COLORIMETRY[1]

János D. Schanda

---

[1] **CHAPTER 9 of the** OSA/AIP Handbook of Applied Photometry (ed.: Dr. Casimer DeCusatis IBM, Poughkeepsie, NY USA).

9.4.2.3 Small field colorimetry

9.4.3 Uniform chromaticity scales and their use in defining correlated colour temperature

9.4.3.1 Colour temperature, correlated colour temperature and distribution temperature

9.4.4 Colorimetry of surface colours

9.4.4.1 Colorimetric properties of materials

9.4.4.2 CIE Standard illuminants and sources

9.4.4.2.1 Standard illuminants

9.4.4.2.2 Standard sources

9.4.4.2.3 Daylight simulators

9.4.4.2.4 Secondary standard illuminants and sources

9.4.4.3 Recommendations on surface colour measurement

9.4.4.3.1 Standard of reflectance factor

9.4.4.3.2 Standard measuring geometry

9.4.4.4 Colour space, and colour difference

9.4.4.4.1 CIE Colour spaces

9.4.4.4.2 CIE colour difference specifications

9.4.4.5 Further recommendations on surface colour measurement

9.4.4.5.1 Metamerism

9.4.4.5.2 Whiteness

9.4.5 Colorimetry of sources

9.4.5.1 Chromatic adaptation

9.4.5.2 Colour rendering

9.5 Further questions of colorimetry

9.5.1 Colour order systems

9.5.1.1 Munsell system

9.5.1.2 The Natural Colour System (NCS system)

9.5.1.3 Further colour order systems

9.5.2 Colour appearance models

9.5.2.1 ATD colour vision model

9.5.2.2 RLAB colour appearance model

9.5.2.3 Nayatani and co-worker's model of colour appearance

CHAPTER 9
COLORIMETRY

János D. Schanda

CIE Executive Director of Central Bureau, Vienna, Austria

and

Department for Image Processing and Neural Computing, University Veszprém, Hungary

9.1 INTRODUCTION

The term colour is used with a number of different meanings in different technologies. The lamp manufacturer understands the physical stimulus produced by his lamp, in everyday life often the pigment is termed colour, in psychophysics the human sensation is called colour. Thus it is wise to distinguish between colour sensation or colour percept, the very fundamental aspects of colour that are formed by our visual system and our brain, and the colour stimulus, the physical quantity producing the colour perception. Materials used for colouring objects can be pigments, inks, paints, etc., but should not be called colour.

Colorimetry is the science and technology to quantify and describe by the help of mathematical models the human colour percepts.

As colour perception is a psychophysical phenomenon, to understand colorimetric methods it is right to overview first the physiological basis of colour perception. Then some psychophysical experiments that lead to a quantified description of colour matching will be discussed. Based on these findings a standardised method for describing tristimulus colour matches, the CIE system of colorimetry will be presented, followed by the introduction to different colour spaces and colour appearance models.

From the point of view of photometry one of the most important aspects of colorimetry is the quantification of the colour rendering properties of light sources. This will be dealt with together with the introduction of the concept of correlated colour temperature.

Colour measurement is performed by spectrophotometric, spectroradiometric and tristimulus measurements. The technique to conduct such measurements will be discussed together with the description of the fundamentals of the instruments.

The final section will discuss colorimetric properties of visual display units and hard copy printers, their functioning and calibration.

9.2 THE VISUAL BASIS OF COLORIMETRY

9.2.1 The human visual system

Figure 9.1 shows a probable model of the human visual system. Part 1 of the visual system is the optics of the eye, a living camera, that focuses a picture of the visual field onto the retina (part 2 in the figure). The optical nerves of the two eyes are combined, and split in the optic chiasma (part 3), the switching board of the optical signals. Within the lateral geniculate nucleus (part 4) the optical information is subdivided into parts relating to colour, motion, form and depth information, which are first processed separately by the brain and then reunited into a mental picture (part 5.). Our knowledge on the functioning of the different parts of the optical system gets fainter and fainter as we move from part 1 to 5.

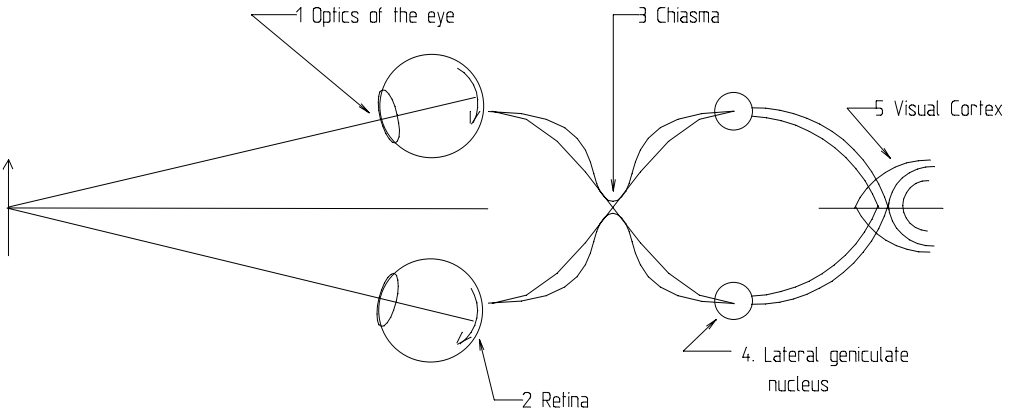

FIGURE 9.1. Model of the human visual system.

Figure 9.2 shows the cross-section of the eye-ball in more detail. Most of the refractive power of the eye comes from the cornea. The ciliary muscle can change the shape of the eye lens, so that the joint refractive power of the cornea and the lens can focus objects at different distances onto the retina. When we look at an object, we try to focus its picture onto the fovea, the part of the retina with the highest visual acuity. (Observe that the visual and optical axis of the eye are approximately 4° apart from each other.) The iris is the coloured annular shaped part of the eye that can be seen from the outside. Its shape changes with light intensity. The "black hole" in the middle of the eye is the pupil, its diameter depends on the shape of the iris and can change from about 2 mm diameter in bright light to about 8 mm in dim light. This is a system to adjust the light entering the eye. From fundamental optics a 1 to 16 fold intensity change can be calculated as the pupil diameter changes from 2 to 8 mm. In reality rays that pass the peripheral regions of the pupil are less effective in producing a light sensation (Stiles-Crawford effect of the first kind). The dynamic range of our eye is much larger, further sensitivity adjustment is of physiological nature. To explain this, we have to investigate the human retina in more detail.

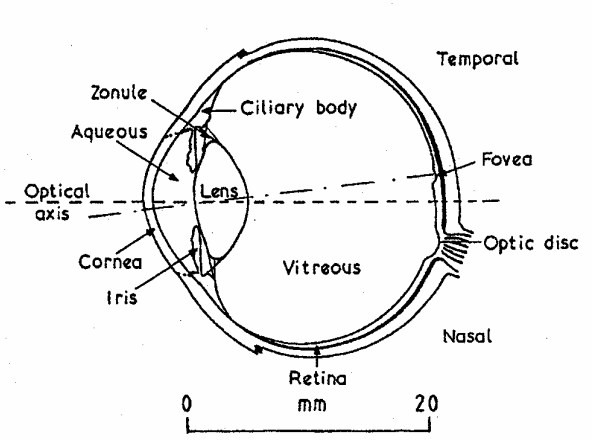

FIGURE 9.2. Cross section of the human eye (*from Handbook of Optics, ed.: M Bass, McGraw-Hill, Inc*.(1)).

9.2.2 The human retina

Figure 9.3 is a schematic drawing of a part of the retina. Light is reaching the retina from the pupil through the vitreous body. First it has to penetrate the layer of the optical nerve, layers of different cells (ganglion-cells, amacrine-cells, bipolar-cells) before it reaches the layer of the rods and cones, responsible for the transformation of optical radiation into light perception. The back of the eye is covered by an almost black layer (the pigment epithelium) that absorbs the light not being absorbed effectively in the rods and cones, and thus decreases the amount of scattered light produced in the eye.

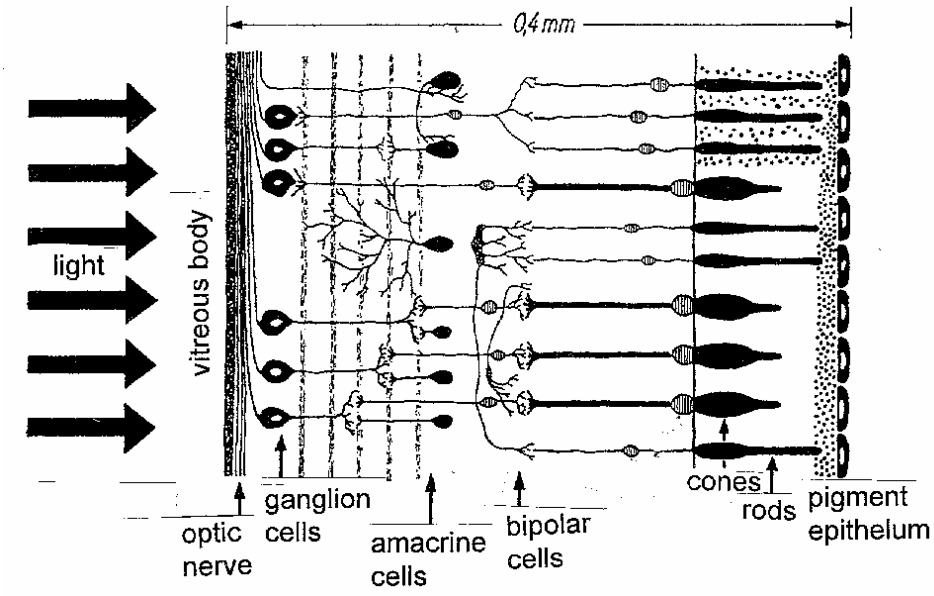

FIGURE 9.3. Schematic drawing of a part of the retina (*from M Richter: Einführung in die Farbmetrik, de Gruyter* (2)).

In the human retina there are about 6,8 million cones, responsible for vision at day-time light levels and evoking colour vision, and about 115 million rods functioning mainly at night-time vision and providing peripheral vision. The distribution of rods and cones is not uniform throughout the retina. The retina has a small pit called fovea. In the fovea we have the highest visual acuity. The approximate diameter of the fovea is - in angular measures - 1,5°. Here the rod population drops considerably. In the central part of the fovea (approximate diameter 1°), called foveola, no rods are present. (This is the reason, e.g. that if looking at a faint star, it can be observed by looking not directly at it, when triing to look at it directly, it seems to disappear.) Figure 9.4 shows the distribution of rods and cones within the retina. Here we see also that in the direction of the blind spot, where the optical nerve leaves the eye, the eye is insensitive. It is interesting that we do not observe this, not even in monocular vision: the brain overpaints the missing information. This phenomenon becomes visible only if one specifically searches for it.

There are several other features of the interior of the eye that have not been dealt with here. We would like to draw attention to only one single entity not shown in the drawing of the eye-ball: The *macula lutea* or *yellow spot*: a pigmented area of approximately 4° visual angle covering the fovea and its neighbouring regions. Owing to individual changes in the pigmentation of this layer and to the discoloration of other transmissive parts of the eye, the spectral sensitivity of individual observers varies, and it changes also with age (4,5).

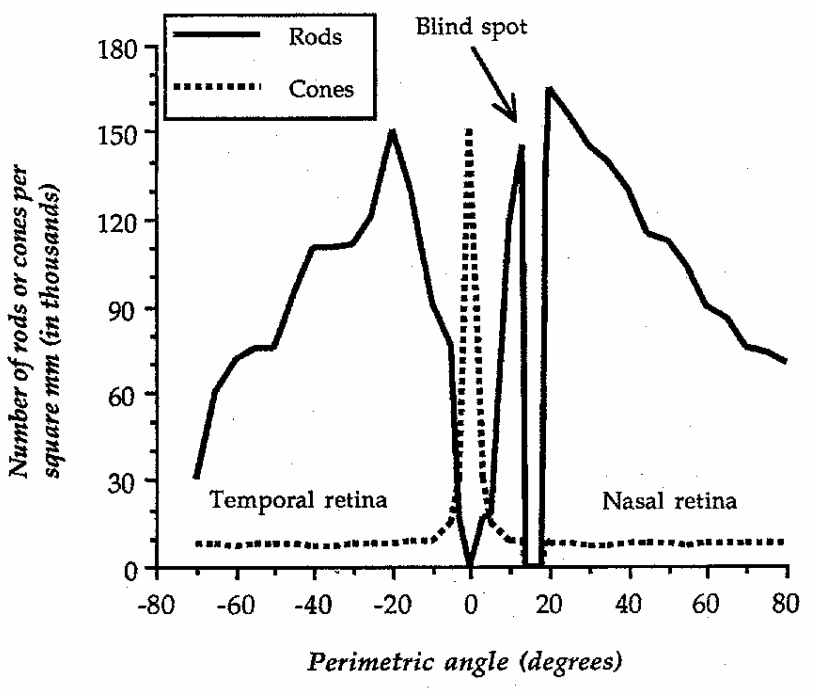

FIGURE 9.4 Distribution of rods and cones within the retina (*from Travis D, Effective colour displays, Academic Pr.*(3)).

As mentioned already, the rods are our receptors at very low light levels, at the so called scotopic luminance levels (below 10^{-3} cd·m^{-2}, as e.g. at moonlight). The rods

contain a single photo pigment that absorbs the light and produces neural signals. These signals are pre-processed in the layers of the different bipolar-, amacrine-, ganglion-, etc. cells and fed via the optical nerves to the brain. Owing to the fact that the rods contain only a single type of photo pigment - called rhodopsin - the rod vision is colour blind: at low light levels we cannot distinguish among different colours, only light intensity differences are sensed. The rod absorption spectrum and the psychophysically determined $V'(\lambda)$-function (see Chapter #X) show reasonably similar spectral dependence, so that one can be pretty sure that the psychophysically determined curve describes the physiological visual mechanism. The $V'(\lambda)$-function has been reproduced in Figure #X **(Insert here reference to Secton XXX!).**

To determine the primary physiological colour vision mechanism, i.e. the cone photo pigment absorption spectra, is not that easy. Microspectrophotometric measurements of human retinal tissue have shown that there are three distinctly different photo pigments in the human cones. The measurements show reasonable agreement with so called suction electrode photoelectric measurements (6) obtained on monkey cone cells where the minute electric currents produced by the illuminated cone sucked into a micro pipette were investigated. Thus from physiological measurements one can assume that the cones of the human retina contain three different photo pigments, where two have rather similar spectral sensitivity and the third one is distinctly different. It is usual to call the three cone sensitivities Long Wave Sensitive (or L-), Medium Wave Sensitive (or M-) and Short Wave Sensitive (or S-) cone sensitivity (see e.g.(7)). (In older literature we find also the symbols R(ed), G(reen) and B(lue), or to distinguish them from real lights the symbols ρ, γ and σ, to identify these visual sensitivities.) The precision of direct physiological investigations is not sufficient to develop from these measurements cone sensitivity functions with an accuracy high enough to be used to model the visual mechanism. They serve merely for comparison with cone sensitivity functions derived from phsychophysical experiments (e.g. heterochromatic brightness matching experiments). Some psychophysically derived cone excitation functions are seen in Figure 9.5.

The L-, M- and S-cones are distributed more or less randomly in the retinal mosaic of receptors, but their concentration in the retina is not equal. The relative abundance of the L- to M- to S-cones is approximately as 40 : 20 : 1 (8). This ratio holds for a large part of the retina. The central part of the fovea, the foveola, however, lacks S-cones, thus it is blue colour blind, or tritanop. (In everyday life we do not realise this because our eyes permanently scan the visual field, and via the so-called *micronystagmus* and *saccades* the brain receives more than one package of information on the field just viewed.)

One can assume that the primary visual physico-chemical process leading to colour sensation is the absorption of photons by the cone photo pigments, producing electrical signals. We will not go into detail on the production of these signals (see e.g. (6)), we would only like to mention that there is physiological evidence that the primary signals are processed by the layers of the bipolar-, amacrine- and ganglion-cells, leading to a signal (pair) that is coded as light intensity related, and two signals (pairs) that are colour coded. The primary photochemical process is most probably a linear one: the primary photoelectric signal produced by a cone is linearly depending on the number of photons absorbed by the cone; the subsequent coding processes are, however, highly non-linear. This makes the investigation of the visual processes by

psycho physical techniques (experimental techniques where a psychical response is registered, produced by a physical stimulus) most difficult.

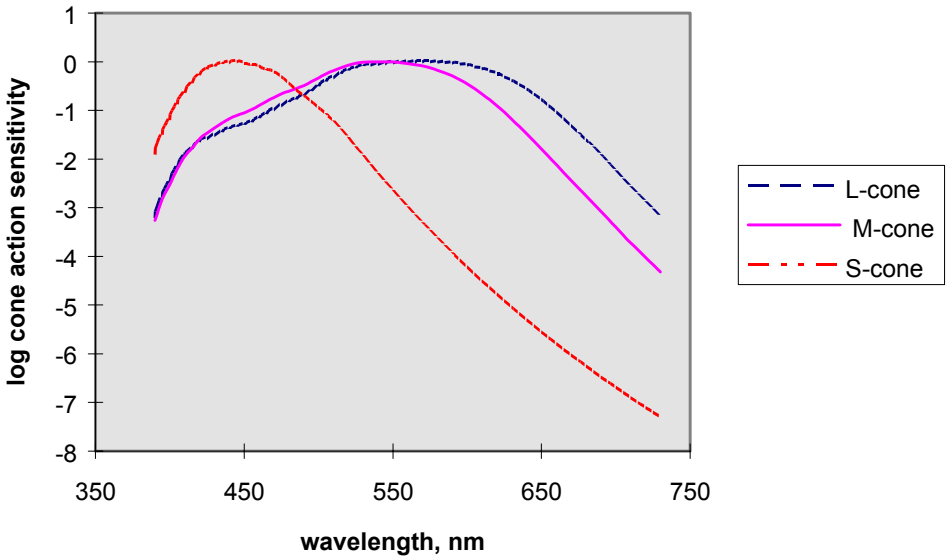

FIGURE 9.5. Relative log cone action spectra.

As a working model the retinal colour vision can be modelled by the scheme as seen in Figure 9.6.

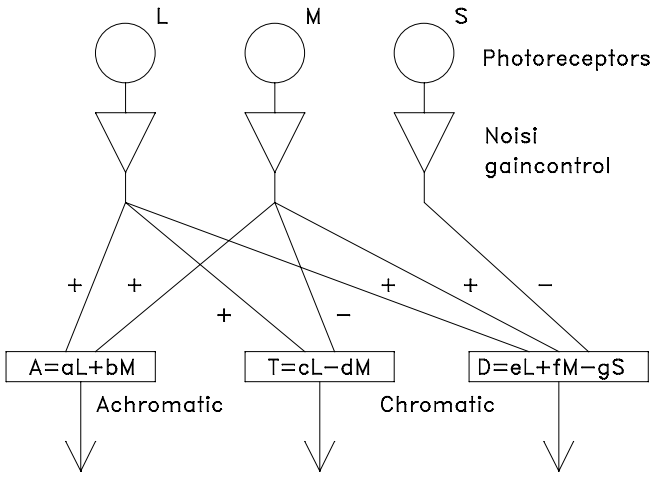

FIGURE 9.6. Schematic model of initial stages of human colour vision: The L, M and S cone signals are processed in a noisy gain control system and fed into an achromatic channel and two opponent chromatic channels. a ... g show percentage contributions of the three cone processes in the establishment of the achromatic and chromatic signals (nerve pulse chains).

The nerve pulses can be followed by physiological techniques, and it can be shown - with some simplifications - that three kinds of signals are carried along the visual pathway. All signals are "frequency coded", i.e. in an un-excited state the nerve cells fire at a given rate, if excited, the firing rate will increase or decrease. The three kinds of signal carriers are:

- nerves that respond to optical excitation differences of neighbouring sites (contrast sensitive cells); at present it is assumed that only the L and M cone signals contribute to this achromatic, contrast signal;
- nerves that respond if excitation becomes overwhelmingly red or green; this is an opponent L versus M excitation; and
- nerves that respond if excitation becomes overwhelmingly yellow or blue; produced by antagonistic excitations coming from the added L plus M cone excitation versus the S cone excitation.

Also response speed differences have been observed, where the contrast channel proved to be the quickest and the blue channel inherently slower than the other two.

Physiological experiments have shown that, with some simplification, beyond the retina the achromatic (contrast) information is carried by the magnocellural pathway and the chromatic information by the parvocellular one (see e.g. (9, 10)).

9.2.3 Colour deficiency

Human colour vision varies from one observer to the other. The majority of the human observers belongs to one class, having very similar cone spectral sensitivity functions. As they are the majority, their colour vision is called "normal". What has been discussed up to now is valid for the so-called colour normal observer. About eight per cent of men and less then half a per cent of women show congenitally different cone spectral sensitivities. They are called colour deficient observers, as most of them can differentiate less precisely among colours than the colour normal. It is usual to classify the colour deficient observers into the following main classes:

- dichromats,
- anomalous trichromats,
- monochromats.

Dichromats cannot distinguish among all the colours that colour normals (often called also normal trichromats) can. They can produce colour matches using only two - not three - properly chosen primaries.

The most common types of dichromatism is *protanopia*. Protanopes find it difficult to distinguish between red and green hues. The red sensitivity of protanopes is much lower than that of normal trichromats (approximately 1 % of men and 0,02 % of women are protanopes), a probable cause of protanopia could be that the L-cones are missing (and probably their place has been filled up by M-cones).

Deuteranopia is a dichromatism, where again the discrimination ability between red and green hues is impaired, but no colour is appearing appreciably dimmer than for normal trichromats. It is not quite sure whether in case of deuteranopia the M-cones are missing or whether it is caused by a second stage abnormality, an impairment of the red-green channel. About 1,1 % of men and 0,01 % of women are deuteranope.

Tritanopia is a very rare form of dichromatism. It manifests itself in a severely reduced discrimination of the bluish and yellowish content of colours. Probable cause could be the missing of the S-cones. As S-cones presumably do not contribute to the luminance channel (see Figure 9.6), there is no loss in luminance perception. We have seen that there are no S-cones in the foveola and therefore the foveola is tritanope. Only about 0,002 per cent of men are tritanope, in women this type of dichromatism is extremely rare.

Monochromatism can have two forms: *Rod monochromats* have no colour discrimination ability and their brightness sensation resembles that of scotopic vision. Most probably their cone-system does not function. Its occurrence frequency is: 0,003 % in men and 0,002 % in women.

Cone monochromats have no colour discrimination ability what-so-ever, but approximately normal brightness sensation. This deficiency might be caused by either the missing of both the M- and S-cones, or problems with the colour difference channels.

Anomalous trichromats can discriminate among every colour where normal trichromats can, only their ability to do this is different from that of normal trichromats.

Protanomaly manifests itself in some reduction in the discrimination of the reddish and greenish hues, with reddish colours appearing dimmer than normal. It might be caused by a somewhat shifted absorption spectrum of the L-cones. Protanomalous observers make up about 1 % of the male and 0,02 % of the female population.

Deuteranomalous observers have some reduction in the discrimination of the reddish and greenish content of colours, it might be caused by an abnormal M-cone spectrum, having its maximum shifted towards that of the L-cones. Deuteranomaly is the most common form of anomalous trichromacy: Almost 4,9 % of the male population and 0,38 % of the female population show this deviation from normal trichromacy.

Recent molecular genetic investigations (see e.g. (11,12)) showed correlation between different kinds of anomalous forms of trichromacy and a single amino acid substitution at a given position of the M- and L-cone pigment.

9.2.4 Colour pseudo-stereopsis

Before we leave the realms of physiology, we have to deal with one further subject: The *colour pseudo-stereopsis*, a phenomenon that red and blue letters printed on a dark background look if they were not in the same plane. Figure 9.7 shows the phenomenon: For most observers the red letters are standing out in front of the plane and the blue ones are lying behind it. Some observers might not see the phenomenon or even might find an opposite effect. An explanation of the effect after Hunt is the following: The effect is caused by the fact that the pupils of the eyes are not always central with the optical axis. The eye is unable to focus both the red light and the blue light simultaneously onto the retina. As known, blue light has always a larger refraction than red light. Thus if the pupils of the observer are displayed outwards relative to the optical axis, as seen in Figure 9.7.a, the rays from an object at O are dispersed by refraction: the images of blue (B) light in the two eyes will be closer to one another than in the case of red (R) light. The red light therefore appears to emanate from an object that is closer than an object from which blue light appears to

emanate. Figure 9.7.b shows the situation for an observer who sees no colour pseudo-stereopsis effect, and Figure 9.7.c shows the situation for an observer whose pupils are displaced inwards relative to the optical axis and therefore for whom the effect is reversed. Colour pseudo-stereopsis has to be considered e.g. in computer display colour design as the unconscious readjustment of the focusing of the eyes is fatiguing.

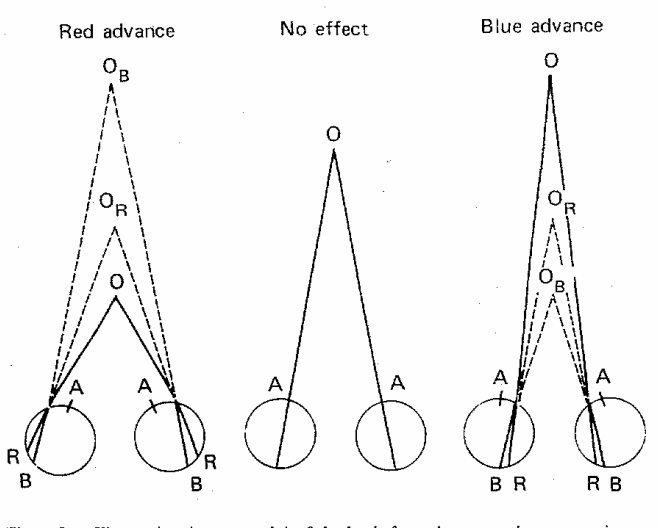

FIGURE 9.7. An explanation for pseudo-stereopsis after Hunt (13).

9.2.5 Colour vision model

Based on above considerations, a colour vision model can be elaborated. Such a model is always an oversimplification of the visual mechanism, but it helps to memorise the functioning of the system and to explain the fundamental experimental findings.

9.2.5.1 The first level: The cone signals

Both the physiological data and the psycho-physical finding that colours can be matched with the mixture of three independent colours (see next section: 9.3 Psychophysical experiments to quantify colour matches) suggest that the primary visual mechanism is trivalent. We have seen that there is enough evidence to assume three cone types in the retina (L-, M- and S-cones) as shown in Figure 9.5. In that retinal area where we have good colour and form recognition capability (a central region of approximately 10° to 15° diameter, but not in the very central region of less than 1° diameter (the foveola)) the relative abundance of the three cone classes is, as mentioned, L : M : S = 40 : 20 : 1. The L- and M-cones behave rather similarly, their spectral sensitivity is not very much different, their speed of response is similar, etc. The S-cones behave differently: they respond much slower than the L- and M-cones, and their spectral sensitivity is also markedly different; also there are much fewer S-cones in the retina than L- or M-cones.

9.2.5.2 The second level: The antagonistic colour signals

Anthropologists speculate that the L- and M-cones differentiated from each other only at a late stage of evolution and still show many common features. One of these could be that the L- and M-cone signals combine to form the "luminance-channel" of vision, i.e. one of the visual pathways from the eyes to the brain contains signals, where both L- and M-cones feed into spatially antagonistic structures, leading to contrast information signals. It is possible to build from the spectral sensitivity of the L- and M-cones a spectral sensitivity curve that practically duplicates the $V(\lambda)$-function. In Figure 9.6 the M + L cone signal represents this schematically. A signal, where L- and M-cones work antagonistically against each other, is propagating in a colour-difference channel, carrying red versus green information. A second colour difference channel could combine the M + L cone response antagonistically with the S-cone response producing a yellow versus blue signal. Neurophysiological investigations have shown the existence of such pathways. All three signals have such structures that there is a quiescent firing rate when there is no excitation in the pathway (i.e. there is no light stimulation difference between the centre-surround for the luminance channel, and it is achromatic for the two colour difference channels). As soon as differences occur in the centre-surround, and/or red-green, and/or yellow-blue primary excitation, the firing rate in the respective channels will change (increase or decrease) and the information on luminance and hue is mediated towards the brain.

In this simplified model other couplings between the single levels of neural pathway have been omitted. Such couplings function as feed-back to control the overall sensitivity and relative sensitivity in the different pathways, and make the system non-linear. Also the influence of the rods has been left out of this picture. Their signal most probably combines with the L+M signal. Some authors consider also inputs from the S-cones into the M+S and L-M channels, but most recent publication assume the model as depicted in Figure 9.4.

Above model of colour vision corresponds well with the psycho physical observation that in human perception a mental picture exists of pure red, yellow, green and blue, and we can well think of a yellowish green or red but never of a yellowish blue. Similarly red and green are exclusive, no reddish green exists (or vice versa).

9.2.5.3 The third level: the mental processing

The first two levels of colour perception are - at least at this elementary level - reasonably well understood. For less is known how the final stages of colour perception function. There are a few peculiarities of colour vision, most probably stage three phenomena, which are important to understand the colorimetric issues of photometry.

Colour constancy is one phenomenon whose interpretation can be given only partly on the basis of first and second stage mechanisms: If daylight and incandescent light are seen side by side it is apparent that the incandescent light is much more yellow than daylight. If, however, we look at a white paper, illuminated by daylight or incandescent light only, our visual mechanism adjusts itself to the illuminant and in both cases we will say that paper is white. Part of this adjustment - chromatic

adaptation - is probably taking place at retinal levels: It can be due to the bleaching of one of the cone pigments and to selective gain control between the different channels. The phenomenon is, however, partly mental: for well-known objects the colour of illumination can be grossly changed and the observer will still seem to see the object in its original colour.

Also a further "transformation" of the colour information takes place in the brain: From the luminance and two opponent colour difference signals brightness, hue and saturation perception is formed: luminance, determined by flicker-photometric experiments (see Chapter #XX), corresponds to brightness only if the colour is almost achromatic. Highly chromatic colours show higher brightness at the same luminance level than less chromatic ones (so called Helmholtz-Kohlrausch effect). In the concept of a model one assumes that the brain adds information from the chromatic (i.e. colour difference) channels to the luminance information in creating the percept of brightness. (As we will see in Section 9.5.2, some model builders try to construct a brightness descriptor using vector addition analogy.)

The concept of *hue* - as used in the elementary description of colours based on the hue circle - is also a mental concept, and we do not find its physiological analogy in level one or level two colour perception.

Further items, where higher mental processing seems to work, are *lightness* and *saturation*. The colour stimulus should - transformed to the mental picture - produce signals of brightness, hue and *chromaticness* (called also *colourfulness*). As mentioned, brightness can be thought as composed by the achromatic signal and the chromatic signals. Hue is somehow related to the chromatic signals and for an engineering approach it is easy to visualise it as the angle between a starting point in a three dimensional diagram, as seen in Figure 9.8, and the particular hue described by vectorial sum of the red/green and yellow/blue signals. Also the "strength" of the colour, the chromaticness can be visualised in such a diagram. The human visual system has, however, the peculiar property that looking at a real scene it relates the brightness and the chromaticness to that of a mental reference white: to the brightness of a surface in the picture that it assumes to be white. Thus, if in a scene the brightness of a particular object is decreased, e.g. due to the fact that it is moved from direct sunlight into a shaded area, the perceived *lightness* of this object will stay unchanged. We are able to distinguish a white surface that is in the shadow from a grey one in sunlight, even if the stimulus reaching the eye from the white surface (i.e. its luminance) is lower than that of the grey one.

Similarly, for colours of objects (so-called related colours) not the absolute length of the colourfulness arrow is the most important mental characteristic of what is the result of the colour channel signals, but a quantity somehow related to the apparent brightness. This characteristic is called *saturation*, and is something that seems again to stay constant when the coloured object is moved from a place with high illumination to one where the illumination level is lower.

In the third level of the visual mechanism different features, such as form, movement, colour, of the real world seen are pre-processed at different locations of the brain and then are integrated into the final mental picture. Although little is known for sure in this field, the area of physiological and psycho physical research is developing fast, and it is a continuous endeavour in engineering research to apply the

newest findings of vision research. For further reading on the topography of the human visual cortex see the excellent review of Eric Schwartz (14).

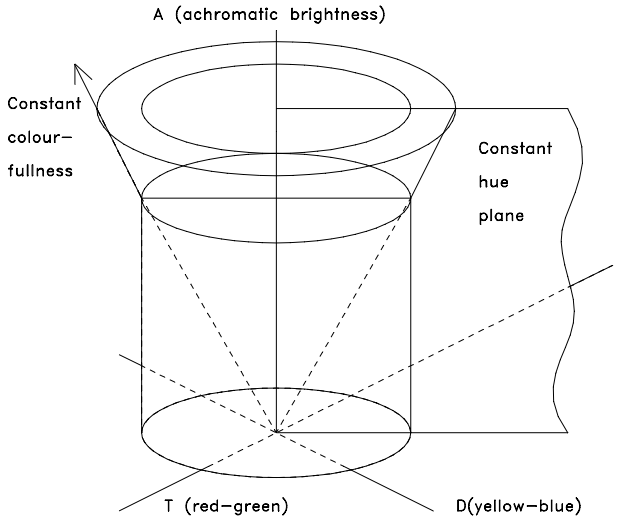

FIGURE 9.8. A three dimensional representation of the mental representation of a colour percept.

9.3 PSYCHOPHYSICAL EXPERIMENTS TO QUANTIFY COLOUR MATCHES

9.3.1 Additive colour mixture experiments

The fundamental experiment in colorimetry is depicted in Figure 9.9. A test colour stimulus ***C*** is selected. This colour stimulus can be an arbitrary light, coloured or white, only its intensity should be so high that when the light reflected from the white screen is viewed, as depicted in the figure, the eye should be stimulated in the photopic region, preferably to a level, as in normal daylight (i.e. an illumination of the white screen of approximately 1000 lx should be set). This colour stimulus illuminates one half of a bipartite field (the test field) in the masking screen and is observed by the observer's eye. The other half of the bipartite field (the matching field) is illuminated by the additive mixture of three lights. Additive mixture means here that the three lights irradiate the common white surface in such a form that by viewing this surface the three sources cannot be seen as independent light sources any more, only the mixed light reflected from the screen can be perceived. There is only a single constraint on the selection of the colour of the three sources: the three colours have to be independent, i.e. it should not be possible to produce the colour of one of the lights via mixing given proportions of the other two. It is convenient to select saturated red (**R**), green (**G**) and blue (**B)** lights as constituents of the additive mixture. Means to adjust the intensity of the three sources are shown as well. These are essential parts of the experiment. The intensity of the three lights has to be chosen so that they are strong enough to produce matches with the test stimulus. It is convenient to choose the units of the three lights (i.e. unity setting of the light adjusting means) so that they produce a white mixture.

Let us first choose a colour stimulus $\boldsymbol{C_1}$ (e.g. the light of an incandescent lamp filtered with an orange filter). One can adjust the intensity of the **R, G, B** lights to match this light. These quantities shall be $\boldsymbol{R_1}$, $\boldsymbol{G_1}$, $\boldsymbol{B_1}$ (we will call them the *tristimulus values).* In mathematical form one describes the colour match as

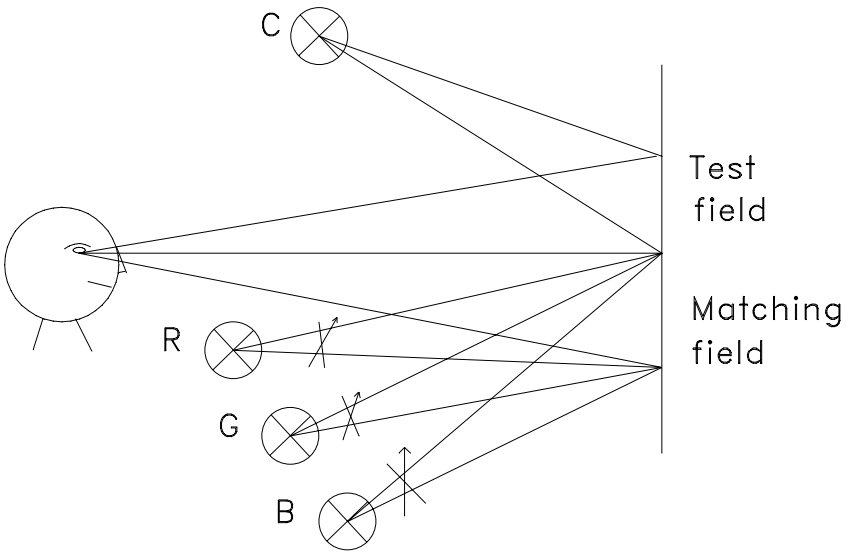

FIGURE 9.9 Basic colour matching experiment

$$C_1 \equiv R_1 + G_1 + B_1 \qquad \text{... 9.1}$$

where "≡" is read as "matches".

Let us now choose a second colour stimulus $\boldsymbol{C_2}$ (e.g. the light of the incandescent lamp filtered with a green filter). This will be matched by the quantities $\boldsymbol{R_2}$, $\boldsymbol{G_2}$, $\boldsymbol{B_2}$:

$$C_2 \equiv R_2 + G_2 + B_2 \qquad \text{... 9.2}$$

Experimenting with different $\boldsymbol{C}$ colour stimuli, one will see that to every colour a unique setting of the ***R, G, B*** values is needed. If we experiment with saturated test colours, then once we will observe that we are unable to establish a colour match: by the mixture of two matching stimuli, we reach an approximate match, and the adding of the third one makes the match worse. Slightly modifying the experimental set-up the colour match can be established: the third light whose intensity was set to zero to establish the best approximation is re-directed to fall onto the test half screen, i.e. one establishes a two/two colour match (let us assume for simplicity that the Red matching stimulus is the one that behaves peculiarly, naturally with other test stimuli it could be the Green or the Blue just as well):

$$\boldsymbol{C_3 + R_3 \equiv G_3 + B_3} \qquad \text{... 9.3}$$

As we would like to express the test stimulus by the three matching stimuli we re-arrange the equation to read:

$$C_3 \equiv G_3 + B_3 - R_3 \qquad \text{... 9.4}$$

The adding of one of the matching stimuli to the test stimulus is mathematically expressed as subtracting the stimulus on the matching side (naturally there is nothing like a negative colour stimulus)

9.3.2 Grassmann's laws

As a next step in our experiments let us irradiate the test field side once with C_1 and C_2 separately, and then with the sum of C_1 and C_2 (with the orange and green lights of the previous paragraph it will produce a yellow light patch). We will observe that colour match is obtained if the matching field is illuminated with intensities $R_1 + R_2$, $G_1 + G_2$, $B_1 + B_2$, i.e. colour matching is additive.

Mathematically one can formulate the laws of additive colour matching in the following form (15):

1/ symmetry law: If colour stimulus ***A*** matches colour stimulus ***B,*** then colour stimulus ***B*** matches colour stimulus ***A***.

2/ transitivity law: If ***A*** matches ***B*** and ***B*** matches ***C***, then ***A*** matches ***C.***

3/ proportionality law: If ***A*** matches ***B***, then αA matches αB, where α is any positive factor.

4/ additivity law: If ***A, B, C, D*** are any four colour stimuli, then if any two of the following three conceivable colour matches hold:

$$A \equiv B,\ C \equiv D,\ (A + C) \equiv (B + D) \qquad \text{... 9.5}$$

then so does the remaining match

$$(A + D) \equiv (B + C) \qquad \text{... 9.6}$$

where ***(A+C), (B+D), (A+D), (B+C)*** denote, additive mixtures of ***A*** and ***C, B*** and ***D, A*** and ***D, B*** and ***C,*** respectively.

(These four laws are often called the stronger form of trichromatic generalisation of colour matching). It is a mathematical description of what was stated by Grassmann in 1853 - 1854 (16). A modern verbal formulation of Grassmann's laws is given by Hunt (13) in the following form:

1. To specify a colour match, three independent variables are necessary and sufficient.
2. For an additive mixture of colour stimuli, only their tristimulus values are relevant, not their spectral composition.
3. In additive mixtures of colour stimuli, if one or more components of the mixture are gradually changed, the resulting tristimulus values also change gradually.

There are some constrains that have to be considered if Grassmann's laws are applied:

1. Matches have to be always made under similar observational situation. If an observer sets a match where the fields have different spectral compositions, the match will not necessarily hold if he moves his eye, does not look centrally at the fields, or the sizes of the fields are changed.

2. The light exposure of the eyes will effect the state of *adaptation*. Although the persistence of colour matches is rather high, with very high irradiation the spectral sensitivity of the eye can be influenced.

3. If a larger area of the retina (e.g. a 10° field) is used for colour match, a failure of the proportionality law is found.

9.3.3 Towards a system of colorimetry

Grassmann's laws will be followed as long as above constrains are obeyed, and a colorimetric system based on additivity and proportionality can be used.

As will be seen in Section 9.4, such a system can be built on the analogy of the photometric system, only as colour is three dimensional (we need three independent variables to describe colour, or to obtain a colour match) three integrals of the form of Equ. 'XXX (see Chapter 'YYY, Section 'ZZZ)**(Pls. insert numbers!)** will be needed to describe colour:

$$T_i = k \int_{380\text{nm}}^{780\text{nm}} \Phi_{e\lambda}\, \bar{t}_i(\lambda)\, \mathrm{d}\lambda, \quad i = 1, 2, 3 \qquad \ldots\ 9.7$$

where $\bar{t}_i(\lambda)$ stand for three weighting functions of the stimulus, called colour matching functions, T_i describes the colour stimulus in the trichromatic system.

The principles to reach an expression as equation 9.7 are the following:

First the units of the matching stimuli have to be set. This can be done, e.g. by setting them so that the mixture of the unit amounts provide a colour match with a particular white stimulus, such as produced by an equienergetic spectrum (having equal amounts of energy per wavelength interval throughout the visible spectrum. Using the symbols **[R], [G], [B]** for these unit amounts of matching stimuli, equation 9.1 can be written in the form:

$$\boldsymbol{C}_1 \equiv r_1[\mathbf{R}] + g_1\,[\mathbf{G}] + b_1\,[\mathbf{B}] \qquad \ldots\ 9.8$$

where r_1, g_1, b_1 represent the amount of light taken from the **[R], [G], [B]** matching stimuli (called also tristimulus values). $\boldsymbol{C}_1$ has a spectral distribution ($\boldsymbol{C}_1(\lambda)$) and one could write an equation like 9.8 for every 2003.09.17. wavelength band of the spectrum and then add these to obtain $\boldsymbol{C}_1$. The additivity and multiplicativity of colorimetry permits this and via this technique we can reach an equation like 9.7, where $\bar{t}_i(\lambda)$ provide the monochromatic constituents of the tristimulus values (they were actually called spectral tristimulus values, at present the term *colour matching functions* is preferred, since by the help of them colour matching is performed).

As will be seen from the next section, this principle can be used in praxis, the CIE system of colorimetry is built around these fundamental experimental findings.

9.4 CIE COLORIMETRY

9.4.1 The colour equation

We have seen that despite the fact that colour is a perception and underlies individual variations, some fundamental rules can be elaborated. These permit predictions to outline, how colours change when the stimuli are changed, and how colour matches can be obtained. Based on them, a colour measuring system enabling the specification of colours can be worked out, at least to that extent that colours with the same numerical specification will look similar to the vast majority of observers. CIE (from its French name: Commission Internationale de l'Éclairage, International Commission on Illumination) is the international organisation that undertook the task of developing these specifications. As seen in the previous section, colorimetry needs conventions. Such conventions are necessary because two colour stimuli looking similar under one viewing condition might look different when seen under other conditions (field of view, adaptation, direction of viewing, etc., see Section 9.3.2).

Condition 1 of CIE colorimetry is that the colour matches on which the system is based have to be performed with an approximately 2° bipartite visual field, central fixation and dark surround.

The schematic drawing of such a trichromatic match experiment is shown in Figure 9.10. In one of the basic investigations, performed by WD Wright (see (17)) the monochromatic wavelengths 700 nm, 546,1 nm and 435,8 nm were used as red (R), green (G) and blue (B) stimuli. (The red stimulus can be selected using an interference filter, the green and blue stimuli are emission lines of a mercury discharge.) In the trichromator means have to be available to set the intensity of the three matching stimuli and to measure these intensities. To construct the colour matching functions to be used in the integrals, as discussed in Section 9.3.3, monochromatic radiation has to used as test stimulus.

The three matching stimuli are mixed in a photometer sphere (often called Ulbricht-sphere) and viewed via the exit port of the sphere. A mirror blends the light coming from the test stimulus into one half of the 2° viewing field. A black light trap absorbs the light of the test lamp not hitting the white reflecting plate. Two light baffles in the sphere (not shown in the figure) secure that no direct light from the sources or the mixture field reaches the observer.

Condition 2 of the CIE trichromatic match concerns the magnitude of the selected 700 nm, 546,1 nm and 435,8 nm matching stimuli (called also reference colour stimuli, or primary stimuli or primaries): The units of the three primaries have been set to such values that their mixture should provide a colour match with an equienergetic white test stimulus, i.e. a stimulus where at every wavelength in the visible spectrum the same amount of power is propagating ($\mathrm{d}S(\lambda)/\mathrm{d}\lambda = S_\lambda = \text{const.}$). Taking 1 cd/m^2 of red light as 1 red unit, to achieve such a match 4,5907 cd/m^2 of green and 0,0601 cd/m^2 of blue light has to be taken, and the mixture of them matches the equienergetic white stimulus of 5,6508 cd/m^2. Thus the chosen three new units have the following luminance:

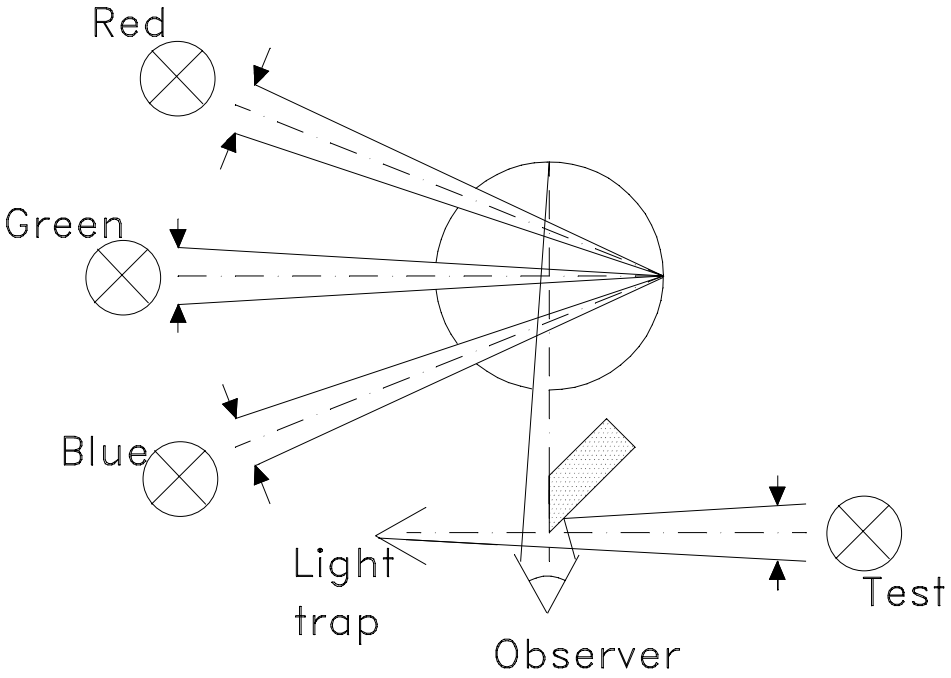

FIGURE 9.10 Schematic drawing of the principles a visual colorimeter.

Table 4-1:

Luminance of the selected **R**, **G**, **B** matching stimuli

red:	1,0000	cd/m^2	= 1 new **R** unit
green:	4,5907	cd/m^2	= 1 new **G** unit
blue:	0,0601	cd/m^2	= 1 new **B** unit

If now an arbitrary colour is matched with the so selected **R**, **G**, **B** matching stimuli, the amounts of the three matching stimuli expressed in the above new units are called (*R*, *G*, *B*) tristimulus values, and the colour match is expressed as:

$$C \equiv R[R] + G[G] + B[B] \quad \ldots 9.9$$

where ≡ reads "matches".

If monochromatic test stimuli are used, one observes that e.g. a 520 nm green stimulus cannot be matched by any combination of the three matching stimuli. One comes nearest to the match if only blue and green matching stimuli are used, but exact colour match can only be obtained if some red light is mixed to the test stimulus:

$$C(520\text{ nm}) + R[R] \equiv G[G] + B[B] \quad \ldots 9.10$$

i.e. the colour mixture of given amounts of the green and blue matching stimuli will match the mixture of the test and red stimuli. This is shown schematically in Figure 9.11. Here, to obtain a colour match, the pivoting mirror Mp in the red channel directs

the light onto the side of the test stimulus. Mathematically the fact that from one of the primaries light is mixed with the light of the test stimulus is written with a negative sign for that stimulus:

$$C \equiv -R[\mathrm{R}] + G\,[\mathrm{G}] + B\,[\mathrm{B}] \qquad \ldots\ 9.11$$

It should be, however, quite clear that this does not mean "negative light"!

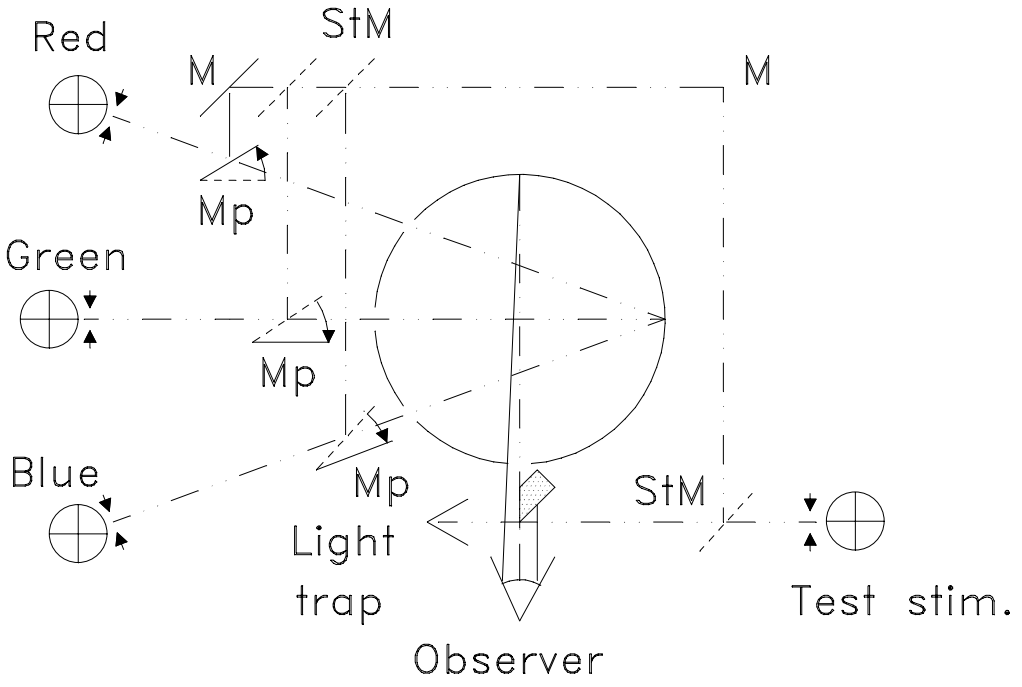

FIGURE 9.11 Schematic view of a visual colorimeter.

9.4.1.1 Tristimulus values and colour matching functions

If between 380 nm and 780 nm all the monochromatic radiation of equal power within a small wavelength band are matched with the combination of the **R**, **G**, **B** primaries, the so called *colour matching functions* (CMF) designated by the symbols $\bar{r}(\lambda)$, $\bar{g}(\lambda)$ and $\bar{b}(\lambda)$ are obtained. The CIE standardised such CMF as average curves in 1931. They are called the *colour matching functions* of the *CIE 1931 Standard Colorimetric Observer* and are shown in Figure 9.12.

As colour matches are additive, if 1 unit of power of light with wavelength λ_1 [$\boldsymbol{C}(\lambda_1)$] is matched with the **R**, **G**, **B** primaries:

$$\boldsymbol{C}(\lambda_1) \equiv R_1[\mathbf{R}] + G_1[\mathbf{G}] + B_1[\mathbf{B}] \qquad \ldots\ 9.12$$

and 1 unit of power of light with wavelength λ_2 [$\boldsymbol{C}(\lambda_2)$] is matched with the **R**, **G**, **B** primaries:

$$\boldsymbol{C}(\lambda_2) \equiv R_2[\mathbf{R}] + G_2[\mathbf{G}] + B_2[\mathbf{B}] \qquad \ldots\ 9.13$$

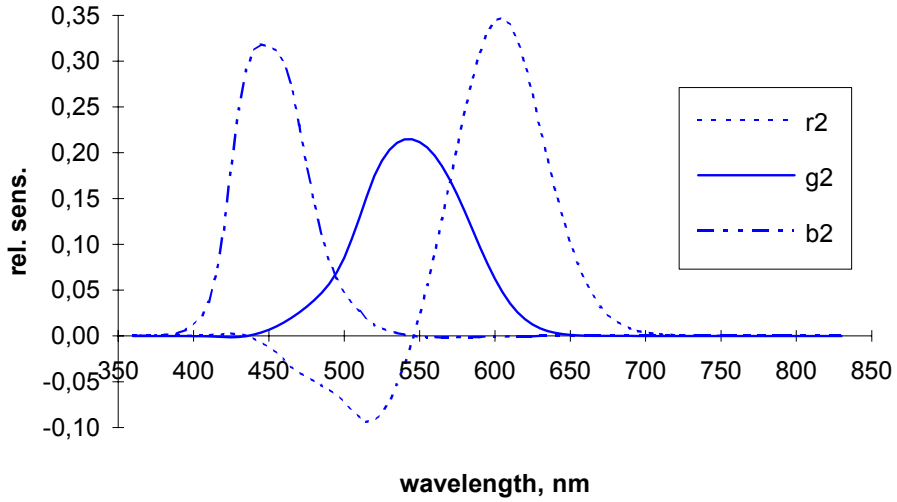

FIGURE 9.12 $\bar{r}(\lambda), \bar{g}(\lambda), \bar{b}(\lambda)$ colour-matching functions of the CIE 1931 Standard Colorimetric Observer.

then the additive mixture of the two monochromatic lights $\boldsymbol{C}(\lambda_1) + \boldsymbol{C}(\lambda_2)$ will be matched with the additive mixture of the two amounts of the primaries:

$$\boldsymbol{C}(\lambda_1) + \boldsymbol{C}(\lambda_2) \equiv (R_1 + R_2)[\mathbf{R}] + (G_1 + G_2)[\mathbf{G}] + (B_1 + B_2)[\mathbf{B}] \qquad \ldots\ 9.14$$

This reasoning can be extended to three, four, ... etc. monochromatic components, so that if the spectral power distribution of a stimulus is known, its tristimulus values can be determined by adding the R_i G_i, B_i weighted spectral constituents of the stimulus. The R, G, B tristimulus values of a stimulus with $P(\lambda)$ spectral power distribution are:

$$\begin{aligned} R &= k \sum_{380\text{ nm}}^{780\text{ nm}} P(\lambda)\ \bar{r}(\lambda)\Delta\lambda \\ G &= k \sum_{380\text{ nm}}^{780\text{ nm}} P(\lambda)\ \bar{g}(\lambda)\Delta\lambda \qquad \ldots\ 9.15 \\ B &= k \sum_{380\text{ nm}}^{780\text{ nm}} P(\lambda)\ \bar{b}(\lambda)\Delta\lambda \end{aligned}$$

or using the integral form

$$R = k \int_{380\text{ nm}}^{780\text{ nm}} P(\lambda)\bar{r}(\lambda)\mathrm{d}\lambda, \quad G = k \int_{380\text{ nm}}^{780\text{ nm}} P(\lambda)\bar{g}(\lambda)\mathrm{d}\lambda, \quad B = k \int_{380\text{ nm}}^{780\text{ nm}} P(\lambda)\bar{b}(\lambda)\mathrm{d}\lambda \qquad \ldots 9.16$$

Here k is a constant that can be used to couple the colorimetric (photometric) quantities to the radiometric ones: as seen from Table 4-1 the luminance of a colour matched by the amounts R red units, G green units and B blue units will be:

$$L = 1{,}0000R + 4{,}5907G + 0{,}0601B \qquad \ldots\ 9.17$$

This means that the constant k can be chosen in such a way that if $P(\lambda)$ is a radiometric quantity, the L value will be a corresponding photometric quantity, e.g. if $P(\lambda)$ is measured in W/(sr·m^2) then L will be provided in cd/m^2.

9.4.1.2 G,R,B colour space

To visualise a trichromatic colour system, the **R**, **G**, **B** primaries can be thought of as the basis vectors of a three dimensional vector space. Figure 9.13 shows such a representation. Here a plane has been drawn where the **R**, **G**, and **B** vectors have unity values. Also the cone of monochromatic colour stimuli are shown. The **R**, **G**, and **B** vectors are located on the surface of this cone, as they are monochromatic lights (i.e. if the monochromatic test stimulus has the value of 700 nm, or 546,1 nm, or 435,8 nm, only one of the *R*, *G*, *B* tristimulus values will be different from zero). The two extremes of the monochromatic spectrum locus (380 nm and 780 nm) have been connected by a straight line, we will see that here are located the purple colours. From this representation it is also easy to see that only colour stimuli that lie within the tetrahedron drawn up by the three basic vectors can be realised by simple additive mixture, for all other stimuli, thus also for most of the monochromatic ones, from one of the basic vectors negative amount has to be taken, i.e. in the colour mixture one of the primaries has to be mixed to the test stimulus to achieve a colour match. This is equivalent with the finding in Figure 9.12 that the $\bar{r}(\lambda), \bar{g}(\lambda), \bar{b}(\lambda)$ functions show negative lobes, and that at the wavelengths of the matching stimuli two of the functions are always zero, and a single one shows positive value.

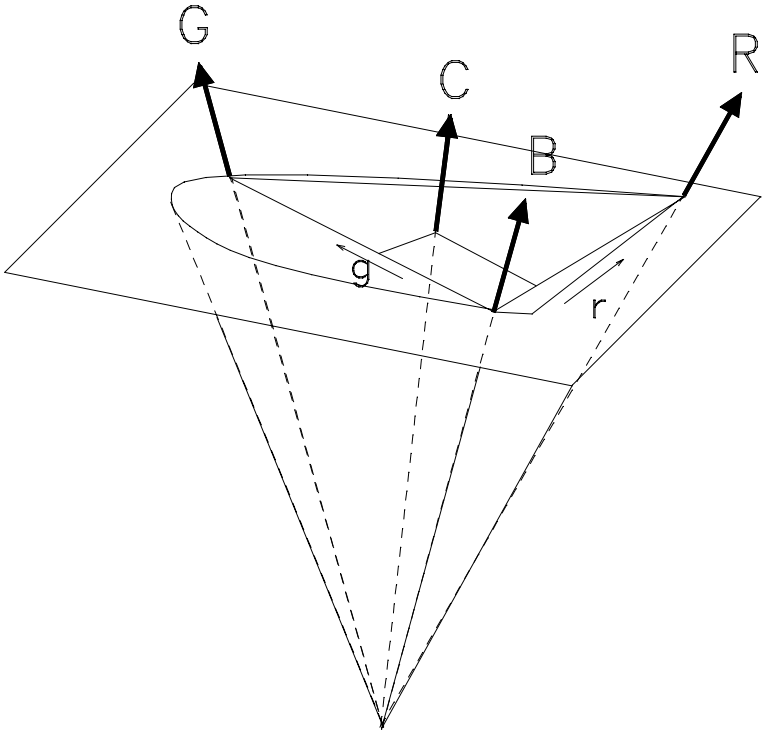

FIGURE 9.13 Schematic representation of the **RGB** colour space, where **R, G, B** are the primaries of the system; **C** is a colour stimulus, a plane has been drawn where the primaries have unit values; r, g are the chromaticity co-ordinates in this plane..

9.4.2 X,Y,Z colour space

9.4.2.1. CIE 1931 Standard Colorimetric Observer

For those who have a good concept of vector calculus, the construction of the **R**, **G**, **B** colour space can be easily conceived it the following form: Let us assume an *n* dimensional spectrum space, where a colour stimulus is represented by an *n* dimensional vector. The co-ordinates of this vector are the power (or radiance, etc.) values at the *n* wavelengths (e.g. an 81 dimensional space if the colour vector has been defined by its values at 81 wave-length co-ordinates [(780 - 380)/5+1, if measurements have been performed at 5 nm wave-length increments between 380 nm and 780 nm]. The three dimensional colour space is a sub-space of this spectrum space, where any three independent vectors can be used as basis vectors of the colour space. Thus we can choose e.g. such basis vectors that the total volume of the colour cone is within the positive quadrant of the space. Just this has been done by the CIE at the time the CIE trichromatic system was built (18, 19), as it was felt that the manipulation with negative values in the colour matching functions may lead to calculation errors.

The basis vector transformation was done in such a form that

1. the tristimulus values of the colour stimulus of the equienergetic spectrum should again be equal;
2. all the photometric information (luminance, if the stimulus is measured in radiance units) should be in a single value, i.e. one of the colour matching functions should be equal with the V(λ)-function;
3. the tristimulus values of all real colours should be positive and the volume of the tetrahedron should be as small as possible (i.e. the borders of the colour cone should touch the tetrahedron at as many as possible places.

(For further details see (20).)

With above in mind the transformation adopted by the CIE was:

$$\begin{vmatrix} X \\ Y \\ Z \end{vmatrix} = \begin{vmatrix} 2{,}76888 & 1{,}75175 & 1{,}13016 \\ 1{,}00000 & 4{,}59070 & 0{,}06010 \\ 0{,}00000 & 0{,}05651 & 5{,}59427 \end{vmatrix} \cdot \begin{vmatrix} R \\ G \\ B \end{vmatrix} \qquad \text{... 9.18}$$

or in an expanded form:

$$\begin{aligned} X &= 2{,}76888\,R + 1{,}75175\,G + 1{,}13016\,B \\ Y &= 1{,}00000\,R + 4{,}59070\,G + 0{,}06010\,B \\ Z &= 0{,}00000\,R + 0{,}05651\,G + 5{,}59427\,B \end{aligned} \qquad \text{... 9.19}$$

In these equations we see that the *Y* component is identical with Equ. 9.17 and thus contains the luminance information. If the matrix elements are multiplied with 0,176967 (the coefficient of *Y(R)* to get unit *Y* value), the matrix gets a simple form:

$$\begin{vmatrix} 0{,}49 & 0{,}31 & 0{,}2 \\ 0{,}176967 & 0{,}812397 & 0{,}010636 \\ 0 & 0{,}01 & 0{,}99 \end{vmatrix} \qquad \text{... 9.20}$$

where only the *Y* component is carrying six precisely chosen significant digits, all other matrix elements have only two non zero decimal digits. From this it is also evident that the *X* value is composed mainly from the *R* value, but the *G* and *B* values have also significant weight. The *Z* value is almost entirely composed by the *B* value.

The inverse transformation from the *XYZ*-system into the *GRB* one can be done by using the inverse matrix of 9.18:

$$\begin{vmatrix} 0{,}41846 & -0{,}15866 & -0{,}08283 \\ -0{,}09117 & 0{,}25243 & 0{,}01571 \\ 0{,}00092 & -0{,}00255 & 0{,}17860 \end{vmatrix} \quad \ldots 9.21$$

One can see that all three matrices 9.18, 9.20 and 9.21 fulfil the requirement that an equienergetic stimulus has in the system equal tristimulus values.

Colour matching functions can be built in this system on the analogy of the $\bar{r}(\lambda)$, $\bar{g}(\lambda)$ and $\bar{b}(\lambda)$ colour matching functions as introduced in Section 9.4.1.1 and shown in Figure 9.12. The values of the $\bar{x}(\lambda)$, $\bar{y}(\lambda)$, $\bar{z}(\lambda)$ colour matching functions are the tristimulus values of the monochromatic stimuli. Thus equation 9.22 holds for their transformation:

$$\begin{vmatrix} \bar{x}(\lambda) \\ \bar{y}(\lambda) \\ \bar{z}(\lambda) \end{vmatrix} = \begin{vmatrix} 2{,}76888 & 1{,}75175 & 1{,}13016 \\ 1{,}00000 & 4{,}59070 & 0{,}06010 \\ 0{,}00000 & 0{,}05651 & 5{,}59427 \end{vmatrix} \cdot \begin{vmatrix} \bar{r}(\lambda) \\ \bar{g}(\lambda) \\ \bar{b}(\lambda) \end{vmatrix} \quad \ldots 9.22$$

These functions (see Appendix A) form the *CIE 1931 Standard Colorimetric Observer*. They are tabulated in an ISO/CIE Standard (21) at 1 nm intervals to seven significant digits between 360 nm and 830 nm. A graphical representation is given in Figure 9.14. As seen, all the values of these functions are non negative, and the $\bar{y}(\lambda)$-function has exactly the shape of the $V(\lambda)$-function. One peculiarity of this transformation is that the $\bar{x}(\lambda)$-function has turned out to have two maximums.

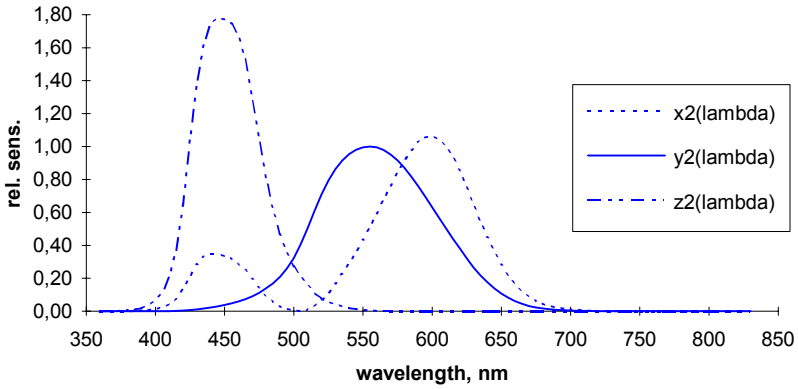

FIGURE 9.14 $\bar{x}(\lambda)$-, $\bar{y}(\lambda)$-, $\bar{z}(\lambda)$- colour matching functions of the CIE 1931 Standard Colorimetric Observer

9.4.2.1.1 Tristimulus values and chromaticity co-ordinates

Using the $\bar{x}(\lambda)$-, $\bar{y}(\lambda)$-, $\bar{z}(\lambda)$-functions, the *X*, *Y*, *Z* tristimulus values of a colour stimulus ($S(\lambda)$) can be calculated exactly in the same way as described in connection with equation 9.16:

$$X = k \int_{380\,\text{nm}}^{780\,\text{nm}} S_\lambda(\lambda)\bar{x}(\lambda)\mathrm{d}\lambda, \quad Y = k \int_{380\,\text{nm}}^{780\,\text{nm}} S_\lambda(\lambda)\bar{y}(\lambda)\mathrm{d}\lambda, \quad Z = k \int_{380\,\text{nm}}^{780\,\text{nm}} S_\lambda(\lambda)\bar{z}(\lambda)\mathrm{d}\lambda \quad \ldots 9.23$$

If $S(\lambda)$ is a radiometric quantity (e.g. spectral radiance), then with k = 683 lm/W the corresponding photometric quantity (in our case luminance) is received for Y. This is the proper use of these equations for *self luminous colours*. (For surface colours see Section 9.4.4.)

Unfortunately the X, Y, Z tristimulus values are not very easy to interpret and it is not very easy to "see" the colour they specify. As the luminance measure has been condensed into the Y tristimulus value, it seemed to be reasonable to transform from the X, Y, Z space into another space where Y is one of the co-ordinates and the other two are describing chromaticity. To do this the CIE introduced the chromaticity co-ordinates x, y, z and defined them in the following form:

$$x = \frac{X}{X+Y+Z}, \quad y = \frac{Y}{X+Y+Z}, \quad z = \frac{Z}{X+Y+Z} \qquad \ldots\ 9.24$$

As $x + y + z = 1$, it is enough to use two of the chromaticity co-ordinates to describe the chromaticity of the stimulus. It is usual to use x and y, and to plot the chromaticities in a *chromaticity diagram*. Figure 9.15 shows the CIE *x,y chromaticity diagram* with the spectrum locus, the equi-energetic stimulus and the CIE red, green and blue matching stimuli drawn in.

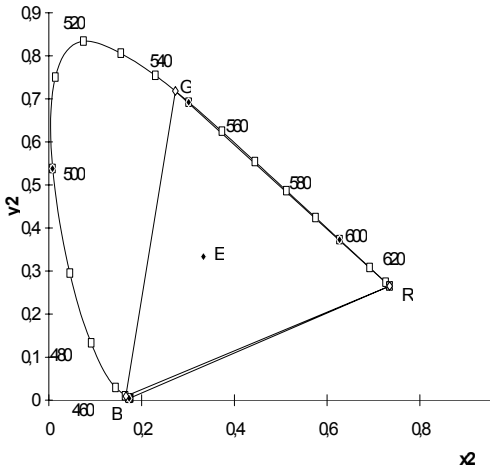

FIGURE 9.15 *xy*-chromaticity diagram with the spectrum locus, the equi-energetic stimulus (*E*) and the CIE 1931 **R,G,B** matching stimuli.

In the chromaticity diagram the chromaticity point of two additive mixed colours is located on the line joining the chromaticity points of the two constituent colours. The mixture of red and blue produces purple colours, and thus the two ends of the spectrum locus have been joined by a line, the purple boundary of the chromaticity chart. As seen, the triangle span by the **R, G, B** primaries covers only a part of the locus of the possible chromaticities, the area located within the boundaries of the spectrum locus and the purple boundary. Chromaticities outside the triangle can be matched with the **R, G, B** primaries only if one of the primaries is mixed with the test stimulus.

9.4.2.1.2 Alternative description of chromaticity

It is relatively easy to learn the approximate hue of a monochromatic light described by its wavelength. Thus it is convenient to use as one of the descriptors of a colour a wavelength related quantity. This is done in the chromaticity diagram in the following way: One assumes as reference an achromatic (*N* for neutral) chromaticity (often called the “white point"). Such a reference chromaticity could be the chromaticity of the equienergetic radiation, shown in Figure 9.15 by the point *E*. We will see that in practice many other reference points are possible, as e.g. the chromaticity of average day-light illumination. In Figure 9.16 *N* is such a reference point.

Let us first consider the chromaticity represented by point *C* and draw from point *N* a straight line through the chromaticity point of the test colour (point *C*) to the spectrum locus. The intersection of this line and the spectrum locus is shown in the figure by *DW*, the wavelength of the monochromatic radiation corresponding to this spectrum chromaticity is called dominant wavelength (λ_D).

If the test chromaticity is within the triangle set by the reference point *N* and the two end points of the spectrum locus, as shown by *C'*, then one uses the concept of the complementary wavelength, as shown by the point *CW* in the diagram. The concept of dominant wavelength is a first approximation for a correlate with hue. We will see later that constant dominant (or complementary) wavelength does not mean exactly constant hue.

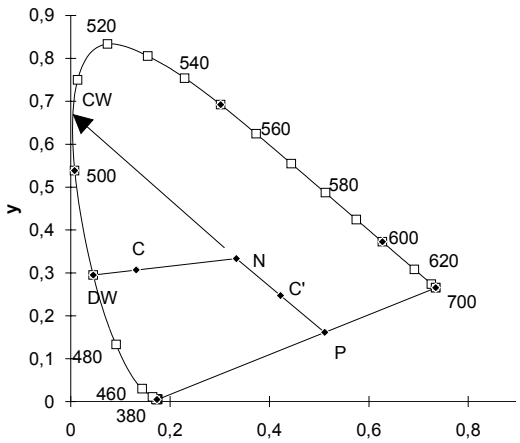

FIGURE 9.16 Concept of dominant wavelength, complementary wavelength and excitation purity in the *xy*-diagram.

As a second descriptor of chromaticity the concept of excitation purity is used: The ratio of the distance between the neutral point and the test colour ($\overline{NC}$) divided by the distance between the neutral point and the chromaticity point of the corresponding dominant wavelength ($\overline{ND}\,\overline{W}$). Point *DW* describes the chromaticity of maximum purity for the test colour *C*. In case of purple colours, the chromaticity point on the purple line where the line defining the complementary wavelength intersects the purple line is used as the chromaticity of maximum purity.

For chromaticity point *C:*

$p_e=(y_C - y_N)/(y_{DW} - y_N)$ or $p_e=(x_C - x_N)/(x_{DW} - x_N)$ ... 9.24

and for chromaticity point C':

$p_e=(y_{C'} - y_N)/(y_P - y_N)$ or $p_e=(x_{C'} - x_N)/(x_P - x_N)$ ... 9.25

Excitation purity is the first approximation to a correlate of saturation. Again, just as in case of dominant wavelength, this is only a very crude approximation, but helps to visualise some phenomena.

As to describe a colour stimulus, always three quantities are needed, alternative possibilities are to use

- *X, Y, Z* tristimulus values;
- *Y* tristimulus value (for a self luminous object a photometric quantity, e.g. luminance *L*) and the *x, y* chromaticity co-ordinates;
- *Y* tristimulus value (i.e. luminance: *L*), dominant (or complementary) wavelength λ_D and excitation purity p_e.

One should never forget that three quantities are needed to describe a colour, thus λ_D and p_e alone are not enough, a brightness correlate (e.g. luminance) is needed to get a full description.

9.4.2.1.3 The chromaticity of the additive mixture of two stimuli

If two colour stimuli are given, as e.g. the red and green phosphor primaries of a CRT display, the chromaticity of the additive mixture of the two stimuli can be calculated in the following way:

Let the tristimulus values of the red phosphor at maximum intensity setting be X_R, Y_R and Z_R, and those of the green phosphor: X_G, Y_G and Z_G. The corresponding chromaticity co-ordinates are: x_R, y_R, and x_G, y_G. In the mixture a_R amount of red and a_G amount of green light will be used. Thus the tristimulus values of the additive mixture will be:

$X = a_R X_R + a_G X_G$; $Y = a_R Y_R + a_G Y_G$; $Z = a_R Z_R + a_G Z_G$ ... 9.26

and the corresponding chromaticity co-ordinates:

$$x = \frac{a_R X_R + a_G X_G}{a_R (X_R + Y_R + Z_R) + a_G (X_G + Y_G + Z_G)}$$

$$y = \frac{a_R Y_R + a_G Y_G}{a_R (X_R + Y_R + Z_R) + a_G (X_G + Y_G + Z_G)}$$

... 9.27

Expressing the X_R, Y_R, Z_R, and X_G, Y_G, Z_G with the corresponding chromaticity co-ordinates and luminance values (Y_R and Y_G), the following equations are reached:

$$x = \frac{\frac{a_R Y_R x_R}{y_R} + \frac{a_G Y_G x_G}{y_G}}{\frac{a_R Y_R}{y_R} + \frac{a_G Y_G}{y_G}} \qquad \text{... 9.28}$$

$$y = \frac{a_R Y_R + a_G Y_G}{\frac{a_R Y_R}{y_R} + \frac{a_G Y_G}{y_G}}$$

here $a_R Y_R$ is the luminance of the amount of the red stimulus taken, and $a_G Y_G$ is the amount of the green stimulus used in the mixture. As seen, the chromaticity co-ordinates of the mixture are the luminance weighted averages of the two constituents. This is often called the centre of gravity law of colour mixture.

9.4.2.2. CIE 1964 Supplementary Standard Colorimetric Observer

As discussed in section 9.2.2 ´The human retina´, the central area of the retina is covered by the macula lutea or yellow spot. This yellow pigmentation functions as a colour filter and masks the real absorption spectra of the cone pigments. Owing to this, the colour matching functions differ if fields considerably larger than 2° are used for the colour matches.

In 1964 the CIE standardised another set of colour matching functions to be used "whenever more accurate correlation with visual colour matching of fields of larger angular subtense (more than 4° at the eye of the observer is desired"(22,23) based on the extensive work of Stiles and Burch (24, 25) as well as of Speranskaya (26), where the colour matches were performed in a 10° field.

It turned out that luminance is non-additive in this 10° field because in this larger field of view rod-vision also participates in the perceived brightness (termed rod-intrusion) and this participation depends on the intensity of the stimulus (at lower luminance levels rod intrusion becomes more important(27, 28), Because of this fact, this colorimetric system was not coupled with a photometric one. Otherwise the colorimetric system for the 10° observer was built up in the same form as that for the 2° observer. It is called the CIE 1964 Supplementary Standard Colorimetric Observer (sometimes termed also the 10° observer). The colour matching functions of the CIE 1964 Supplementary Standard Colorimetric Observer are distinguished from those of the CIE 1932 Standard Colorimetric Observer by a subscript 10. This subscript is used also for the tristimulus values and chromaticity co-ordinates calculated by using the 10° observer. Figure 9.17 shows the 10° colour matching functions, for comparison also the 2° colour matching functions are shown in this figure.

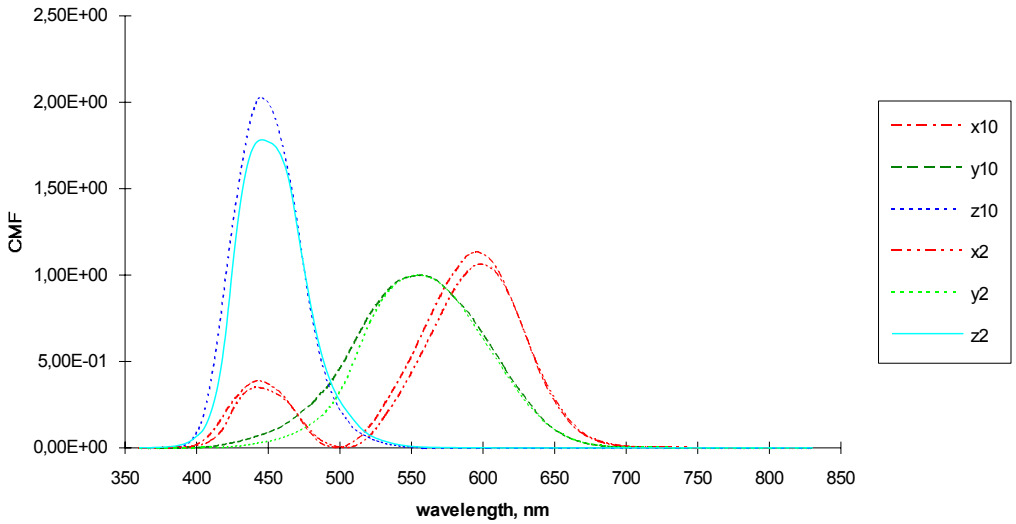

FIGURE 9.17 CIE 1932 2° and CIE 1964 10° colour matching functions.

Thus, in case of the 10° observer, equations similar to 9.23 are used:

$$X_{10} = k \int_{380\,\mathrm{nm}}^{780\,\mathrm{nm}} S_\lambda(\lambda)\bar{x}_{10}(\lambda)\mathrm{d}\lambda,$$

$$Y_{10} = k \int_{380\,\mathrm{nm}}^{780\,\mathrm{nm}} S_\lambda(\lambda)\bar{y}_{10}(\lambda)\mathrm{d}\lambda, \qquad \ldots\ 9.29$$

$$Z_{10} = k \int_{380\,\mathrm{nm}}^{780\,\mathrm{nm}} S_\lambda(\lambda)\bar{z}_{10}(\lambda)\mathrm{d}\lambda$$

where, however, the use of $k = 683$ lm/W is not recommended. In this case, for self-luminous stimuli $k = Y_{10}$ is used.

Chromaticity co-ordinates are reached in the same way as in the 2° system:

$$x_{10} = \frac{X_{10}}{X_{10} + Y_{10} + Z_{10}}, \quad y_{10} = \frac{Y_{10}}{X_{10} + Y_{10} + Z_{10}}, \quad z_{10} = \frac{Z_{10}}{X_{10} + Y_{10} + Z_{10}} \qquad 9.30$$

By using the x_{10}, y_{10} chromaticity co-ordinates an x_{10}, y_{10} chromaticity diagram can be built, the properties of which are similar to those of the 2° chromaticity diagram.

The CIE 1964 Supplementary Standard Colorimetric Observer is used if the colour patches to be matched are larger than 4° in diameter. It is important to realise that in a field of view as large as 5° to 10° the influence of rod vision (termed rod intrusion) cannot be neglected. Consequently the 10° observer should be used only if the light intensity is high enough so that rod intrusion can be neglected (CIE is at present (1995) working on a recommendation on this subject).

9.4.2.3. Small field colorimetry

It is well known that at visual angles below 1° the colour matching properties of the eye change again - the eye becomes more and more tritanopic. Although such small field colour matches are common in many modern applications of colorimetry, as e.g. in VDU colour graphics, there are no standards to describe the colour matches for field angles smaller than 2°. Photometric investigation have shown that the $V_M(\lambda)$ - function (29) describes the brightness of small fields well (30), but no extension to colorimetry has been officially agreed (CIE TC 1-36 is working on a recommendation that could be used down to a 1° visual angle).

9.4.3 Uniform chromaticity scales and their use in defining correlated colour temperature

Although the CIE x, y and x10, y10 chromaticity diagrams can be used to describe properties of colour stimuli, they suffer from the drawback that equal perceptual colour differences are at widely different distances in these diagrams. This drawback was recognised shortly after the introduction of the CIE 1931 colorimetric system, distances corresponding to 10 times the just perceptible colour differences in case of constant luminance are seen in Figure 9.18 (31).).

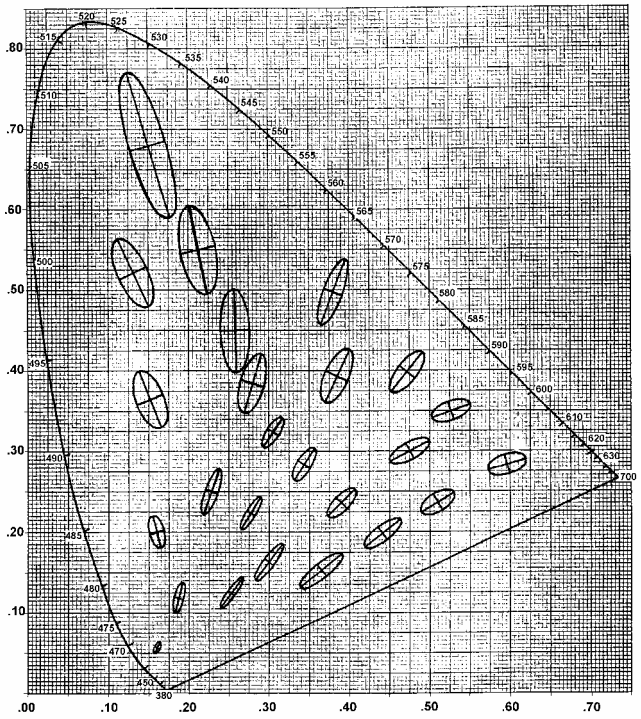

FIGURE 9.18 The CIE *x,y* diagram with ellipses representing small colour differences.

In a later paper Brown and MacAdam (32) extended these investigations to colours with different luminances. It has also been realised that colour space is not Euclidean, i.e. also a surface of constant luminance in this space will not be a two dimensional surface, and no projection exists that will transform this surface into a flat surface showing equal chromaticity differences as equal distances.

During the years many transformations have been tried to get to reasonably equidistant chromaticity scales. At present we use the CIE 1976 uniform chromaticity diagram, called also *u′, v′* diagram. The *u′, v′* co-ordinates are obtained from the x, y co-ordinates by the following equations:

$$u' = 4X / (X+15Y+3Z) = 4x / (-2x+12y+3) \quad \ldots 9.31$$

$$v' = 9Y / (X+15Y+3Z) = 9y / (-2x+12y+3)$$

In some applications still an older uniform chromaticity scale diagram(*u*, *v* diagram) is used, the co-ordinates of which can be calculated from the *u*', *v*' co-ordinates :

$$u = u' , \quad v = (2/3)v' \quad \ldots 9.32$$

Figure 9.19 shows the *u*', *v*' diagram with the location of the equienergetic stimulus S_n. The *u*', *v*' diagram can be used to define some correlates of colour perception. Let *C* be an arbitrary stimulus, a correlate of its hue in this diagram is the *CIE 1976 u,v hue-angle*

$$huv = \text{arctg}[(v' - v'n) / (u' - u'n)] = v^* / u^* \quad \ldots 9.33$$

here h_{uv} lies between 0° and 90° if both $u' - u'_n$ and $v' - v'_n$ are positive, between 90° and 180° if $v' - v'_n$ is positive and $u' - u'_n$ is negative, between 180° and 270° if both $v' - v'_n$ and $u' - u'_n$ are negative, and between 270° and 360° if $v' - v'_n$ is negative and $u' - u'_n$ is positive (for *u**, *v** see later).

The *CIE 1976 u,v saturation* is a correlate of the colour perception saturation:

$$suv = 13[(u' - u'n)^2 + (v' - v'n)^2]^{1/2} \quad \ldots 9.34$$

In Figure 9.19 S_n is shown as the location of the equienergetic stimulus, but it can be any other suitable neutral stimulus.

9.4.3.1 Colour temperature, correlated colour temperature and distribution temperature

We have seen that in a chromaticity diagram - for the purpose of defining a colorimetric system - the locus of the spectral stimuli and of the equienergetic stimulus are of particular importance. A further locus of special significance is the locus of the black body radiators.

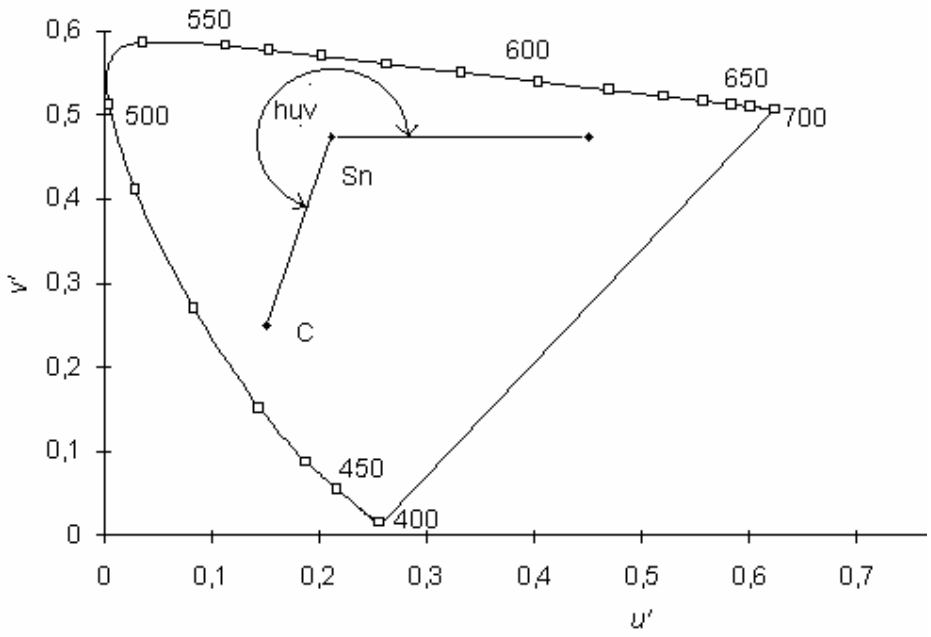

FIGURE 9.19 CIE 1976 u',v' diagram with the location of the equienergetic stimulus S_n, a colour stimulus C, shown are also the CIE 1976 u,v hue-angle h_{uv} and along the spectrum locus the location of some dominant wavelengths.

It is well-known that black bodies, or cavity radiators, called also Planckian- or full radiators are radiators where the spectral power distribution is defined by the absolute temperature (measured in K) of the cavity. Human eye experiences light reflected from an aselective surface (whose spectral radiance factor is near to unity and is wavelength independent) as "white" if irradiated by a full radiator the temperature of which is within approximately 2700 K and 20.000 K if no other clue of "white" light is in the field of vision. This wide range of "white" light sensation gives special significance to the chromaticity locus of full radiators.

The spectral power distribution of a full radiator can be calculated using Planck's formula:

$$Me = c1\lambda^{-5}[\exp(c2/\lambda T)-1]^{-1} \qquad \ldots\ 9.35$$

where as long as we deal only with chromaticities, i.e. with relative spectral power distributions, only the constant c_2 is of importance (see Sec. 9.4.4 on Surface colours):

$$c2 = 1{,}4388\text{x}10^{-2}\ \text{mK} \qquad \ldots\ 9.36$$

Figure 9.20 shows the loci of Planckian radiators in the x,y chromaticity diagram. It is convenient to describe the chromaticity of a full radiator by simply stating its temperature.

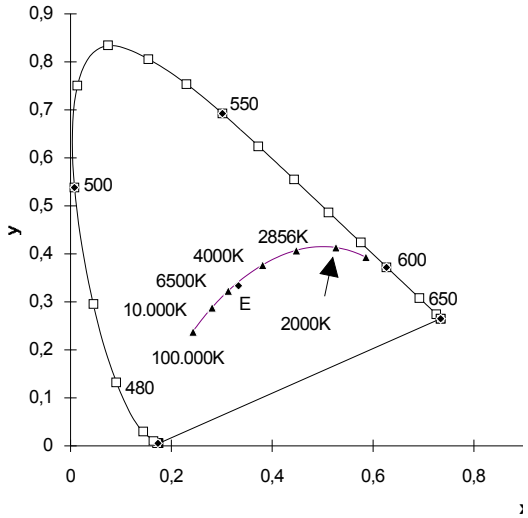

FIGURE 9.20 *x,y* diagram with locus of Planckian radiators.

As we have seen in discussing colour matches two colour stimuli are indistinguishable for the human eye if their tristimulus values are equal and they are seen under the same observational conditions. Thus lights of non Planckian distribution but with a chromaticity equal to that of a full radiator will evoke the same visual colour effect then a full radiator. (Colours of surfaces irradiated with the full radiator and the radiator with non Planckian spectral distribution might have different colour, this phenomenon will be described by *colour rendering*, see Section 4.4.x.) Due to this fact it is convenient to characterise these non-full radiators by stating the absolute temperature of the full radiator with the same chromaticity. This "temperature" is called *colour temperature*.

Sometimes the chromaticity of a radiator does not equal exactly with the chromaticity of a full radiator, but lies very near to it. Also in this case one would like to use the term colour temperature. To distinguish between the cases of exact colour match with a full radiator, and only an approximate one, one uses the term *correlated colour temperature* to describe the non-perfect match. At present the correlated colour temperature is defined as the temperature of that full radiator whose chromaticity approximates most closely the chromaticity of the test radiator in the CIE 1960 *u*,*v* chromaticity diagram (i.e. the two chromaticities have to lie on the line that is perpendicular to the tangent of the Planckian locus at the given point, on a so called *iso temperature line*:). Figure 9.21. shoes a section of the *x,y* diagram with some iso temperature lines (see (33)).); for the possibility to describe correlated colour temperature in the CIELUV and CIELAB spaces see (34, 35), for the calculation of correlated colour temperature (36-38).

A further terms used sometimes in colorimetry and photometry are the distribution temperature and ratio temperature.

Distribution temperature is the “temperature of the Planckian radiator whose relative spectral distribution $S_b(\lambda)$ is the same or nearly the same as that of the radiator considered ($S_t(\lambda)$ in the spectral range of interest”(39). Mathematically this means that the distribution temperature of a source in a given wavelength range, λ_1 to λ_2, is the

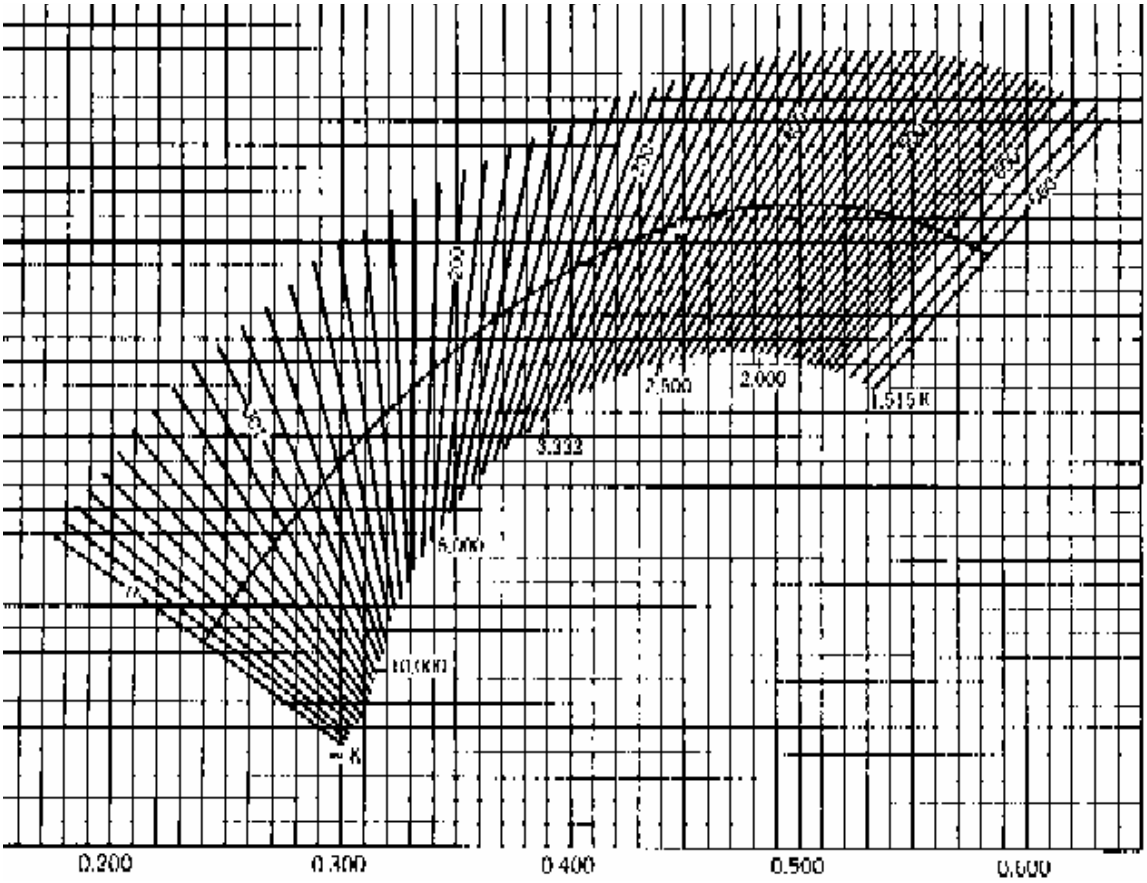

FIGURE 9.21 CIE 1931 x,y chromaticity diagram showing iso-temperature lines (after (33).

temperature T_D, of the Planckian radiator for which the following integral is minimised by adjusting of a and T:

$$\int_{\lambda_1}^{\lambda_2} \left[1 - S_t(\lambda) / a\, S_b(\lambda, T) \right]^2 d\lambda \qquad \ldots\ 9.37$$

for the expression of $S_b(\lambda)$ see equation 9.35 and 9.36; in colorimetry and photometry it is usual to select $\lambda_1 = 400$ nm and $\lambda_2 = 750$ nm.

The concept of T_D should be used only for an extended wavelength range as stated above and for radiation whose spectral distribution is a continuous function of wavelength in that range.

If the value of the distribution temperature has to be transferred from one incandescent lamp to an other one of the same type, the concept of *ratio temperature* might be used: Two irradiation measurements are made using narrow band filters near to 460 nm and 660 nm on the calibrated source and the ratio of the two readings is taken. Then the current and tension of the second lamp is adjusted till the same ratio reading is obtained. In this case the two lamps have the same ratio temperature and it is assumed that also their distribution temperature will be the same (for further details see 39, 40)).

9.4.4 Colorimetry of surface colours

9.4.4.1 Colorimetric properties of materials

The stimulus reaching the eye is usually radiation reflected by a surface, or radiation penetrating through a layer of material. These substances may modify the spectral power distribution of the radiation by reflection (specular and diffuse (see Chapter X Sec. xxy) or transmission. Let us assume an opaque surface. As discussed in Chapter X Sec. xxy such a surface can be characterised by its spectral radiance factor $\beta(\lambda)$. If this material surface is irradiated by a light source, the colour stimulus will be the radiation reflected back into the eye. Thus in equation 9.23 and 9.29 $S_\lambda \cdot \beta(\lambda)$ has to be written instead of S_λ :

$$X = k \int_{380\,\mathrm{nm}}^{780\,\mathrm{nm}} S(\lambda) \cdot \beta(\lambda) \cdot \bar{x}(\lambda)\mathrm{d}\lambda, \quad Y = k \int_{380\,\mathrm{nm}}^{780\,\mathrm{nm}} S(\lambda) \cdot \beta(\lambda) \cdot \bar{y}(\lambda)\mathrm{d}\lambda,$$

$$Z = k \int_{380\,\mathrm{nm}}^{780\,\mathrm{nm}} S(\lambda) \cdot \beta(\lambda) \cdot \bar{z}(\lambda)\mathrm{d}\lambda \qquad \ldots\ 9.38$$

here we used the symbol $S(\lambda)$ and not $S_\lambda(\lambda)$ to denote that not the absolute spectral power distribution is needed for the calculations. For characterising the colorimetric properties of the surface, we need only the relative spectral power distribution function. As discussed in Section 9.2.5.3 (see discussion on saturation) our mental picture of a coloured surface does not change with the level of illumination (within the limits of normal photopic vision, say 300 lx and 30.000 lx illumination). This is reflected in CIE colorimetry by the fact that in calculating the tristimulus values of surface colours only the relative spectral power distribution of the illuminant is used and the normalising constant k is calculated as:

$$k = \frac{1}{\int S(\lambda)\bar{y}(\lambda)\mathrm{d}\lambda} \qquad \ldots\ 9.39$$

i.e. the tristimulus values are normalised to the Y value of the illumination. Chromaticity co-ordinates, x, y and u', v', both for the 2° observer and the 10° observer are calculated exactly in the same way, as discussed in Sections 9.4.2 and 9.4.3 (see Equations 9.24, 9.30, 9.31):

$$x = \frac{X}{X+Y+Z}, \quad y = \frac{Y}{X+Y+Z}, \quad z = \frac{Z}{X+Y+Z}, \qquad \ldots\ 9.40$$

$$x_{10} = \frac{X_{10}}{X_{10}+Y_{10}+Z_{10}}, \quad y_{10} = \frac{Y_{10}}{X_{10}+Y_{10}+Z_{10}}, \quad z_{10} = \frac{Z_{10}}{X_{10}+Y_{10}+Z_{10}} \qquad 9.41$$

$$\mathrm{u}' = 4X / (X+15Y+3Z) = 4x / (-2x+12\mathrm{y}+3) \qquad \ldots\ 9.42$$

$$\mathrm{v}' = 9Y / (X+15Y+3Z) = 9y / (-2x+12\mathrm{y}+3)$$

and similarly for the 10 degree observer.

9.4.4.2 CIE Standard illuminants and sources

9.4.4.2.1 Standard illuminants

Equations 9.38 to 9.42 can be calculated by using any illuminant spectral distribution. The attained tristimulus values and chromaticity co-ordinates depend both of the reflectance characteristics of the material and the emission spectrum of the illuminant. Therefore, to be able to compare colorimetric characteristics of materials, it was necessary to agree on a smaller number of representative spectral distributions. This has been done by defining some spectral power distributions, called *illuminants.* These are described only with the tabulated values of the spectral power distribution and are used to calculate the tristimulus values and chromaticity co-ordinates. In order to perform visual observations, realisable sources are needed. These are called *standard sources*.

In 1931 the CIE standardised three illuminants and standard sources (in these definitions we give the temperature values as correct in the International Practical Temperature Scale of 1968):

- CIE Standard Illuminant A: An illuminant having the same relative spectral power distribution as a Planckian radiator at a temperature of 2856 K.
- CIE Standard Illuminant B: An illuminant having the relative spectral power distribution near to that of direct sunlight. (This illuminant is now obsolete.)
- CIE Standard Illuminant C: An illuminant representing average daylight with a correlated colour temperature of about 6800 K. (For the definition of correlated colour temperature see Section 9.4.3.1. This illuminant is now obsolete.)

A series of daylight illuminants were suggested in 1963 and standardised in 1967 (19, 41). The relative spectral power distribution of these illuminants can be calculated along the following lines:

First the correlated colour temperature of the daylight (D) has to be chosen: T_c. With this value of T_c one calculates the 1931 x_D chromaticity of the daylight:

- for correlated colour temperatures from approximately 4000 K to 7000K:

$$x_D = -4{,}6070\,\frac{10^9}{T_c^3} + 2{,}9678\,\frac{10^6}{T_c^2} + 0{,}09911\,\frac{10^3}{T_c} + 0{,}244063 \qquad \ldots\ 9.43$$

- for correlated colour temperatures from 7000K to approximately 25 000 K:

$$x_D = -2{,}0064\,\frac{10^9}{T_c^3} + 1{,}9018\,\frac{10^6}{T_c^2} + 0{,}24748\,\frac{10^3}{T_c} + 0{,}237040 \qquad \ldots\ 9.44$$

With known x_D value the y_D value can be obtained, and by the help of both the spectral power distribution of the Daylight illuminant can be calculated:

$$y_D = -3{,}000 x_D^2 + 2{,}870 x_D - 0{,}275 \qquad \ldots\ 9.45$$

and

$$S(\lambda) = S_0(\lambda) + M_1 S_1(\lambda) + M_2 S_2(\lambda) \qquad \ldots\ 9.46$$

where $S_0(\lambda)$, $S_1(\lambda)$, $S_2(\lambda)$ are functions of wavelength, λ, given in the table Appendix 9.1, and M_1, M_2 are factors whose values are related to the chromaticity co-ordinates x_D and y_D as follows:

$$M_1 = \frac{-1{,}3515 - 1{,}7703\,x_D + 5{,}9114\,y_D}{0{,}0241 + 0{,}2562\,x_D - 0{,}7341\,y_D} \qquad \text{... 9.47}$$

$$M_2 = \frac{0{,}0300 - 31{,}4424\,x_D + 30{,}0717\,y_D}{0{,}0241 + 0{,}2562\,x_D - 0{,}7341\,y_D}$$

Although based on this calculation procedure the relative spectral power distribution of any daylight illumination between 4000 K and 25 000 K can be calculated, for practical reasons it has been recommended to restrict the daylight illuminants used to a few illuminants. Besides *CIE Standard Illuminant A* now *CIE Standard Illuminant D65* is the other primary standard illuminant of colorimetry:

- *CIE Standard Illuminant D65*: An illuminant representing a phase of daylight with a correlated colour temperature of approximately 6504 K.

Note:

At the time of defining CIE Standard Illuminant A and preparing the definition how to calculate the daylight illuminant spectral power distribution, older versions of the International Practical Temperature Scale were valid. To keep the spectral power distributions unaltered, the assigned colour temperatures have been changed. In 1931 the temperature of that black-body whose spectrum equals that of Standard Illuminant A was 2848 K (The c_2 constant in Planck's equation, see Equation 9.35 was $1{,}4350 \cdot 10^{-2}$ m·K, now it is $1{,}4388 \cdot 10^{-2}$ m·K, see Equation 9.36, this brings the temperature of the of Standard Illuminant A on the present day International Practical Temperature Sale to 2856 K. Similar changes were necessary for the Daylight Illuminants (D_{65} had originally a correlated colour temperature of 6500 K, due to the change in the 1948 International Practical Temperature Scale as amended in 1960, with c_2 changing from $1{,}4380 \cdot 10^{-2}$ m·K to the 1968 value of c_2 = $1{,}4388 \cdot 10^{-2}$ m·K, the correlated colour temperature of illuminant D65 increased by the factor of 1,4388/1,4380, and due to this fact the originally defined spectral power distribution is now reached at T_c = 6504.

The CIE standardised the illuminants A and D_{65} (often written as D65) as its primary colorimetric illuminants and one of them should be used whenever possible. As secondary colorimetric standards the illuminants D50, D55 and D75 are recommended, having correlated colour temperatures of approximately 5000 K, 5500 K and 7500K. For all these illuminants the tabulated relative spectral power distribution values as reproduced in Appendix 9.2 are the official ones. Figure 9.22 shows the relative spectral power distribution of CIE Standard Illuminants A and D65.

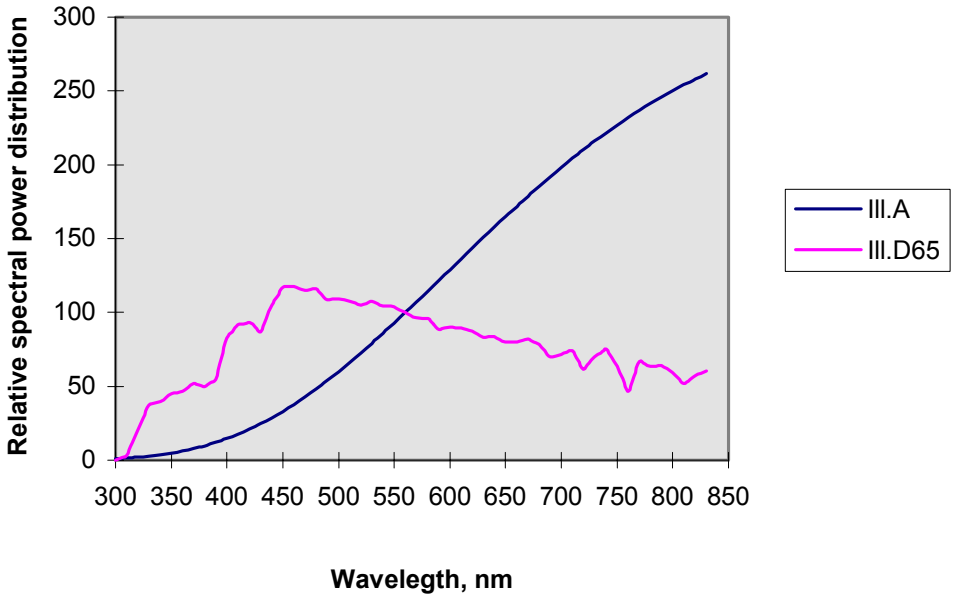

FIGURE 9.22 Relative spectral power distribution of CIE Standard Illuminants A and D65.

9.4.4.2.2 Standard sources

For practical colorimetry one needs sources with spectral power distribution corresponding to those of the standard illuminants. Illuminant A is to be realised by a gas-filled tungsten filament lamp operating at a correlated colour temperature of 2856 K. In the original definition a source corresponding to Illuminant C was also defined, where the Source A had to be filtered by two filter solutions (19). There is no recommendation for an artificial source to realise illuminant D65 or other D illuminants. Thus, in case of daylight sources we can speak only about *daylight simulators*.

9.4.4.2.3 Daylight simulators

CIE elaborated a method to assess the quality of D55, D65 and D75 daylight simulators (42), where the evaluation is done separately in the visible and in the ultraviolet range of the spectrum: For each of these standard illuminants, spectral radiance factor data are supplied for five nonfluorescent metameric sample pairs (see Section 9.4.4.5.2). The colorimetric differences of the five pairs are computed for the test illuminant; the average of these differences is taken as the visible range metamerism index and is used as a measure of the quality of the test illuminant as a simulator for nonfluorescent samples. For fluorescent samples (see Section 9.4.4.5.1), the quality is assessed in terms of an ultraviolet range metamerism index, defined as the average of the colorimetric differences computed with the test illuminant for three further pairs of samples, each pair consisting of a fluorescent and a nonfluorescent sample which are metameric under the standard illuminant. Test sources are then categorised by two letters, depending on the calculated metamerism indices for the

visible and UV ranges. Category letter A means excellent simulation, B is still very good, for C to E category sources the simulation becomes worse and worse. The CIE published also a computer program to calculate the visible and UV category classes (43).

During the years many attempts were made to build good daylight simulators (for a review of the subject see (44)). Practical needs call for two types of sources: those used in instruments (spectral or tri-stimulus) and those used in viewing booths, where test and reference samples are illuminated side by side and viewed visually. The still best laboratory instrument source uses a high pressure xenon arc lamp as source, and a three-fold light path with individual correction filters in each path (45, 46). Other commercial systems might use filtered xenon arc lamps or halogen incandescent lamps. It is usual to have a fine tuning possibility to adjust UV to visible radiation proportions. Liu and co-workers described an optimisation algorithm for designing D65 simulators (47). For viewing booth application, special fluorescent lamps are often used. Figure 9.23 shows the spectral power distribution of such a fluorescent lamp compared with illuminant D65. As seen, the spectral match is poor, mainly due to the mercury emission lines.

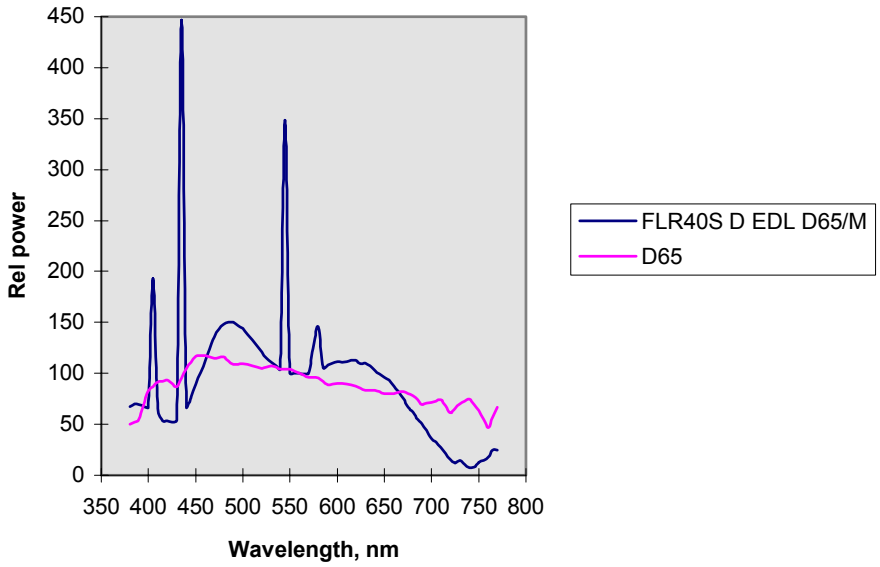

FIGURE 9.23 Relative spectral power distribution of illuminant D65 and of a fluorescent lamp built to simulate this illuminant.

9.4.4.2.4 Secondary standard illuminants and sources

Many practical lighting situations differ considerably from the standard incandescent light (Illuminant A) and daylight (D65) situations. Problems are encountered also if visual estimates are needed and no practical source is available. There is a considerable move among colorimetrists to standardise a realisable daylight spectral distribution, suggestions were made to accept filtered tungsten lamp light as indoor daylight (excluding the UV part of the emission) (48), and to standardise filtered Xe-lamp or fluorescent lamp light as approximations of D65 and D50 (49).

The spectra of 12 of representative fluorescent lamps have been published by the CIE (19) for the use when colours of surfaces have to be judged under different indoor lighting situations. Three of them should take priority whenever such problems occur. Figure 9.24 shows the relative spectral power distribution of these lamps. F2 is a standard fluorescent lamp of medium colour temperature, F7 is one of daylight colour temperature and broad band spectrum, while F11 comes nearest to modern so called “tree band” fluorescent lamps (such phosphors are now widely used in the modern small diameter compact fluorescent lamps).

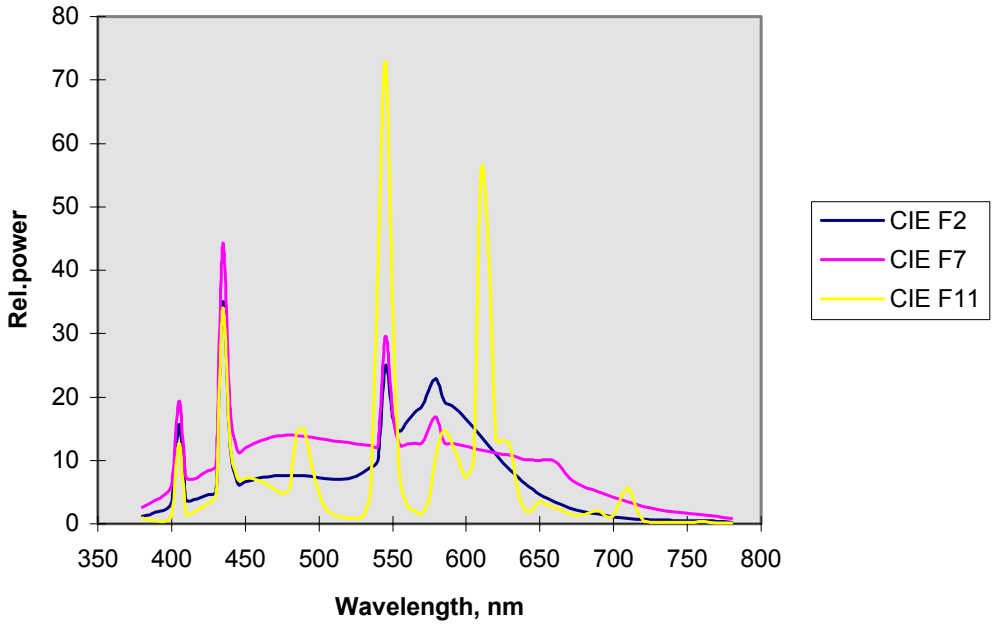

FIGURE 9.24 Relative spectral power distribution of three selected fluorescent lamps of 4230 K (F2), 6500 K (F7) and 4000 K (F11) correlated colour temperature.

9.4.4.3 Recommendations on surface colour measurement

9.4.4.3.1 Standard of reflectance factor

The perfect reflecting diffuser is recommended as the reference standard for surface colour measurement (19). It is defined as the ideal isotropic diffuser with a reflectance equal to unity.

For practical colorimetry we need material standards. The classical secondary reference reflectance factor standard is the pressed barium sulphate plate. It is prepared in using a special $BaSO_4$ press and high grade $BaSO_4$ powder. Pressed barium sulphate tablets can be made with reasonable reproducibility by using colorimetric grade powder. They show good diffuse reflectance characteristics (are Lambertian reflectors). The $BaSO_4$ plates are, however, highly fragile and have to be prepared fresh before use (maximum recommended shelf life 2 - 3 days.

In recent years the $BaSO_4$ secondary reflectance factor standards have been superseded by the so called "halon" white standards: This material is a

polyfluorinated resin. The raw material has to be pressed into a sample holder. A thickness of 5 mm is recommended, to assure perfect opacity. An ideal packing density is about 2,5 g cm^{-3} (50, 51). Such fluorocarbon samples, now commercially available under the trade mark 'SPECTRALON', are robust, can be used for a considerable time before replacement. Recently also coloured SPECTRALON samples have been produced.

Another class of secondary colour standards are the white and coloured ceramic and glazed tiles. These are very robust, can be cleaned relatively easily, but are usually glossy. They can be used only for checking the calibration stability of a colorimeter, or as a transfer standard if the two instruments have the same measuring geometry. Problems can also occur if the laboratory temperature changes, as many of the ceramic tiles are thermochromic, i.e. change their reflectance spectrum with temperature (see e.g. (52 - 54)).

9.4.4.3.2 Standard measuring geometry

As the reflection properties of average samples might differ considerably from those of an ideal standard, i.e. they are neither totally diffuse (Lambertian) nor are they reflecting only regularly (mirror like), at different locations and with different instruments reproducible measurements can only be achieved if the measuring geometry used is the same. The CIE standardised four measuring geometries(19): 45°/normal, normal/45°, diffuse/normal and normal/diffuse. Here the first angle description refers to irradiation, the second to observation:

Case a) 45°/normal (symbol: 45/0): The specimen is irradiated by one or more beams whose effective axes are at an angle of $45° \pm 2°$ from the normal to the specimen surface. The angle between the direction of viewing and the normal to the specimen should not exceed 10°. The angle between the axis and any ray of an irradiating beam should not exceed 8°. The same restriction should be observed in the viewing beam.

Case b) normal/45°(symbol: 0/45): The specimen is irradiated by a beam whose effective axis is at an angle not exceeding 10° from the normal to the specimen surface. The specimen is viewed at an angle of $45° \pm 2°$ from the normal to the specimen surface. The angle between the axis and any ray of the irradiating beam should not exceed 8°. The same restriction should be observed in the viewing beam.

Case c) diffuse/normal (symbol d/n): The specimen is irradiated diffusely by an integrating sphere. The angle between the normal to the specimen surface and the axis of the viewing beam should not exceed 10°. The integrating sphere may be of any diameter provided the total area of the ports does not exceed 10 percent of the internal reflecting sphere area. The angle between the axis and any ray of the viewing beam should not exceed 5°.

Case d) normal/diffuse (symbol: 0/d): The specimen is irradiated by a beam whose axis is at an angle not exceeding 10° from the normal to the specimen surface. The reflected flux is collected by means of an integrating sphere. The angle between the axis and any ray of the irradiating beam should not exceed 5°. The integrating sphere may be of any diameter provided the total area of the ports does not exceed 10 percent of the internal reflecting sphere area.

For the conditions 'diffuse/normal' and 'normal/diffuse' the regularly reflected component of specimens with mixed reflection may be excluded by the use of a gloss trap. If a gloss trap is used, details of its size, shape and position should be given.

In the 'normal/diffuse' condition the sample should not be measured with a strictly normal axis of irradiation if it is required to include the regular component of reflection. Similarly, in the 'diffuse/normal' condition the sample should not be measured with a strictly normal axis of view if it is required to include the regular component of reflection.

Case a), b) and c) give values of reflectance factor, $R(\lambda)$. For directional viewing with a sufficiently small angular spread, these reflectance factors become identical to radiance factors. For case d), for viewing with an integrating sphere, in ideal case the reflectance is measured. Thus, in the limit, the '45/0' condition gives the radiance factor $\beta_{45/0}$; the '0/45' condition gives the radiance factor $\beta_{0/45}$; the 'd/0' condition gives the radiance factor $\beta_{d/0}$; and the 'o/d' condition gives the reflectance ρ.

9.4.4.4 Colour space and colour difference

One could build a colour space by plotting e.g. the *X, Y, Z* tristimulus values or the *x,y* chromaticity co-ordinates and the *Y* tristimulus value in a rectangular co-ordinate system. As seen in Section 9.4.3, in such a representation the colour differences in different parts of the colour space would be very unequal. During the past decades several attempts were made to transform the *Y,x,y* system into a colour space that is more even. Owing to the fact that there was no single new colour spaces that was really much superior to all others, in 1976 the CIE standardised two alternative spaces as interim solution to reach international agreement of usage.

9.4.4.4.1 CIE Colour spaces (19)

*CIE 1976 (L*u*v*) — CIELUV colour space*

This space builds on the uniform chromaticity scale described in Section 9.4.3. It is a three-dimensional, approximately uniform, colour space produced by plotting in rectangular co-ordinates *L*, u*, v** quantities defined by:

$$L^* = 116\,(Y/Y_n)^{1/3} - 16 \quad \text{for } Y/Y_n > 0{,}008856$$
$$u^* = 13\,L^*\,(u' - u_n') \qquad \text{... 9.48}$$
$$v^* = 13\,L^*\,(v' - v_n')$$

where *Y, u', v'* describe the colour stimulus considered and Y_n , u_n', v_n' describe the specified white object colour stimulus, i.e. the stimulus that would be produced if the illuminant illuminated the ideal perfect reflecting diffuser (in practice this is the stimulus produced by the illuminating source).

In Section 9.2.5.3 we have mentioned that our mental picture of a colour can be described by the dimensions of lightness, saturation, chroma and hue. In the CIELUV system the following approximate correlates have been defined:

CIE 1976 lightness:

$$L^* = 116\,(Y/Y_n)^{1/3} - 16 \quad \text{for} \quad Y/Y_n > 0{,}008856 \qquad \text{... 9.49}$$

CIE 1976 u, v saturation

$$s_{uv} = 13\,[(u' - u_n')^2 + (v' - v_n')^2]^{1/2} \quad \ldots\ 9.50$$

CIE 1976 u, v chroma

$$C_{uv}^* = (u^{*2} + v^{*2})^{1/2} = L^* s_{uv} \quad \ldots\ 9.51$$

CIE 1976 u,v hue-angle

$$h_{uv} = \arctan\,[(v' - v_n') / (u' - u_n')] = \arctan\,(v^*/u^*) \quad \ldots\ 9.52$$

*CIE 1976 (L*a*b*) — CIELAB colour space*

This is another approximately uniform colour space produced by plotting in rectangular co-ordinates L^*, a^*, b^* quantities defined by the equations:

$$L^* = 116\,(Y/Y_n)^{1/3} - 16$$

$$a^* = 500\,[(X/X_n)^{1/3} - (Y/Y_n)^{1/3}] \quad \ldots\ 9.53$$

$$b^* = 200\,[(Y/Y_n)^{1/3} - (Z/Z_n)^{1/3}]$$

where

$$X/X_n > 0{,}008856;\ Y/Y_n > 0{,}008856;\ Z/Z_n > 0{,}008856. \quad \ldots\ 9.54$$

and X, Y, Z describe the colour stimulus considered, and X_n, Y_n, Z_n describe the specified white object colour stimulus.

Similarly to the CIELUV system, attributes corresponding to the perceived lightness, chroma and hue have been defined (no correlate of saturation is possible in this system as it has no chromaticity diagram):

*CIE 1976 lightness (*this is the as in the CIELUV system):

$$L^* = 116\,(Y/Y_n)^{1/3} - 16 \quad \text{for} \quad Y/Y_n > 0{,}008856 \quad \ldots\ 9.49$$

CIE 1976 a, b chroma

$$C_{uv}^* = (a^{*2} + b^{*2})^{1/2} \quad \ldots\ 9.55$$

CIE 1976 a, b hue-angle

$$h_{uv} = \arctan\,(b^*/a^*) \quad \ldots\ 9.56$$

Note:

Both in the equations for L^* and in those for a^* and b^* a modified formula can be used if $X/X_n < 0{,}008856$, or $Y/Y_n < 0{,}008856$, or $Z/Z_n < 0{,}008856$:

$$L^* = 903{,}3\,(Y/Y_n) \quad \text{for } Y/Y_n \le 0{,}008856 \quad \ldots\ 9.57$$

and

$$a^* = 500\,[f(X/X_n) - f(Y/Y_n)] \quad \ldots\ 9.58$$

$$b^* = 500\,[f(Y/Y_n) - f(Z/Z_n)]$$

where

$$f(X/X_n) = 7{,}787\,(X/X_n) + 16/116 \quad \text{for} \quad X/X_n \le 0{,}008856$$

$$f(Y/Y_n) = 7{,}787\,(Y/Y_n) + 16/116 \quad \text{for} \quad Y/Y_n \le 0{,}008856 \quad \ldots\ 9.59$$

$$f(Z/Z_n) = 7{,}787\ (Z/Z_n) + 16/116 \quad \text{for} \quad Z/Z_n \leq 0{,}008856$$

For further specification details see the original CIE publication (19).

9.4.4.4.2 CIE colour difference specifications

Both in CIELUV and in CIELAB spaces the colour difference between two stimuli can be calculated as the vector difference between the *L*, u*, v** or the *L*, a*, b** co-ordinates:

$$\Delta E_{uv}^* = [(\Delta L^*)^2 + (\Delta u^*)^2 + (\Delta v^*)^2\ ]^{1/2} \quad \ldots\ 9.57$$

and

$$\Delta E_{ab}^* = [(\Delta L^*)^2 + (\Delta a^*)^2 + (\Delta b^*)^2\ ]^{1/2} \quad \ldots\ 9.58$$

In both cases also a lightness ($\Delta L^* = L^*_1 - L^*_2$), a chroma ($\Delta C^* = C^*_1 - C^*_2$) and a hue-difference can be defined. This latter is done as the colour difference minus the sum of the lightness and chroma differences:

CIE 1976 u, v hue-difference

$$\Delta H_{uv}^* = [(\Delta E_{uv}^*)^2 - (\Delta L^*)^2 - (\Delta C^*_{uv})^2]^{1/2} \quad \ldots\ 9.59$$

CIE 1976 a, b hue-difference

$$\Delta H_{ab}^* = [(\Delta E_{ab}^*)^2 - (\Delta L^*)^2 - (\Delta C^*_{ab})^2]^{1/2} \quad \ldots\ 9.60$$

As neither the CIELUV nor the CIELAB colour spaces are perfectly equidistant, the calculated colour difference will not correspond to the perceived one well enough. Research continued after 1976 to reach to a better colour difference formula, both for threshold data (i.e. just perceptible colour differences) and acceptability data (industrial permissible colour differences between standard and test batch).

Among the many suggested modifications of the CIE formulae the most successful was the so-called CMC formula, adopted among others by the ISO Textile Committee to evaluate industrial colour differences(55). It has been also established that perceived colour differences depend on the individual colour vision of the observer, the viewing situation (colour and lightness of background, size of samples, distance between the samples compared, etc.), , texture of the sample, luminance of the sample, etc. (56).

— *CIE 1994 (ΔL^*, ΔC^*_{ab}, ΔH^*_{ab}) colour-difference model (CIE94):*

Based on above consideration, the CIE recommended in 1995 a new colour difference formula, called CIE 1994 colour difference, ΔE^*_{94} (57) as an extension of the CIELAB formula:

$$\Delta E_{94}^* = \left[\left(\frac{\Delta L^*}{k_L S_L} \right)^2 + \left(\frac{\Delta C^*_{ab}}{k_C S_C} \right)^2 \left(\frac{\Delta H^*_{ab}}{k_H S_H} \right)^2 \right]^{1/2} \quad \ldots\ 9.61$$

where ΔL^*, ΔC^*_{ab}, ΔH^*_{ab} are the lightness, chroma and hue differences (see Equation 9.60).

The S_L, S_C and S_H *weighting functions* adjust the total colour-difference to account for variation in perceived colour-difference with variation in the colour standard location in CIELAB colour space. Experiments have shown that increasing chroma of the standard results in decreased chroma and hue difference (58, 59). Current best estimates are:

$$S_L = 1; \qquad S_C = 1 + 0{,}045\ C^*_{ab}; \qquad S_H = 1 + 0{,}015\ C^*_{ab} \qquad \ldots\ 9.62$$

where C^*_{ab} is the chroma of the standard. A Note in the CIE report states that when neither member of the colour-difference pair can logically be assigned as standard, their mean chroma $(C^*_{ab,1} \cdot C^*_{ab,2})^{1/2}$ might be used in the calculation.

The k_L, k_C and k_H are *parametric factors* and are thought to correct for variation in experimental conditions from the defined reference conditions, for which

$$k_L = k_C = k_H = 1 \qquad \ldots\ 9.63$$

In the textile industry it is common practice to use:

$$k_L = 2;\ k_C = k_H = 1 \qquad \ldots\ 9.64$$

A test of the new formula is described in (60).

The *reference conditions* are summarised in the CIE report as:

- Illumination: source simulating the spectral relative irradiance of CIE Standard Illuminant D65.
- Illuminance: 1000 lux.
- Observer: normal colour vision.
- Background field: uniform, neutral grey with $L^* = 50$.
- Viewing mode: object.
- Sample size: larger than 4 degrees subtended visual angle.
- Sample separation: minimum sample separation achieved by placing the sample pair in direct edge contact.
- Sample colour-difference magnitude: = to 5 CIELAB units.

Sample structure: homogeneous colour without visually apparent pattern or nonuniformity."

This enumeration presents at the same time toe most important factors, where for a deviation from the reference condition a parametric factor could be introduced. Up to now no such factors have been recommended, excepting the mentioned practice of textile industry (where at present the CMC formula is still prevailing).

9.4.4.5 Further recommendations on surface colour measurement

9.4.4.5.1 Metamerism

It can happen that two stimuli have different spectral distribution but their tristimulus values are identical. Such stimuli are called to be *metameric* (in contrast to a metameric match, if the two stimuli have identical spectral distribution, they are called non-metameric matches). Figure 9.25 shows the reflectance spectra (spectral radiance factors) of two samples that are metameric if illuminated with CIE Standard Illuminant D65 and observed with the CIE 1964 Supplementary Standard Observer

(they are two samples used in calculating the visible goodness of fit of a D65 simulator, see Section 9.4.4.2.3 (42).

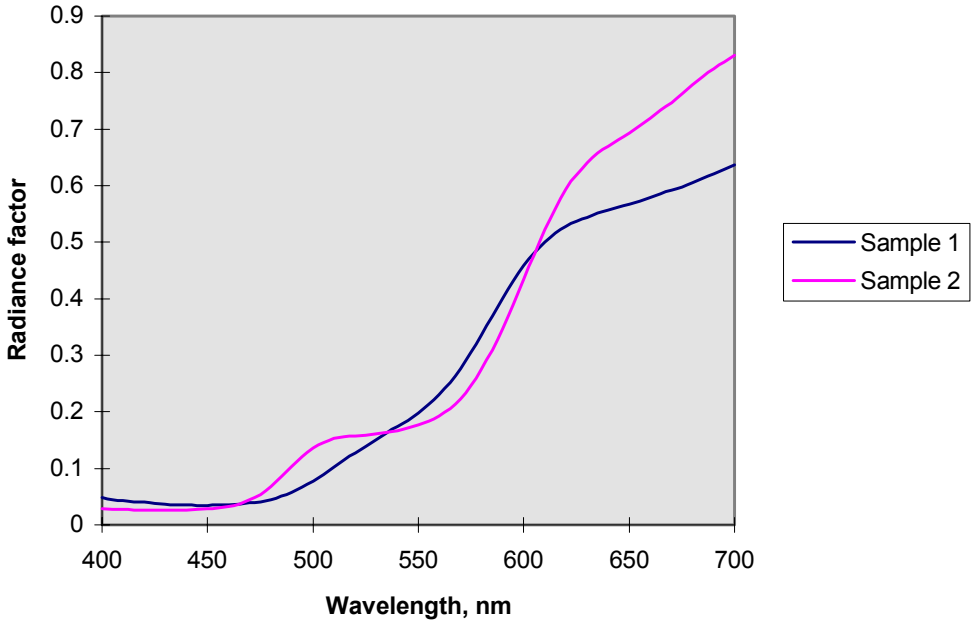

FIGURE 9.25 Spectral radiance factor of two metameric reflecting samples (for D65 and CIE 1964 Observer).

The tristimulus values are defined by equations 9.38. Two material samples having spectral radiance factors: $\beta_1(\lambda)$ and $\beta_2(\lambda)$ are metameric under illuminant *m* and observer *n* if for

$$T_{i,1} = k \int_{380nm}^{780nm} S_{\lambda,m}\beta_1(\lambda)\bar{t}_{i.n}(\lambda) \quad \text{and} \quad T_{i,2} = k \int_{380nm}^{780nm} S_{\lambda,m}\beta_2(\lambda)\bar{t}_{i.n}(\lambda)$$

it holds that $T_{i,1} = T_{i,2}$ ... 9.65

where $T_{1,1} = X_1$, $T_{2,1} = Y_1$, ..., $\bar{t}_{3,2} = \bar{z}_2$

If another illuminant is used, or an observer looks at the samples whose spectral sensitivities deviate from the standard curves, the two stimuli will not match. We describe the mismatch under the test source or the deviate observer by the help of the observed colour-difference.

In practice we distinguish two special metamerism indices: change in illuminant and change in observer.

The *special metamerism index: change in illuminant* (19) is obtained for two specimens ($\beta_1(\lambda)$ and $\beta_2(\lambda)$) whose tristimulus values are identical for one illuminant (usually D65 is used as reference illuminant) but differ for a test illuminant. Suitable test illuminants are CIE Standard Illuminant A or one of the F illuminants discussed in Section 9.4.4.2.4. (Practical application has to show which test illuminant is most suitable: if the question is whether the two samples look very different or not both

under daylight and tungsten light, then D65 reference and A test illuminant will be suitable, if comparison has to be made under industrial or commercial lighting, then probably one of the F illuminants will be more suitable).

The measure of the metamerism index is the ΔE^* colour difference calculated using either CIELAB or CIELUV colour-difference equation (Equation 9.57 or 9.58), and either the 2° or the 10° standard observer (see Sections 9.4.2.1 and 9.4.2.2), depending on the practical situation.

The *special metamerism index: change in observer* is based on similar calculations (61): Four deviate observers have been defined. First one calculates the colour-difference using the Standard Observer (CIE 1931 or 1964) and the Deviate Observer in equation 6.95. This supplies a metamerism index. All four deviate observer spectra are used to determine a range of mismatches from which an ellipse showing the range of mismatches is calculated.

Recent investigations have shown (62 - 64) that while the illuminant metamerism index is well established and widely used in industry, the observer metamerism index needs further re-formulation.

9.4.4.5.2 Whiteness

Whiteness is a psychometric quantity. Whiteness percept is experienced in a rather large part of the chromaticity diagram, and one is able to scale the three dimensional colour space — with reasonable accuracy — into a one dimensional whiteness scale. The presently used whiteness scale was developed (see (65 - 68)) and standardised by the CIE (19) in the mid seventies.

The CIE whiteness descriptor consists of a whiteness scale and a tint formula describing greenishness or reddishness:

$$W = Y + 800(x_n - x) + 1700(y_n - y) \quad \ldots\ 9.66$$

where W is the whiteness descriptor, Y is the Y-tristimulus value of the sample, x, y are the chromaticity co-ordinates of the sample, x_n, y_n are the chromaticity co-ordinates of the perfect diffuser. A higher W value means greater whiteness. The whiteness formula can be used both with the CIE 1931 and the CIE 1964 Standard Colorimetric Observer.

The tint formula is different for the 2° and the 10° Observers:

$$T_W = 1000(x_n - x) - 650(y_n - y) \quad \ldots\ 9.67$$

and

$$T_{W,10} = 900(x_{n,10} - x_{10}) - 650(y_{n,10} - y_{10}) \quad \ldots\ 9.68$$

A more positive T_W or $T_{W,10}$ value indicates greater greenishness, a more negative value indicates more reddishness.

The use of the whiteness and tint formulae is restricted to the range:

$$40 < T_W < 5Y\text{-}280 \text{ and } -3 < T_W < +3 \quad \ldots\ 9.69$$

both for the 2° and the 10° Observers.

Above scales are non-linear, thus equal whiteness- or tint-scale differences do not mean perceptually equal whiteness or tint differences.

Ganz and co-workers (69) have recently described a method how the whiteness and tint scale-values can be visualised in the CIELAB colour space.

9.4.5 Colorimetry of sources

9.4.5.1 Chromatic adaptation

In Section 9.3.3 we have already discussed that the human visual organ has the peculiar capability to adjust itself to the chromaticity of the illumination, thus e.g. a white paper is perceived as white when seen both under incandescent light and daylight. This faculty of the visual system is called chromatic adaptation. For its mathematical description many attempts were made during the past century.

The theory and method to describe chromatic adaptation postulated by von Kries is one of the best-known and widely applied methods although it has many flaws and can be regarded only as a first approximate description of the phenomenon.

The von Kries hypothesis assumes that the L-, M-, S- cone sensitivity functions (see Section 9.2.2) show in a non excited state given sensitivities, so that one can assign to their relative sensitivity unity coefficients. The stimulation of the retina will produce a new equilibrium between the non-bleached/bleached amount of the three photopigments, leading to a new state of the relative sensitivity of the three cone types. According to von Kries hypothesis, to reach the new equilibrium, the sensitivities of those cone-types that were more strongly excited have to be multiplied by a coefficient smaller than one. In a photographic film the three film sensitivities are in a fixed relationship. If the film has been designed for daylight exposures and one uses it in tungsten light, the abundance of long wavelength radiation in the incandescent light produces a reddish-yellowish haze. The human visual system counteracts the development of this haze by turning the long- and medium wave sensitive cones to a lower sensitivity state.

For complete chromatic adaptation one assumes that a reference white surface will be seen white both under the test and reference light. Let us denote the cone responses for the white surface for the test illuminant by $L_{w,t}$, $M_{w,t}$, $S_{w,t}$ and for the reference illuminant by $L_{w,r}$, $M_{w,r}$, $S_{w,r}$. The cone responses for a chromatic stimulus will be: L_t, M_t, S_t and L_r, M_r, S_r, respectively. The visual signal under the test light source will depend on the $L_t/ L_{w,t}$, $M_t/ M_{w,t}$, $S_t/ S_{w,t}$ ratios, and similarly for the reference conditions.

We are seeking the cone signals of that stimulus that produces the same colour percept under the reference illuminant as the stimulus with the L_t, M_t, S_t cone responses produced under the test source, it is necessary that for both states of adaptation the white reduced visual signals should be equal:

$$L_t/ L_{w,t} = L_r/ L_{w,r}, \quad M_t/ M_{w,t} = M_r/ M_{w,r}, S_t/ S_{w,t} = S_r/ S_{w,r} \quad ... \ 9.70$$

Thus the *corresponding colour stimulus* under the reference conditions will be

$$L_r = L_t \cdot(L_{w,r} / L_{w,t}), \quad M_t = M_r \cdot (M_{w,r} /M_{w,t}), \quad S_t = S_r \cdot(S_{w,r} /S_{w,t}) ... \ 9.71$$

here $L_{w,r} / L_{w,t}$, $M_{w,r} /M_{w,t}$, $S_{w,r} /S_{w,t}$ are the von Kries coefficients that scale the cone sensitivities in such a form that irrespective of the chromaticity of the illuminant the white point stays constant. This is only approximately the case in practice.

To answer the question what the tristimulus values of a colour stimulus will be under the reference light source (X_r, Y_r, Z_r,) if its tristimulus values under the test light

source are X_t Y_t, Z_t, first the X_r, Y_r, Z_r, and the corresponding achromatic stimulus (white point) tristimulus values have to be transformed into the *LMS* space. This is a similar transformation to that described in Section 9.4.2.1, when we transformed from the *RGB* space into the *XYZ* one (see equation 9.18). The coefficients of the matrix transformation depend on the chosen *L, M, S* primaries. The chromatic adaptation transformation procedure recommended by the CIE (70) uses the slightly modified transformation proposed by Hunt and Pointer (71):

$$\begin{vmatrix} L \\ M \\ S \end{vmatrix} = \begin{vmatrix} 0{,}40024 & 0{,}70760 & -0{,}08081 \\ -0{,}22630 & 1{,}16532 & 0{,}04570 \\ 0 & 0 & 0{,}91822 \end{vmatrix} \bullet \begin{vmatrix} X \\ Y \\ Z \end{vmatrix} \qquad \ldots \ 9.72$$

Earlier transformations (e.g. (72) were based on other assumptions regarding the most probable form of the *LMS* primaries, which lead to somewhat different numerical results (see CIE method of colour rendering calculation (73)).

To be able to determine the $L_{w,r}$ / $L_{w,t}$, $M_{w,r}$ /$M_{w,t}$, $S_{w,r}$ /$S_{w,t}$ coefficients, this transformation has to be performed first for the achromatic stimuli under both illuminants and for the test stimulus (X_t Y_t, Z_t,). Then the cone excitations for the corresponding colour can be determined by using Equation 9.71. To reach the *X, Y, Z* tristimulus values of the corresponding colour the matrix transformation uses the inverse matrix of 9.72:

$$\begin{vmatrix} X \\ Y \\ Z \end{vmatrix} = \begin{vmatrix} 1{,}85995 & -1{,}12939 & 0{,}21990 \\ 0{,}36119 & 0{,}63881 & 0 \\ 0 & 0 & 1{,}08906 \end{vmatrix} \bullet \begin{vmatrix} L \\ M \\ S \end{vmatrix} \qquad \ldots \ 9.73$$

The present CIE recommendation (70) applies a non-linear formula instead of the simple von Kries coefficient law (for details see the original publication and the papers by Nayatani and co-workers that led to this recommendation (74, 75)).

9.4.5.2 Colour rendering

Light source colour is described by stating the chromaticity of the emitted light or the corresponding correlated colour temperature (CCT), see Section 9.4.3.1. As general purpose light sources are used to illuminate objects, beside the light source colour (or lamp colour) also the colour appearance of the illuminated objects is of importance. This is done by comparing the appearance of the object colours with that as seen when illuminated by a reference illuminant.

The basic idea behind the presently used colour rendering index calculation method(73) is that we assume that colours are seen “natural” if illuminated by daylight or by black-body radiation. The colour of the objects illuminated by the test lamp and by the selected reference illuminant is the compared and the colour differences calculated. From these colour differences the colour rendering indices for the each test colour sample (selected object colour) are calculated. The average of some of these *special colour rendering indices* provides the *general colour rendering index*.

Figure 9.26 shows the flow chart of calculating the colour rendering indices. First the correlated colour temperature of the test lamp has to be determined (see Section

9.4.3.1), based on this result a reference illuminant is chosen: for a CCT below 5000 K the black-body with equal CCT has to be selected, above 5000 K a daylight phase with equal CCT is taken. The small remaining chromaticity difference between the test lamp and reference illuminant chromaticity is corrected by a von Kries type chromatic adaptation transformation (see Section 9,4.5.1).

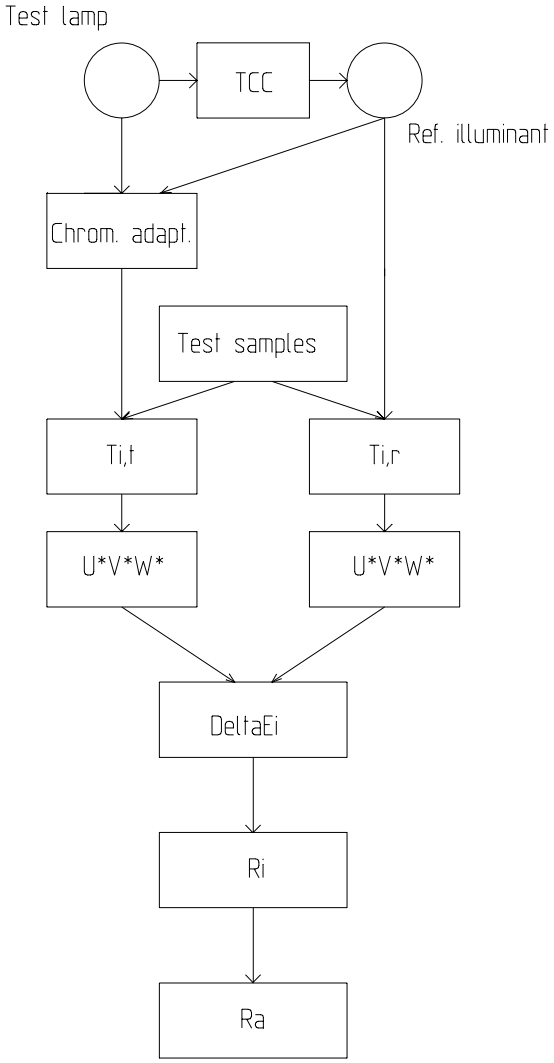

FIGURE 9.26 Flow chart for calculating colour rendering indices.

The next step is to select representative test colour samples. The CIE test method uses eight less saturated Munsell (see Section 9.5.1) samples of medium lightness spanning the colour gamut of general purpose object colours, and six further test samples, partly highly saturated, partly representative of often encountered object colours, as e.g. human complexion and leaf green. Then the tristimulus values for all 14 test samples are then calculated both for the test lamp and the reference illuminant ($T_{i,\mathrm{t}}$ and $T_{i,\mathrm{r}}$, using the terminology of equation 9.65, where i refers to the test sample).

At the time the CIE test method for colour rendering calculation was elaborated, an older transformation into an approximately equidistant colour space (the so-called U^*, V^*, W^* space) was used. This is still used to perform these calculations. In this space colour differences are calculated in the same form as shown in Equation 9.58, only the ΔU^*, ΔV^*, ΔW^* quantities are used.

The ΔE colour difference will be zero if the colours under the test lamp are rendered exactly as under the reference illuminant. It was thought that in this case the colour rendering index should be equal to 100. The scale was so devised that one of the most common fluorescent lamps of those days, the so-called warm white lamp, should have a general colour rendering index (see below) of approximately 50. Based on these principles the *special colour rendering index* formula is as follows:

$$R_i = 100 - 4{,}6 \cdot \Delta E_i \qquad \ldots\ 9.74$$

The general colour rendering index is calculated from the first eight R_i values as their arithmetic mean:

$$R_a = \frac{1}{8}\sum_{i=1}^{8} R_i \qquad \ldots 9.75$$

At present the CIE is working on updating the colour rendering index calculation method. Most probably first an update to the now accepted chromatic adaptation transformation (70) and colour difference calculation (57) will take place, the final goal is the use an accepted colour appearance model (see Section 9.5.2) to describe colour rendering.

9.5 FURTHER QUESTION OF COLORIMETRY

In the previous section we summarised the most important colorimetric rules and procedures where international agreement exists. There are two major items where there is yet no international consensus, but where the concepts are used widely and where very active research is going on. These items are the colour order systems, coupled to them is the question of colour atlases, and the colour appearance models. In this section a short overview of these problems of colorimetry will be presented.

9.5.1 Colour order systems

During the centuries many artists and scientists tried to systematise colours. One of the first colour solid devised along the lines of colour perception (see Section 9.2.5.3) is the Forsius colour solid (76). Owing to limited space we will not be able to discuss here items like Newton's or Goethe's colour circle, the many trials to devise from pigment mixtures colour order systems — and related colour atlases. We will concentrate on the two system used most often at present, the Munsell and the NCS system, and will mention shortly a few other systems that are also in use.

9.5.1.1 Munsell system

Munsell, an artist, started with the development of a colour notation system in 1905 (see(77), which was followed by the first collection of samples, the Atlas of the Munsell Colour System in 1915. The system was developed in a number of steps leading up to the Optical Society of America Munsell Renotation System in 1943 (78).

The Munsell system is built along the three perceptual quantities: hue, chroma (describing saturation) and value (describing lightness). Figure 9.27 shows the schematic structure of the Munsell system.

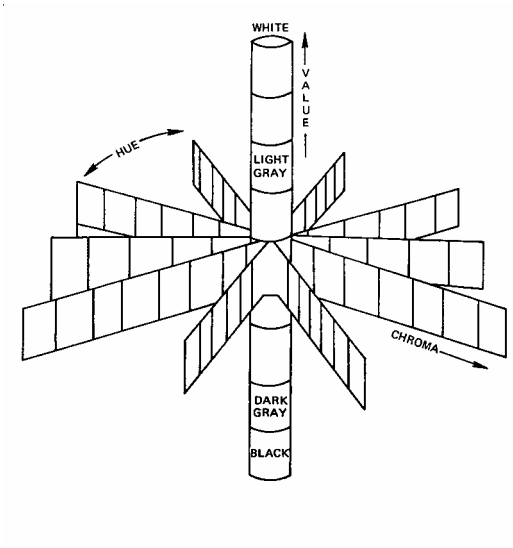

FIGURE 9.27 Schematic view of the Munsell system., after Hunter (79).

The hue circle is devided into five major steps, Yellow (*Y*), Red (*R*), Purple (*P*), Blue (*B*), Green (*G*), and its intermediate steps, *YR, RP, PB, BG GY*. Every such step is further subdivided into 10 substeps, see Figure 9.58.

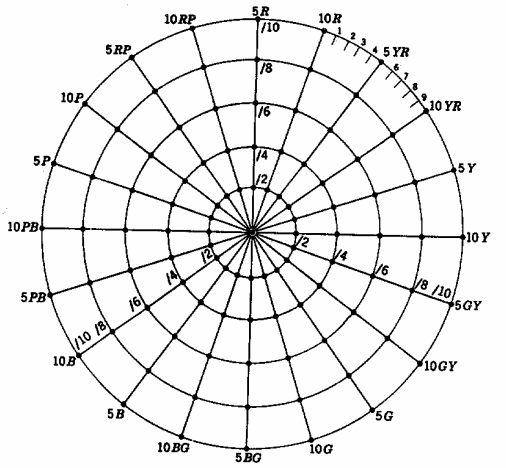

FIGURE 9.28 Organisation of the Munsell hue circle after Wyszecki & Stiles (80)

Figure 9.29 shows a page of constant Munsell hue, with the white - black axis.

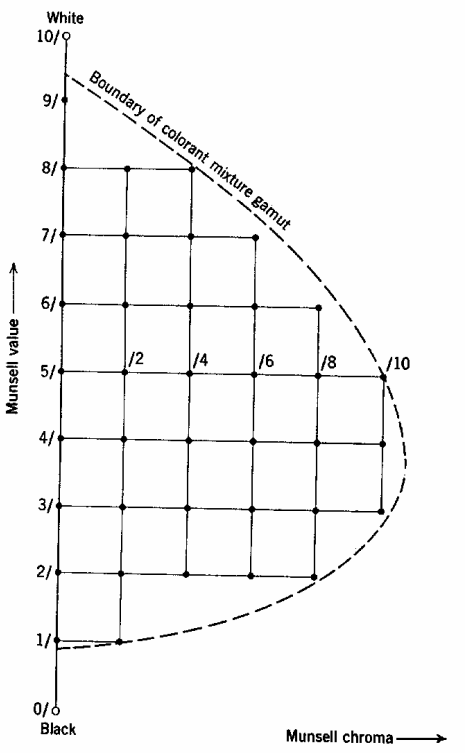

FIGURE 9.29 Organisation of colours of constant Munsell hue (80)..

The Munsell colour notation first specifies the hue, then states the value and chroma in the form Value/Chroma, e.g. 5 *YR* 8/4 for a light yellowish pink (this is the sample used in colour rendering calculations to represent human complexion colour). The Munsell Book of Colour is the manifestation of the system.

Unfortunately there is no exact transformation between the CIE system and the Munsell system. Only the *Y* tristimulus value has an exact definition:

$$Y = 1{,}2219\ V - 0{,}23111\ V^2 + 0{,}23951\ V^3 - 0{,}021009\ V^4 + 0{,}0008404\ V^5 \quad \ldots \quad 9.76$$

where V is the Munsell Value describing the lightness of the sample. This equation in, however, non-invertible. Approximations for the value scale (81) have been proposed and lookup table programs exist also for value and chroma calculations (82).

9.5.1.2 The Natural Colour System (NCS system)

The Swedish NCS system is built on the Hering colour theory (83) that states that "there are six elementary colours, each of which shows no resemblance to any of the others"; and that "all perceived colours can be described by their resemblance to the elementary colours only". The six elementary colours are the two achromatic ones, white and black, and the four chromatic ones, yellow, red, blue and green. Tonnquist states that "for each elementary colour there is an elementary attribute (whiteness *w*, blackness *s*, yellowness *y*, redness *r*, blueness *b* and greenness *g*, giving the resemblance of a given colour to the elementary colour on a scale of 0 to 100".

Yellow — blue and red — green are mutually exclusive colour perceptions, therefore the NCS system places these perpendicularly to each other, with 90° between the adjacent colours, as seen in Figure 9.30.

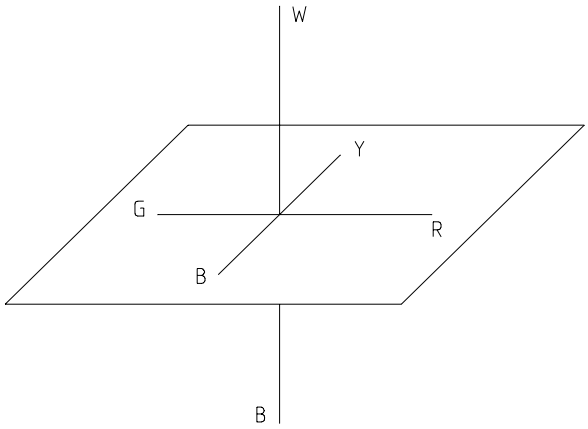

FIGURE 9.30 Antagonistic Red — Green Yellow — Blue and White — Black axes in the NCS system.

Figure 9.31 shows the NCS hue-circle and Figure 9.32 shows one hue-leaf of the NCS system with equal blackness and chromaticness (resambleness with pure colour, i.e. with a colour without blackness or whiteness content) lines.

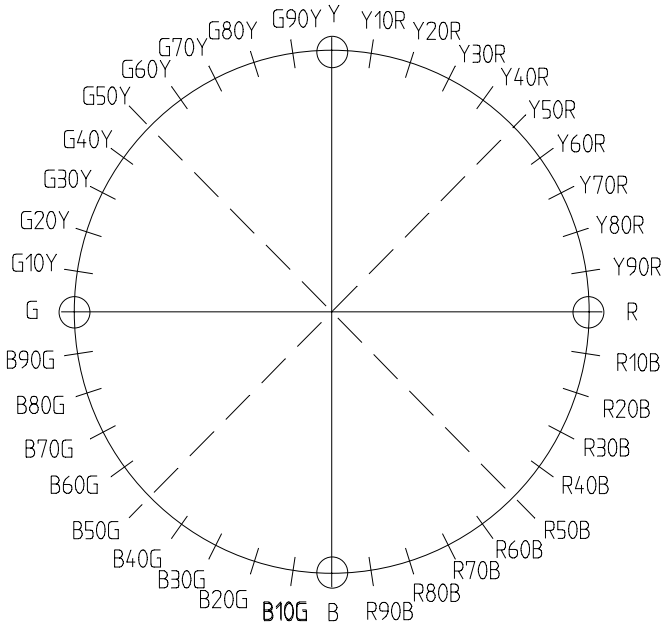

FIGURE 9.31 NCS hue circle with the four unic chromatic hues.

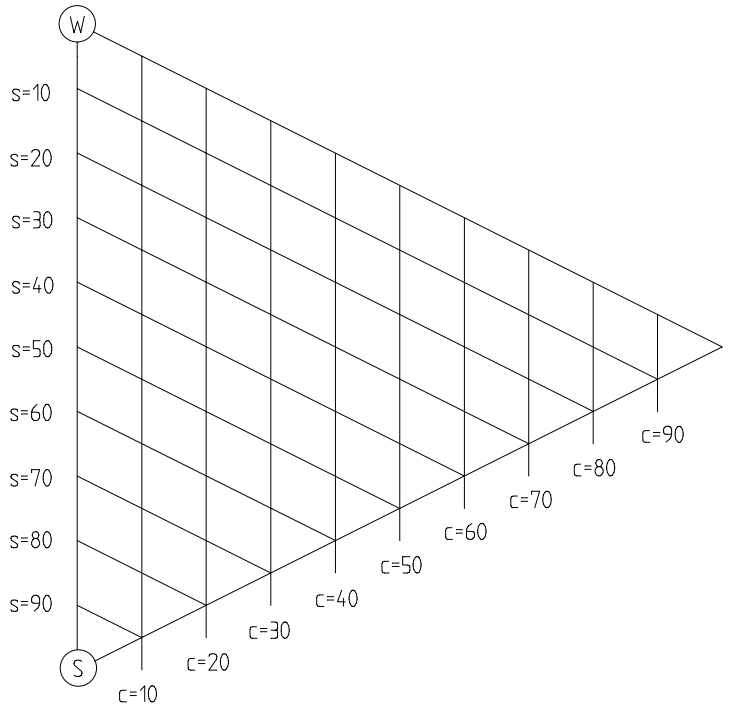

FIGURE 9.32 NCS constant-hue triangle with lines of equal chromaticness and equal blackness.

The NCS system is backed by an NCS atlas, which is, however, only to exemplify the system and not the actual manifestation. These samples of the NCS atlas have been measured and the CIE tristimulus values for each colour sample are available. Derefeldt and Sahlin have shown that there is no simple relationship between the NCS and CIELAB systems (84).

9.5.1.3 Further colour order systems

At this place we would like to briefly mention some of the other colour order systems that find application in different application areas.

The *OSA—UCS system* (77, 85, 86) has been built by placing the samples on a cuboctahedron lattice. A sample located in the centre of the cuboctahedron has 12 nearest neighbours at the 12 corner points of the solid. The lattice has three axes with colorimetric meaning, an L axis representing lightness and two opponent axes: j and g. The system has a transformation into the CIE XYZ system.

The *DIN system* (87) attempts to show equal colour distances in defined colour series of hue, saturation and darkness degree. It has been planned to be an aid for technical purposes. The hue and saturation scales of the system do not differ essentially from those of other colour order systems, but the brightness description is considerably different. For different colours not the equal luminous reflectance but the relative luminance factors are kept equal. The relative luminance factor is the quotient of the luminous reflectance Y of the colour and of the optimal colour of equal chromaticity Y_0. Optimal colours are those whose reflectance curve consists of only zero or unity values and have not more than two transitions between unity and zero values.

The DIN system uses many ideas derived from the *Ostwald system* (88, 89) of ordering colours.

The *Coloroid Colour System* (90, 91) has been developed to show colour harmony series and is intended for the use of architects and interior designers.

In a series of articles Smith and co-workers have described the interrelationship between different colour order systems (92 - 96).

9.5.2 Colour appearance models

The CIE system of colorimetry has been designed to predict whether two stimuli will match or not. Colour order systems are capable to systematise colour perceptions but are not able to predict colour sensations yet as they will be perceived under different adaptation conditions. Colour appearance models have been designed to predict the human perception of colours. They should model colour vision, present measurement tools for quantities as brightness, colourfulness or unique hue.

There is no international agreement on a colour appearance model, therefore we will describe here — very briefly — four models that compete for acceptance. None of them will be described in detail as they are usually quite complex and need much explanation. The reader has to be referred back to the original literature.

One of the common features of all the colour appearance models is that neither of them is in a final form. From time to time model builders modify their calculation method, introducing some fine-tuning to the model. Therefore the reader is advised to search for the most recent literature to find the latest version of a given model (although every effort was taken to describe the models in their most up to date form at the time of writing this chapter, the author would like to apologise had he missed a facet of development in one case or the other).

9.5.2.1 ATD colour vision model

The ATD model developed by S L Guth (97 - 100) is a multizonal colour vision model. It contains a non-linear receptor gain control and two opponent colours processing stages together with a compression stage of the signals. The first stage mediates apparent brightness and visual discrimination, while the second stage mediates apparent hues and saturation. Brightness is described in this model as the vectorial sum of the *ATD* signals derived from the *LSM* cone signals after adding noise and performing a gain control.

9.5.2.2 RLAB colour appearance model

Based on the Fairchild's chromatic adaptation model (101, 102) Berns and Fairchild described an extension of the CIELAB colour space (103, 104) that can be used as a colour appearance space, especially for the reproduction industry. The original tristimulus values are transformed to a D65 1000 lux illumination reference condition by the above chromatic adaptation transformation, then a somewhat modified CIELAB transformation is performed, depending on the surround conditions. If the corresponding colours under another illuminant have to be determined , inverse transformations can be performed.

9.5.2.3 Nayatani and co-worker's model of colour appearance

A colour appearance model based on the chromatic adaptation model described in Section 9.4.5.1 (70, 74, 75) was developed by Nayatani and co-workers (105). This model has been tested and extended several times during the past years, some of the more important phases are described in (106 - 108). The model predicts brightness and lightness, chroma (saturation), colourfulness and hue angle of the test sample.

In the calculations the adapting luminance is taken into consideration, transformations into the Esteves - Hunt - Pointer primary system are performed, followed by non-linear transformations. From these data lightness/brightness, redness/greenness and yellowness/blueness co-ordinates are calculated. These are then used to calculate the hue angle, the chroma and the colourfulness correlates.

9.5.2.4 The Hunt colour appearance model

The other elaborate colour appearance model is that developed by Hunt (109 - 113). The model takes into consideration the adapting field and the proximal filed luminance level, can scope with the brightness and chromatic surround induction effect, and predicts hue, colourfulness, saturation lightness and brightness of the test sample. The model can also be reversed to calculate the CIE colorimetric data of the corresponding colour for another visual situation.

The model first transforms CIE tristimulus data into a *LMS* cone sensitivity space, performs there a non-linear transformation and considers a number of influencing factors (surround, adapting field, induction, etc.) Then signals that could correspond to the antagonistic yellow/blue, red/green second stage visual signals are calculated. From these signals hue, colourfulness, brightness, lightness chroma and whiteness-blackness quantities are calculated.

The system counts as one of the most advanced representation of quantitative visual modelling and a number of experimental studies dealt with its verification and determining the limits of its applicability (see e.g. (114 - 119). Recently also a CIE guide has been published (120) dealing with the question of testing colour appearance models.

9.6 COLORIMETRIC PRACTICE

In this section some general issues of colorimetric practice will be discussed. Within the limited space it is certainly not possible to cover all the practical aspects of colorimetry, we will be selective in choosing items of interest regarding for photometry. First an overview on the available instrumentation will be given followed by some selected items.

9.6.1 Colorimetric instrumentation

9.6.1.1 Tristimulus instruments

A tristimulus colorimeter consists of a measuring head containing some input optics (cosine corrector for “illuminance” type of measurement or lens-optics for “luminance” type of measurement) three or four filter packages to correct the spectral sensitivity of the detector(s) to the colour matching functions (see Figure 9.14 in Section 9.4.2.1). At present most “illuminance” measuring instruments use Si photo-

voltaic cells as detectors, while the “luminance” measuring instruments might contain photoelectric multipliers.

The detector(s) are usually followed by operational amplifiers to convert the current of the detector into a voltage signal, which is then analogue to digital converted and digitally processed. Figure 9.33 shows the scheme scheme of a tristimulus colorimeter.

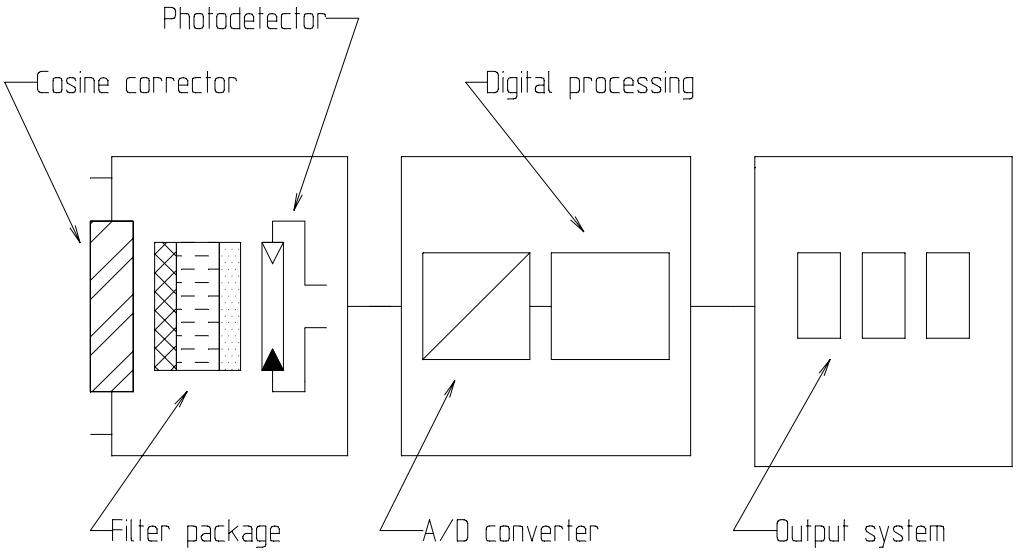

FIGURE 9.33 Schematic view of a tristimulus colorimeter

The most critical part of a tristimulus colorimeter is the filter correction. Usually optical coloured glass filters are used and several such filter-glasses have to be ground and polished to the proper thickness and glued together to achieve a good filter correction.

To achieve better spectral correction in some instruments chips of filter glasses are glued side by side, called partial filtering (see Figure 9.34).

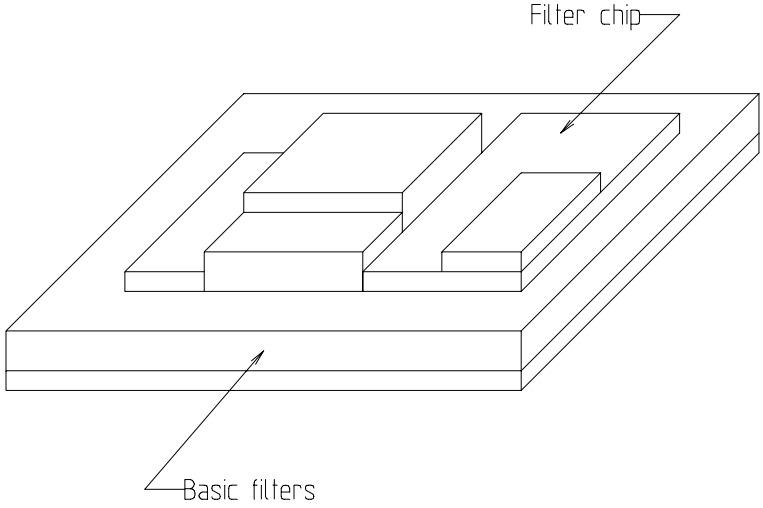

FIGURE 9.34 Spectral correcting filter using both full-filtering and partial filtering (by courtesy of LMT, Berlin (121)).

There is no internationally accepted method for characterising the goodness of fit of the spectral match of the colorimetric detector heads. At present many manufacturers use the method suggested by the CIE for radiometers and photometers (122). This method is based on the so called f_1' error expression of spectral mismatch:

$$f_1' = \frac{\int_0^\infty \left| s^*(\lambda)_{\text{rel}} - \bar{t}_i(\lambda) \right| \mathrm{d}\lambda}{\int_0^\infty \bar{t}_i(\lambda)\,\mathrm{d}\lambda} \cdot 100\% \qquad \ldots\ 9.77$$

where $\bar{t}_i(\lambda)$ is one of the colour matching functions (see Equation 9.38 and 9.65), $s^*(\lambda)_{\text{rel}}$ is the normalised relative spectral responsivity,

$$s^*(\lambda)_{\text{rel}} = \frac{\int_0^\infty S(\lambda)_{\text{m}}\, \bar{t}_i(\lambda)\,\mathrm{d}\lambda}{\int_0^\infty S(\lambda)_{\text{m}}\, s(\lambda)_{\text{rel}}\,\mathrm{d}\lambda}\, s(\lambda)_{\text{rel}} \qquad \ldots\ 9.78$$

and $S(\lambda)_{\text{m}}$ is one of the standard illuminants, in photometry usually Standard Illuminant A, in colorimetry often Standard Illuminant D65. $s(\lambda)_{\text{rel}}$ is the spectral responsivity of the detector - filter combination. f_1' values of the $\bar{y}(\lambda)$-function approximation can be as good as 1 to 1,5 %, for the $\bar{x}(\lambda)$ and $\bar{z}(\lambda)$ functions the approximations are usually poorer, depending to a large extent on the permissible total absorption. (The CIE is working on a method to quantify the spectral mismatch of a colorimeter head, but this technique has not received general acceptance yet (123).) Figure 9.35 shows state of the art instrumental spectral responsivity colour matching functions. Figure 9.35a shows spectral matches achieved by using full-filtering techniques, while Figure 9.35b shows similar data for a partially filtered colour measuring head.

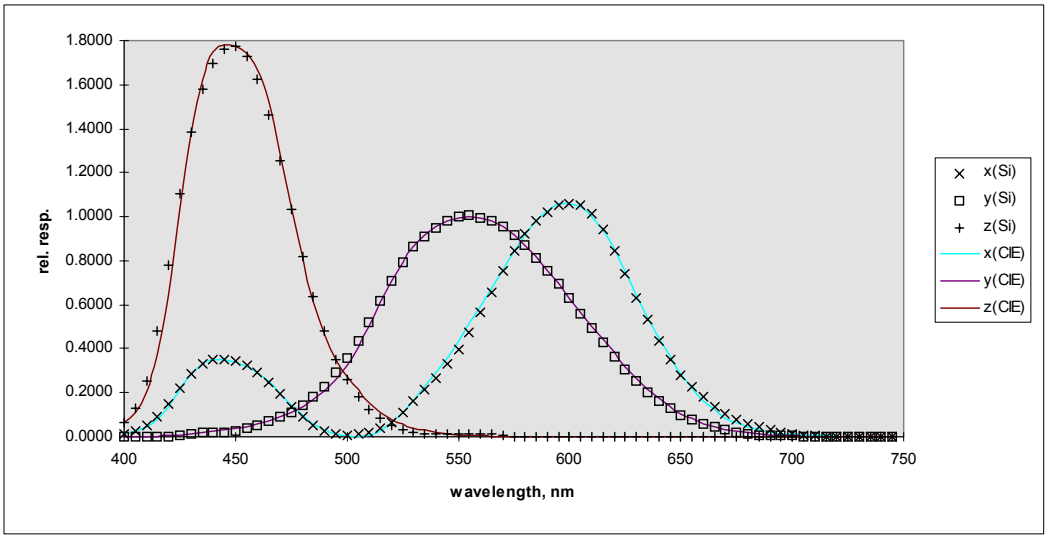

FIGURE 9.35a Spectral sensitivity functions of a tri-stimulus colorimeter with Si-cell and full-filter correction (f_1(x)=2,6, f_1(y)=2,2, f_1(z)=4,3, courtesy of InPhoRa Corp.(124)).

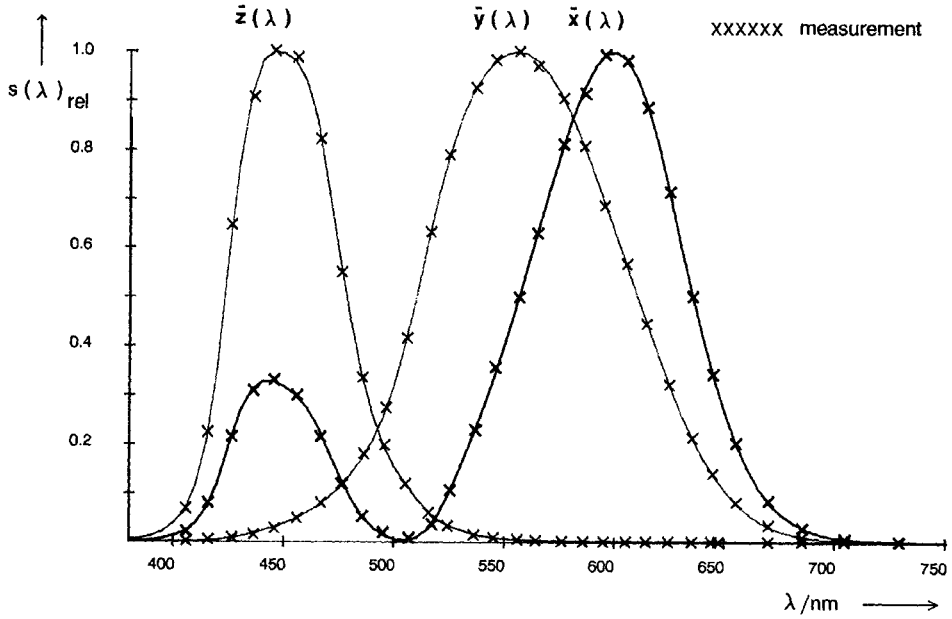

FIGURE 9.35b Spectral sensitivity functions of a tri-stimulus colorimeter with Si-cell and partial-filter correction (courtesy of LMT(121)).

Depending on the application there are other characteristics of a tri-stimulus colorimeter, and of a radiometer in general, that have to be observed. The second most important item is the angular responsivity: For a cosine corrected detector head the irradiance responsivity has to change with the cosine of the angle of incidence, for a radiance type of detector head it should stay constant for a small angular subtense and then drop to zero within a very small range.

Should the colorimeter be used with sources having considerable amount of radiation outside the visible spectrum range, the UV and IR sensitivity is also of importance, as it might lead to stray radiation interference.

If the source to be measured has a non-constant temporal emission , as all a.c. powered gas discharge lamps and all video display units have, then the synchronisation of the measurement cycle to the emission frequency is of outstanding importance as otherwise extremely long measurement times have to be selected to average out the temporal variations of the signal to be measured.

There are measurement situations when the colour has to be determined at different parts of a pictorial scene, as e.g. on a computer picture displayed on a cathode ray tube (CRT) screen. For such purposes tri-stimulus filtered CCD cameras can be used. Figure 9.36 shows instrumental colour matching filters developed for such an instrument (125). The state of the art filter match is in case of the CCD cameras not as good as for Si-photo-voltaic cells, as in this case large surface full filtering has to made, covering all the pixels of the camera. An alternative way would be to filter the pixels of the camera individually as done in the home video recorders. At present the pixel-filtered CCD-cameras colorimetric mismatch is still too high to permit

meaningful colorimetric measurement. However, if the light to be measured is composed of three and only three spectral emissions, as is the case with a CRT display, matrix transformation techniques can be applied to correct for the given CRT — CCD combination (126).

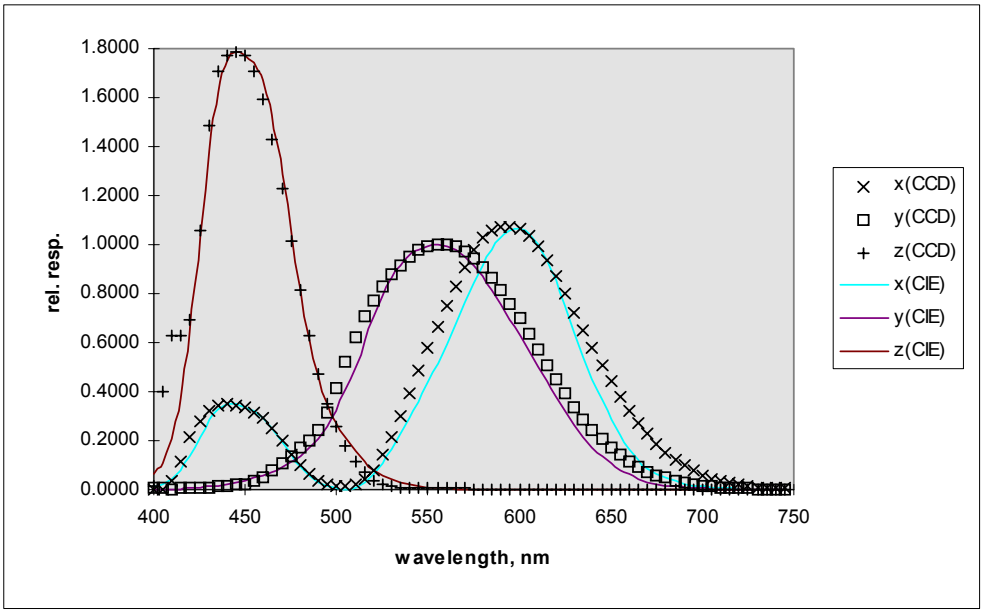

FIGURE 9.36 Spectral sensitivity functions of a tri-stimulus colorimeter built with a CCD camera (f_1(x)=7,5, f_1(y)=3,6, f_1(z)=3,9, courtesy InPhoRa Corp. (125).

A further problem with all types of tristimulus colorimeters is that both the colour matching filters and the detectors show a spectral and absolute sensitivity change with temperature. As the measuring head can be temperature controlled, the main concern occures in case of measuring relatively strong radiation the heat absorption in the filters as a 1 degree Centigrade temperature raise can produce a 0,12 % decrease in absolute sensitivity and a marked shift in the spectral responsivity (depending on the glass types used) (127).

9.6.1.2 Spectroradiometric techniques: Scanning and CCD type instruments

Tri-stimulus instruments suffer from the inherent drawback that the available type of filters is limited, thus a perfect match to the colour matching functions is not possible. The way out is only to determine the emission spectrum and calculate the tri-stimulus values. Traditionally scanning spectrometers are used for this purpose. There are many good commercial instruments available for the measurement of transmission or reflection spectra. Owing to differences in optics and partly in the built-in algorithms to calculate colour co-ordinates, the repeatability of these instruments is usually much better than their absolute accuracy (128-130), which should be checked carefully by using standards calibrated in National Laboratories (131).

Most of the high-end spectroradiometers for colorimetric purposes are custom built instruments. Some items that have to be checked with such systems are summarised in (132) and (133). Most important is that the band-width of the instrument and the wave-length increment by which measurements are made have to be carefully set equal. If one is larger than the other, the instrument will over-sample or under-sample the spectrum, i.e. will measure a spectral band twice or will leave it out completely,

leading to measurement errors, especially if the radiation consists of superposed spectral lines and broad spectral bands.

Recently another type of spectrometer has become available, where the detector is a CCD linear array (or some other variant of that detector type where a high number of single detector elements are sitting side by side. This system permits to use a spectrograph arrangement, i.e. to focus the entire spectrum onto the measuring sensor and thus collect information in parallel over a broad wavelength range. By this technique spectrometers without moving parts can be built.

9.6.2 Light source colorimetry

9.6.2.1 General purpose sources

The colour of incandescent lamps is often determined from distribution temperature measurements (see Section 9.4.3.1). For gas discharge lamps either tristimulus colorimeters or spectroradiometric techniques are used. As the colour of metal halid lamps depends on the angle of view (whether light is collected e.g. in a horizontal plane or vertically upwards or downwards) (134), it is usual to measure the colour, together with the photometric characteristics in a photometer sphere. If a tristimulus colorimeter is used, the spectral match of the filters has to include also the spectral selectivity of the wall paint. As this is difficult to achieve, and shifts of spectral reflection with time cannot be excluded, it is more appropriate to use spectroradiometric methods, where the calibration with an incandescent lamp of known spectral power distribution can correct for selective absorption effects.

It is general practice to measure general purpose gas discharge lamp spectra at 5 nm intervals with 5 nm bandwidth as measurements with higher resolution often only decrease the available light intensity to levels where noise contribution becomes unacceptably high. The attained colorimetric errors produced by the 5 nm abridged measurement compared with a more accurate 1 nm measurement are usually negligible.

If gas discharge lamps are used with magnetic ballast (i.e. not high frequency electronic ballast are used), it is also important to synchronise the measuring cycle to the main frequency , so that at every wavelength radiation is collected for the same amount of time.

Proper stabilisation time of the source is important both in case of low and high pressure gas discharge lamps.

9.6.2.2 LEDs

Light emitting diodes are selective emitters with bandwidths of only a few tens of nanometers. That’s why for their colorimetric measurement tristimulus instruments have to be carefully calibrated in that particular wavelength range where the LED emits. Instrument manufacturers frequently offer special LED measuring tristimulus filter sets tailored for one class of LEDs (i.e. red or yellow or green).

Owing to the narrow emission spectrum of LEDs, spectroradiometric measurements have to be performed at 1 nm steps (with 1 nm bandwidth) in order to achieve the required accuracy.

The spatial light distribution of LEDs can be very different, from narrow beam emitters to almost Lambertian radiators. The spectral characteristics vary somewhat also with angular distribution, but this is generally of smaller importance. Therefore it has become general practice to measure the emitted radiant flux of a LED in a cone of several degrees opening angle, although techniques with integrating spheres have also been described (135).

9.6.2.3 Video Display Units (VDUs)

While the colorimetry of general purpose light sources and of LEDs is more of a technical character, in case of VDUs there are a number of fundamental unsolved problems. In this section we will deal only with cathode-ray-tube (CRT) monitor colorimetry, as the more modern flat-panel display monitors are not advanced well enough to permit real colorimetric work. Flat-panel displays suffer from viewing angle dependent colour, temporal instability, etc. Thus at present they can not be used in applications where colorimetric fidelity is of importance.

The white point on the VDU, the chromaticity produced when all three electron guns are fully energised, is usually set by the manufacturer, although with high-end VDUs nowadays there is the possibility of user defined white point selection. Computer manufacturers often prefer a high temperature (bluish) white point (with a correlated colour temperature of about 9300 K), as this permits higher luminance also in the blue channel. The international standards call for a D65 white point, while graphic arts has settled for an even lower temperature white point (D50) to compromise between daylight and electrical light situations (136, 137). The following table shows the chromaticities of the most often used white points.

Table 9.6.1. Most often used CRT white point settings.

	CCT	x_n	y_n
D50	5000	0,346	0,359
D65	6504	0,313	0.329
D93	9300	0,280	0,312

The white point chromaticity and luminance is important not only as it provides the fundamental setting of the monitor, but also as it defines the anchor point of any transformation from the CIE XYZ system into a more equidistant and appearance conforming system (e.g. CIE-LUV or CIE-LAB, see Section 9.4.4.4).

The calibration of the CRT-monitor, i.e. the determination of the relationship between the digital to analogue converter (DAC) values set by the software and the produced chromaticity co-ordinates and luminance of the emitted colour is based usually on the assumption that the luminance versus DAC value relationship can be described by an exponential function and that the luminance produced by on of the electronic channels of one of the pixels is independent of the setting of the other channels and for that of the other pixels. This is usually termed spatial and channel independence (138 - 141). Depending on the quality of the monitor, neither channel nor spatial independence is fulfilled and more elaborate calibration techniques might be necessary (142, 143).

With a well calibrated VDU it becomes possible to produce photo-realistic pictures. However, their colour appearance will be still different from those produced on hard-copy media. A CIE committee is working on the evaluation of colour appearance models for hard copy and soft-copy comparison (144).

One of the problems in VDU colorimetry is that the coloured patches are seen under other visual angles as for most reflecting objects. Thus e.g. a coloured line has a much smaller angular subtense then prescribed in CIE colorimetry (2° observation angle), and the human colour matching functions differ under these circumstances from those determined under standard conditions (145), see also Section 9.4.2.3. Visual ergonomic colorimetric standards are laid down in an ISO standard (146).

9.6.2.4 Brightness description

In Section 9.2.5.3 we already mentioned that chromatic colours seem to be brighter than achromatic ones with the same luminance. There is no standardised metric to describe this so called "brightness/luminance discrepancy", but a CIE Research None (147) gave a tentative recommendation to quantify this phenomenon (the different colour appearance models, see Section 9.5.2, all deal with the problem, but usually give a less satisfactory result as the CIE empirical approach (148): This model states that for two stimuli that stimulus will seem to brighter for which the following expression is larger:

$$L^{**} = \log(L) + C \qquad \ldots\ 9.79$$

where L is the luminance of the stimulus and C is a chromaticity dependent quantity:

$$C = 0{,}256 - 0{,}184\, y - 2{,}527\, xy + 4{,}656\, x^3 y + 4{,}657\, xy^4 \qquad \ldots\ 9.80$$

If the two stimuli have equal $\log(L) + C$ values they will be seen equally bright. Figure 9.37 shows contour lines of equally bright lights of equal luminance. (For further details on the brightness-luminance relationship see (149).)

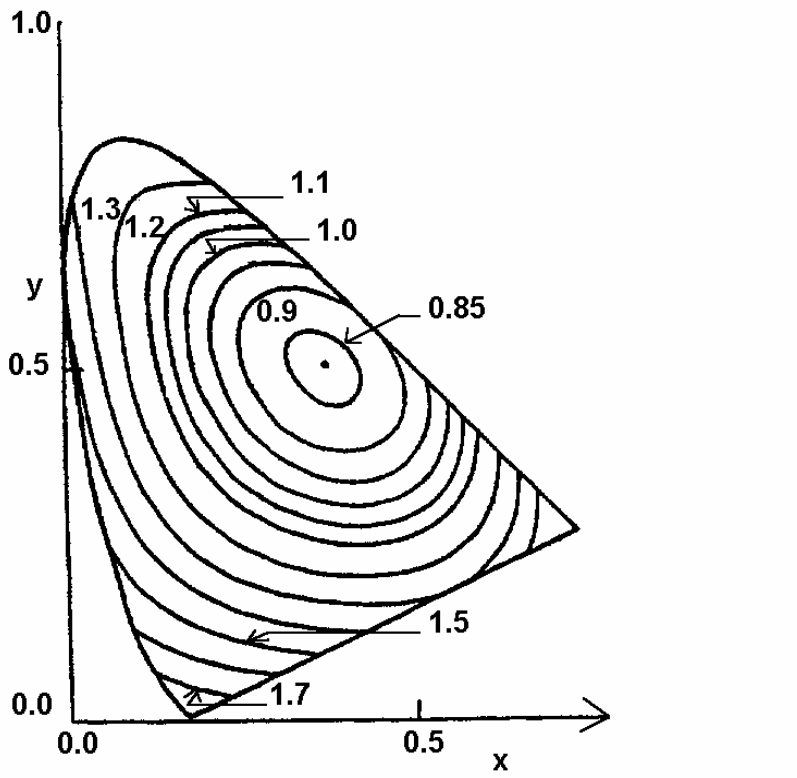

FIGURE 9.37 Contour lines of equiluminous lights of equal brightness.

9.6.2.5 Signal colours

Signal lights have their own photometric and colorimetric problems. They have to be visible, and their colour unambiguously recognisable even from very long distances, this means one has to be able to see them under small angular subtense and low intensity. They should be designed in such a form that even colour deficient people have no difficulty in identifying them.

The first CIE international signal colour recommendations date back to the1950s. Studies performed in different countries led to new recommendations, restricting some of the signal light chromaticity boundaries (150). Figure 9.38 shows in the CIE chromaticity diagram the old and revised signal light colour boundaries of red, yellow, green, blue and white signal colours. It is expected that in a not too distant future these new signal colour boundaries will become an international standard.

The measurement of signal lights provides similar technical problems as that of LEDs, only the strength of the light is usually much higher. If tristimulus instruments are used the goodness of the colorimetric fit is important. Often from each colour to be measured a laboratory standard is prepared by high precision spectroradiometric measurements and the tri-stimulus instrument is used as a colour-difference meter comparing the colour of the test light to that of the standard light. Again, if the fit of the colorimeter is not really good, the spectral distribution of the test should not deviate too much from that of the standard.

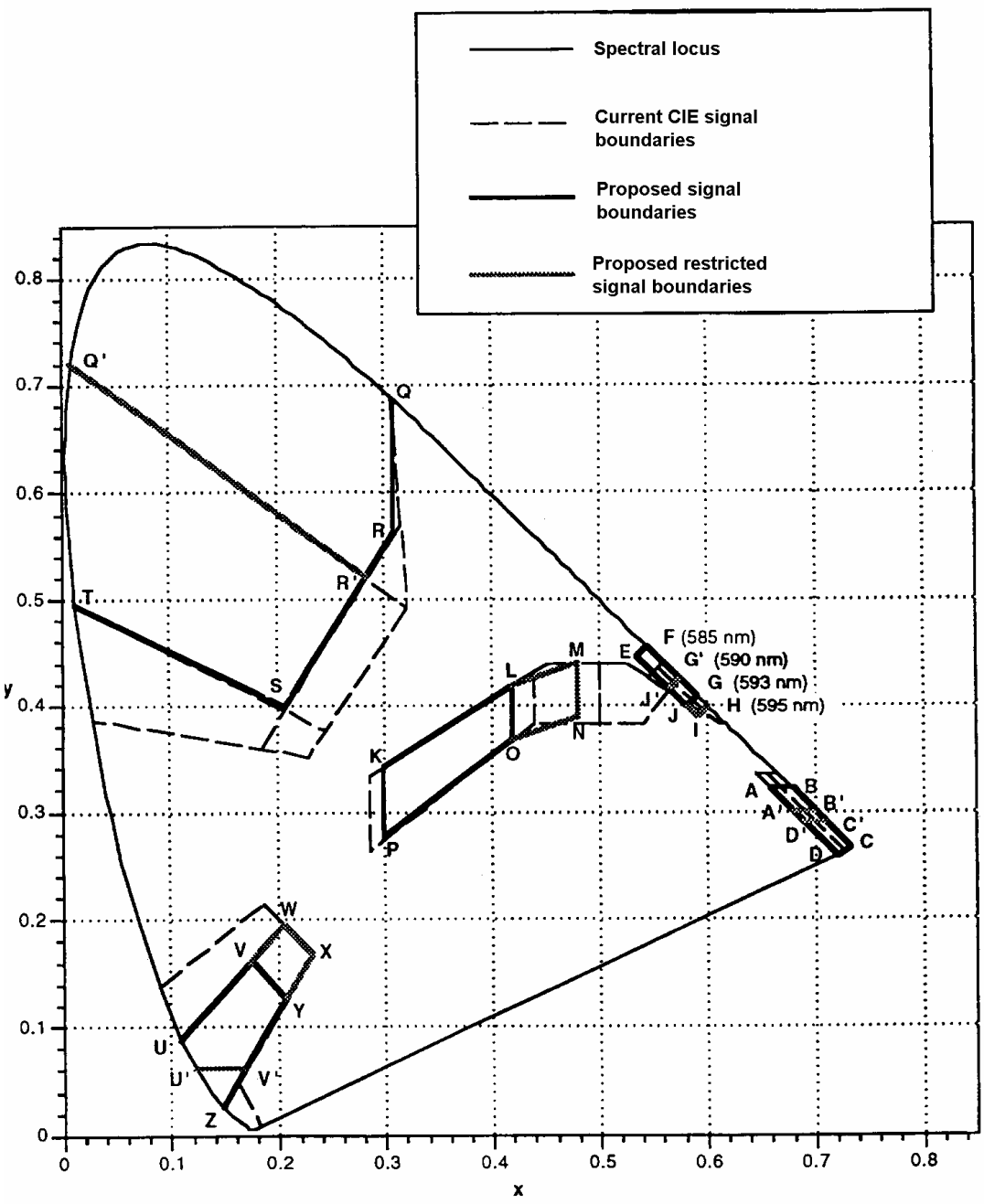

FIGURE 9.38. Original and revised boundaries for colours of signal lights.

Recently signal lights with dichroic filters have been introduced on the market. The spectral transmittance of dichroic filters — as that of all systems working on the principle of interference —shows an angular dependence. To describe completely the colorimetric characteristics of such lights, it is necessary to measure the angle dependence both of the luminance and of the chromaticity. This is especially important if the signal light can be seen under different angles. One has to ascertain that the chromaticity stays for all the relevant angles within the permitted tolerances. If it is a signal light with an incandescent lamp, this has to be checked for the lowest and highest main voltage value, as the colour temperature of the incandescent lamp is highly voltage dependent. In case of gas-discharge lamps, the light source chromaticity tolerances have to be observed. In case of glass-filter signal lights, it is permitted to shine the light into an integrating sphere and measures the average chromaticity of the integrating sphere wall. For dichroic filter signal lights this is not permitted, as the chromaticity of dichroic filtered lights is changing with viewing angle. Such a measurement is allowed only if it is ensured that the goniometric variations of the chromaticity are small enough.

9.6.3 Colorimetry of materials

The overwhelming part of all colorimetric work is done on materials: textiles, plastics, paper, etc. Questions related to the measurement technology of these substances would go far beyond the limits of this book, and we would like to refer in this respect to the many specialised monographs and books dealing with the theoretical and practical aspects of measuring material sample colour. (See general references at the end of the bibliographic section). At this point only a single question will be discussed, the measurement of fluorescing materials, as the fluorescence measurement is actually a photometric one, consequently falls within the scope of the present book.

9.6.3.1 Fluorescing materials

The general concept *luminescence* is “the emission of light at low temperatures by any process other than incandescence, such as phosphorescence or chemiluminescence”(151). Its special form *fluorescence* refers to emission produced by excitation by optical radiation or particles (electrons, ions, etc.) and where the lifetime of the excited atoms or molecules is less than about 10^{-8} seconds. Excitation by optical radiation is often termed *photo-fluorescence*, but in this section we will use the term fluorescence to describe this latter phenomenon.

Fluorescing materials transform shorter wavelength radiation into longer wavelength radiation, usually UV radiation or short wavelength visible (blue) light into green, orange or red light. Such materials are e.g. the luminophores (or phosphors) used in gas discharge lamps (fluorescent tubes, high pressure mercury lamps, etc.). Paper, textiles and other materials often contain optical brighteners, a special class of fluorescent material, used to increase the "whiteness" sensation. A further class are some fluorescent pigments or inks (used in marker pens, advertisements etc.) producing a strong coloured radiation when irradiated by ultraviolet or short wavelength visible radiation.

Figure 9.39 shows on the example of an orange fluorescent material the four characteristic spectra of a fluorescent specimen (152). β_T is the total spectral radiance factor measured when the sample is properly irradiated by a D65 source, β_S is the reflected radiance factor one would obtain if no fluorescence occured. β_L is the fluorescent part of the radiance factor, i.e. the emitted radiation depending on the irradiation at shorter wavelength, and X is the excitation spectrum showing the relative efficiency of different wavelength radiation to excite the fluorescence. Problems are encountered if the excitation spectrum and the emission spectrum overlap, as shown on this example. (The emission occurring in wavelength regions where there the fluorescence can be still excited is called anti-Stokes emission.)

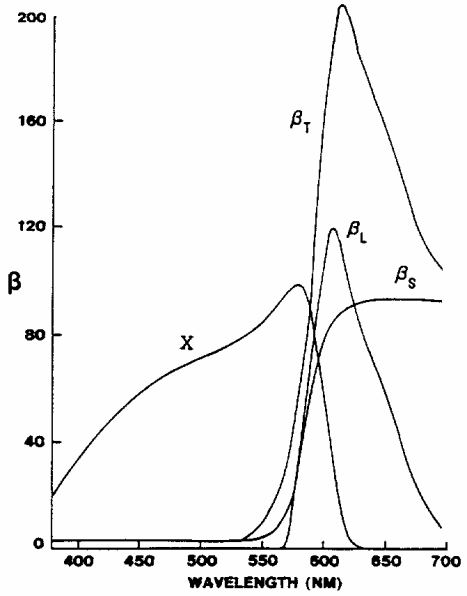

FIGURE 9.39 Total spectral radiance factor β_T and its components on the example of an orange fluorescent sample.

To be able to measure the colour of such surfaces reproducibly, not only the reflected light has to be evaluated but also the emitted one, and the emission has to be excited by a well-known amount of radiation of known spectral composition. The recommended illuminant for such measurements is the CIE Standard Illuminant D65. Unfortunately, the practical realisation of this illuminant (the production of a D65 source) is not easy, and there are no standardised methods how to proceed (42).

Material samples are often measured in photometer spheres where either the irradiation is semi-spherical, or the collection of the radiation is done in the upper hemisphere. Measuring fluorescent samples in such measuring geometry is further complicated by the fact that the absorption by the test sample influences the spectral distribution of the radiation falling onto the sample. Ways to correct for this effect are described in (153).

It is better practice to use a 0°/45° measuring geometry as in this case the spectral distribution of the excitation is not influenced by the absorption of the specimen. Such a measurement is described for the very important class of fluorescent retro-reflective materials in (154).

The most exact technique to measure fluorescent materials is to use the so called two-monochromator method, and scan both the excitation spectrum and the emission spectrum. The schematic layout of such a system is seen in Figure 9.40.

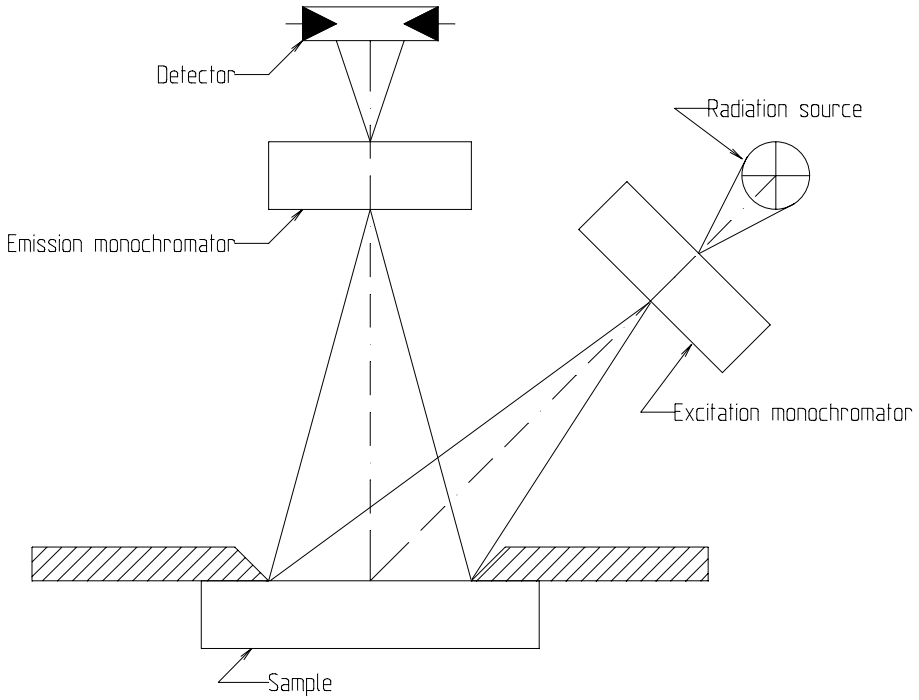

FIGURE 9.40 Schematic layout of a two-monochromator spectroradiometer to measure the total radiance factor, the excitation and emission spectra of fluorescent samples.

The two-monochromator method was first introduced by Donaldson (155), a modern version of the method together with the proper colorimetric evaluation of the measurement results was published in (156). When the two monochromators are scanned in tandem, one gets the true reflection spectrum of the sample. Scanning the excitation monochromator for pre-selected emission monochromator setting provides the excitation spectrum. Usually a complete matrix of intensities determined at the different settings of the excitation monochromator and of the emission monochromator has to be measured. Proper calibration of the responsivity of the two systems, band-pass corrections, etc. restrict such measurements to well equipped laboratories even in the days of fully computerised spectroradiometers.

9.7 SUMMARY AND CONCLUSIONS

The present chapter intended to provide an overview of one of the most intriguing issues of optical radiation measurement, searching for objective correlates of our visual system. Colour is on the one hand an everyday experience, and most of us with a more or less good trichromatic vision take it granted that we see colours and that physics should be able to describe these colours objectively.

Even from the short presentation of the physiological factors of our colour vision system, it became obvious that there are a number of phenomena that cannot be

described by simple objective equations. Colorimetry has to make use of simplification, only this makes it possible to obtain quantifiable results.

It is remarkable that CIE colorimetry, despite of the great number of simplifications and the fact that it has been designed to predict only colour perception equality, performs so well in a number of industries, especially those for which it was not thought originally, as e.g. the textile colouring industry. Just applications that were in mind when the system was founded have most problems with its application. The colorimetry of light-sources, colour rendering descriptions, e.g., are yet not completely adequate. The lighting industry, and in more modern times the colour graphics and colour computer industry need colour appearance description, which is outside of the classical limits of CIE colorimetry.

In the present chapter first we tried to summarise those techniques where international consensus exists. We covered other items where only tentative recommendations are available, or where measurement methods are only available as suggested by individual authors in subsequent sections.

For further reading and detailed description of the single colorimetric methods we had to refer to the international literature. For North-American use further details can be found in the ASTM Standards. A compilation of relevant standards was published in 1994 (157).

At the end of the References section a "Further Reading" part has been included giving the bibliographic references of some books presenting an overview on colorimetry or treating colour as a tutorial subject.

References

1. *Handbook of Optics,* ed.: M Bass, McGraw-Hill, Inc. 1995, ch 24.2, p.24.5.
2. Richter M, *Einführung in die Farbmetrik,* de Gruyter 1981, ch. 4. p. 34.
3. Travis D*, Effective colour displays,* Academic Pr., 1991, ch. 2, p. 37.
4 Pokorny J, Smith VC, Lutze M, *Applied Optics* **26,** 1437 - 1440 (1987).
5 van Norren DV, Voss JJ, *Vision Research* **14,** 1237 - 1244 (1974).
6. Schnapf JL and Baylor DA, *Scientific American* **256,** 32 - 39 (1987).
7. Stockman A, , MacLeod DIA, Johnson NE, *J. Opt. Soc. Am*. **10A**, 2491 -2521 (1993).
8. Walraven PL, Bouman MA, *Vision Research* **6**, 567 (1966).
9. Pokorny J, Smith VC, Scientific basis of visual performance in *Proc CIE Symp on Advances in Photometry*, Vienna, 1994.
10. Martinez-Uriegas E, Chromatic-achromatic multiplexing in human color vision, in *Visual Science and Engineering, Models and Applications*, ed.: Kelly DH, Marcel Dekker, Inc., New York, Basel, Hong Kong, 1994.
11. OSA: Advances in color vision, *1992 Technical Digest Series* Vol. **4**, 1992.
12. Piantanida TP, The molecular genetics of human color vision: From nucleotides to nanometers, in *Visual Science and Engineering, Models and Applications*, ed.: Kelly DH, Marcel Dekker, Inc., New York, Basel, Hong Kong, 1994.

13. Hunt RWG, Measuring colour, Ellis Horwood Ltd, Chichester, 1987.

14. Schwartz EL, Topographic mapping in primate visual cortex: History, Anatomy, and Computation, in Vi*sual Science and Engineering, Models and Applications*, ed.: Kelly DH, Marcel Dekker, Inc., New York, Basel, Hong Kong, 1994.

15. Wyszecki G, Stiles WS, Color Science, Concepts and methods, quantitative data and formulae, 2nd ed., JOHN Wiley & Sons, New York, Chichester, Brisbane, Toronto, Singapore, 1982.

16. Grassmann HG, Theory of compound colours. *Philosophical Magazine*, **4(7)**, 254-264. 1854 (see in Selected papers on Colorimetry - Fundamentals, ed.: MacAdam & Thomson, *SPIE Milestone Series* **MS 77,** Bellingham, USA. 1993).

17. Wright WD, The historical and experimental background to the 1931 CIE system of colorimetry, Proc. Symp. Golden Jubilee of Colour in the CIE, 3-18. *Soc. Dyers and Colourists*, Bradford, 1981.

18. CIE Proc. 8th Session, Cambridge 1931, 19 - 29, Cambridge at the University Press, 1932.

19. Publ. CIE 15.2-1986, Colorimetry, 2nd ed., CIE Central Bureau, Vienna, 1986.

20. Morren L, A few suggestions regarding the CIE publications on colorimetry, in Proc. Symp. Advanced Colorimetry, Vienna, 50 - 54, ed.: Schanda - Hermann, CIE Central Bureau, Vienna, 1993.

21. ISO/CIE Standard 10527-1991, CIE standard colorimetric observer

22. Publ CIE 4-1960. Compte Rendu Quatorzième Session, Bruxelles, 1959, Vol. A, 91 - 109, 1960.

23. Publ CIE 11-1964. Compte Rendu Quinzième Session, Vienne, 1963, Vol. A, 35, 1964.

24. Stiles WS, Burch JM, Interim report to the Comission Internationale de l'Eclairage, Zurich, 1955, on the National Physical Laboratory's investigation of colour-matching, *Optica Acta* **2**, 168, 1955.

25. Stiles WS and Burch JM, N.P.L. colour-matching investigation: Final report (1958), *Optica Acta* **6**, 1-26, 1959.

26. Speranskaya NI, Determination of spectrum colour co-ordinates for twenty-seven normal observers, *Optics and Spectroscopy* **7**, 424-428, 1959.

27. Stiles WS, The average colour-matching functions for a large matching field, in *Visual Problems of Color*, 213 - 249, Chemical Publ. Co., New York, 1961.

28. Shapiro AG, Pokorny J, Smith CV, Rod contribution to large-field color matching, *COLOR Res. & Appl*. **19**/4, 236 - 245, 1994.

29. Publ. CIE 86-1990, CIE 1988 2° spectral luminous efficiency function for photopic vision, CIE Central Bureau, Vienna.

30. Publ. CIE 75-1988, Spectral luminous efficiency functions based upon brightness matching for monochromatic point sources, 2° and 10° fields, CIE Central Bureau, Vienna.

31. MacAdam, DL, Visual sensitivities to color differences in daylight. *J. Opt. Soc. Am.* **32**, 247 - 274, 1942.

32. Brown WRJ, MacAdam DL, Visual sensitivities to combined chromaticity and luminance differences. *J. Opt. Soc. Am.* **39**, 808 - 834,, 1949.

33. Kelly, KL: Lines of constant correlated color temperature based on MacAdam's (*u*, *v*) uniform chromaticity transformation of the CIE diagram. *J. Opt. Soc. Am.* **53**, 999 - 1002, 1963.

34. Schanda J, Dányi M, Correlated color-temperature calculations in the CIE 1976 Chromaticity diagram. *COLOR Res. & Appl.* **2**/4, 161-163, 1977.

35. Schanda J, Correlated colour temperature and the ΔE_{ab}* colour-difference formula, in *Proc. AIC COLOR 77*, 292 -295, ed.: Billmeyer and Wyszecki, Adam Hilger Ltd, Bristol, 1978.

36. Robertson AR, Computation of correlated color temperature and distribution temperature, *J. Opt. Soc. Am.* **58**, 1528 - 1535, 1968.

37. Schanda J, Mészáros M, Czibula G, Calculating correlated color temperature with a desktop programmable calculator, *COLOR Res. & Appl*. **3**, 56 - 69, 1978.

38. McCamy CS, Correlated color temperature as an explicit function of chromaticity coordinates, *COLOR Res. & Appl*. **17**, 142 - 144, 1992.

39. Publ. CIE 114/4-1994, Distribution temperature and ratio temperature, CIE Central Bureau, Vienna, 1994.

40. Mori L, Sugiyama H, Kambe N, An absolute method of color temperature measurement, *Acta Chromatica* **1**, 93 - 102, 1964.

41. Publ. CIE 14A-1968, CIE recommendations on standard illuminants for colorimetry, in Compte Rendu Seizième Session, Washington, 1967, pp. 95-97.

42. Publ. CIE 51-1981, A method for assessing the quality of daylight simulators for colorimetry, CIE Central Bureau, Vienna.

43. CIE D005-1994, A method for assessing the quality of daylight simulators for colorimetry (based on CIE 51.181), CIE Central Bureau, Vienna.

44. McCamy CS, Simulation of daylight for viewing and measuring color, *COLOR Res. & Appl*. **19**/6, 437 - 445, 1994.

45. Gundlach D, Annäherung von Normlichtart D_{65} für Zwecke der Farbmessung, *AIC Color 77*, 218-221, Adams Hilger, Bristol, 1978.

46. Terstiege H, Artificial daylight for measurement of optical properties of materials *COLOR Res. & Appl*. **14**/3, 131 - 138, 1989.

47. Liu Y, Berns RS, Shu Y, Optimization algorithm for designing colored glass filters to simulate CIE illuminant D65, *COLOR Res. & Appl*. **16**/2 89 - 96 1991.

48. Clarke FJJ, Practical standard illuminant representative of interior daylight. In *Proc. 19th Session of the CIE*, Kyoto 1979, pp. 73 - 78, Publ. CIE 50-1980.

49. Hunt RWG, Standard sources to represent daylight, *COLOR Res. & Appl*. **17**/4 293 -294, 1992.

50. Grum F, Saltzmann M, New white standard of reflectance, *18th Session of CIE*, London, Publ. CIE 36-1975.

51. Publ. CIE 46-1979, A review of publications on properties and reflection values of material reflection standards, CIE Central Bureau, Vienna.

52. Malkin F, Verrill J F, The new series of ceramic colour standards. In *Proc. 20th Session of the CIE*, Amsterdam 1983, E37/1-2, Publ CIE 56-1983.

53. Fillinger L, Lukacs Gy, Andor Gy, Színetalonok termokromimusa (Thermochromism of colour standards) *Mérés és Aut*. **24** 342 - 347 1976.

54. Fairchild MD, Grum F, Thermochromism of ceramic reference tiles, *Appl. Opt*. **24** 3432 - 1985.

55. ISO Draft International Standard, Textiles — Test for colour fastness — Part J01: Calculation of small colour differences, ISO/DIS 105-J01/1992.

56. CIE Technical Report, Parametric effects in colour-difference evaluation, *CIE 101 - 1993*, CIE Central Bureau, Vienna.

57. CIE Technical Report, Industrial colour-difference evaluation, *CIE 116 - 1995*, CIE Central Bureau, Vienna.

58. Berns RS, Alman DH, Reniff L, Snyder GD, Balonon-Rosen MR, Visual determination of suprathreshold colour-difference tolerances using probit analysis, *COLOR Res. & Appl*. **16**, 297 - 316, 1991.

59. Luo MR, Rigg B, Chromaticity-discrimination ellipses for surface colours, *COLOR Res. & Appl.* **11**, 25 - 42, 1986.

60. Witt K, Modified CIELAB formula tested using a textile pass/fail data set, *COLOR Res. & Appl*. **19** 273 - 276, 1994.

61. CIE Technical Report, Special metamerism index: change in observer, *CIE 80 - 1989*, CIE Central Bureau, Vienna.

62. North A, Fairchild M, Measuring color matching functions, Part 1, *COLOR Res. & Appl.* **18** 155 - 162 1993.

63. North A, Fairchild M, Measuring color matching functions, Part 2, *COLOR Res. & Appl.* **18** 163 - 170 1993.

64. Rich DC, Jalijali J, Effects of observer metamerism in the determination of human color-matching functions, *COLOR Res. & Appl.* **20** 29 - 35 1995.

65. Berger-Schun A, Description of samples used and their colorimetric measurement, *Die Farbe* **26** 7 - 16 1977.

66. Ganz E, Whiteness: photometric specification and colorimetric evaluation, *Appl. Opt.* **15** 2039 - 2058 1976.

67. Ganz E, Whiteness formulas: a selection, *Appl. Opt*. **18** 1073 - 1078 1979.

68. Brockes A, The evaluation of whiteness, *CIE-Journal* **1** 38 - 39 1982.

69. Ganz E, Pauli HKA, Whiteness and tint formulas of the Commission Internationale de l Eclairage: approximations in the L*a*b* color space, *Appl. Opt*., **34**/16, 2998-2999, 1995.

70. CIE Technical Report, A method of predicting corresponding colours under different chromatic and illuminance adaptations, *CIE 109 - 1994*, CIE Central Bureau, Vienna.

71. Hunt RWG, Pointer MR, A colour-appearance transform for the CIE 1931 standard colorimetric observer, COLOR Res. & Appl. 10 165 - 179 1985.

72. Judd DB, Standard response functions for protanopic and deuteranopic vision, *J. Opt. Soc. Am.* **35** 199 - 220 1945.

73. CIE Technical Report, Method of measuring and specifying colour rendering properties of light sources, *CIE 13.3 - 1995*, CIE Central Bureau, Vienna.

74. Takahama K, Sobagaki H, Nayatani Y, Formulation of a nonlinear model of chromatic adaptation for a light-gray background, *COLOR Res. & Appl*. **9** 106 - 115 1984.

75. Nayatani Y, Takahama K, Sobagaki H, Field trials on color appearance of chromatic colors under various light sources, *COLOR Res. & Appl*. **13** 307 - 317 1988.

76. Forsius SA, Physica, manuscript, 1611, published in Acta Bibliothecae Stockholmiensis 315 - 321 1971.

77. Billmeyer FW Jr, Survey of color order systems, *COLOR Res. & Appl*. **12** 173 - 186 1987.

78. Newhall SM, Nickerson D, Judd DB, Final report of the O.S.A. subcommittee on the spacing of the Munsell colors, *J. Opt. Soc. Am*. **33** 385 - 418 1943.

79. Hunter RS, The measurement of appearance, John Wiley & Sons, New York, 1975.

80. Wyszecki G, Stiles WS, Color science, Concepts and methods, quantitative data and formulae, 2nd ed., pp 508 - 509 John Wiley & Sons, New York 1982.

81. McCamy CS, Munsell value as explicit functions of CIE luminance factor, *COLOR Res. & Appl*. **17** 205 -207 1992.

82. Rheinboldt WC, Menard JP, Mechanized conversion of colorimetric data to Munsell renotations, *J. Opt. Soc. Am*. **50** 802 - 807 1960.

83. Tonnquist G, Philosophy of perceptive color order systems, *COLOR Res. & Appl*. **11** 51 - 55 1986.

84. Derefeldt G, Sahlin C, Transformation of NCS data into CIELAB colour space, *COLOR Res. & Appl*. **11** 146 - 152 1986.

85. MacAdam DL, Colorimetric data for samples of OSA uniform color scales, *J. Opt. Soc. Am.* **68** 121 - 130 1978.

86. Nickerson D, History of the OSA Committee on Uniform Color Scales, *Opt. News* **3** 8 - 17 1977.

87. Richter M, Witt K, The story of the DIN color system, *COLOR Res. & Appl*. **11** 138 - 145 1986.

88. Ostwald W, *Die Farbenlehre*, Unesma, Leipzig, 1915

89. Ostwald W, *The color primer*, translated and edited by F Birren, Van Nostrand Reinhold, New York, 1969

90. Nemcsics A, Color space of the Coloroid Color System, *COLOR Res. & Appl.* **12** 135 - 146 1987.

91. Nemcsics A, Spacing in the Munsell color system relative to the Coloroid Color System, *COLOR Res. & Appl*. **19** 122 - 125 1994.

92 Smith NS, Whitfield TWA, Wiltshire TJ, Research note on the accuracy of the NCS, DIN and OSA-UCS colour atlases, *COLOR Res. & Appl*. **15** 197 - 299 1990.

93 Smith NS, Whitfield TWA, Wiltshire TJ, Comparison of the Munsell, NCS, DIN and Coloroid colour order systems using the OSA-UCS model, *COLOR Res. & Appl*. **15** 327 - 337 1990.

94 Smith NS, Whitfield TWA, Wiltshire TJ, Accuracy of the NCS atlas samples, *COLOR Res. & Appl*. **16** 108 - 113 1991.

95 Smith NS, Whitfield TWA, Wiltshire TJ, NCS, and DIN notations for the OSA-UCS atlas samples, *COLOR Res. & Appl*. **17** 273 - 283 1992.

96 Smith NS, Billmeyer FW Jr., Comparison of the colorcurve and SCA-2541 colour order systems using the OSA-UCS model, *COLOR Res. & Appl*. **19** 363 - 374 1994.

97. Guth SL, Model for color vision and light adaptation, *J. Opt. Soc. Am. A* **8** 976 - 993 1991, and erratum, *J. Opt. Soc. Am. A* **9** 344 1992.

98. Guth SL, Unified model for human color perception and visual adaptation II, *Proc. SPIE* Vol. **1913** 440 - 448 1993.

99. Guth SL, ATD model for color vision I: background; II: applications, *Proc. SPIE* Vol. **2170** 149 - 161 1994.

100. Guth SL, Further applications of the ATD model for color vision, *Proc. SPIE Conf on Device-Independent Color Imaging II*, **2414** 12 - 26 1995.

101. Fairchild MD, Formulation and testing of an incomplete-chromatic adaptation model, *COLOR Res. & Appl*. **16** 243 - 250 1991.

102. Fairchild, MD, A model of incomplete chromatic adaptation, *Proc. 22nd Session of the CIE,* 33 - 34 *CIE 91 - 1991,* CIE Central Bureau Vienna

103. Fairchild MD, Berns RS, Image color-appearance specification through extension of CIELAB, *COLOR Res. & Appl*. **18** 178 - 190 1993, and Erratum to Image color-appearance specification through extension of CIELAB, *COLOR Res. & Appl*. **18** 437 1993.

104. Fairchild MD, Visual evaluation and evolution of the RLAB color space, *IS&T and SID's 2nd Color Imaging Conference: Color Science Systems and Applications,* 9 - 13, IS&T, Springfield, Va., USA 1994.

105. Nayatani Y, Hashimoto K, Takahama K, Sobagaki H, A nonlinear color-appearance model using Estevez - Hunt - Pointer primaries, *COLOR Res. & Appl*. **12** 231 - 242 1987.

106. Nayatani Y, Takahama K, Sobagaki H, Hashimoto K, Color-appearance model and chromatic-adaptation transform, *COLOR Res. & Appl*. **15** 210 - 221 1990.

107. Nayatani Y, Revision of the chroma and hue scales of a nonlinear color-appearance model, *COLOR Res. & Appl*. **20** 143 - 155 1995.

108. Nayatani Y, Sobagaki H, Hashimoto K, Yano T, Lightness dependency of chroma scales of a nonlinear color-appearance model and its latest formulation, *COLOR Res. & Appl*. **20** 156 - 167 1995.

109. Hunt RWG, A model of colour vision for predicting colour appearance in various viewing conditions, *COLOR Res. & Appl*. **12** 297 - 314 1987.

110. Hunt RWG, Errata: A model of colour vision for predicting colour appearance in various viewing conditions, *COLOR Res. & Appl*. **13** 132 1988.

111. Hunt RWG, Revised colour-appearance model for related and unrelated colours, *COLOR Res. & Appl*. **16** 146 - 165 1991.

112. Hunt RWG, Erratum: Revised colour-appearance model for related and unrelated colours, *COLOR Res. & Appl*. **16** 351 1991.

113. Hunt RWG, An improved predictor of colourfulness in a model of colour vision, *COLOR Res. & Appl*. **19** 23 - 26 1994.

114. Luo MR, Clarke AA, Rhodes PA, Schappo A, Scrivener SAR, Tait CJ, Quantifying colour appearance, Part I. LUTCHI Colour appearance data, *COLOR Res. & Appl*. **16** 166 - 180 1991.

115. Luo MR, Clarke AA, Rhodes PA, Schappo A, Scrivener SAR, Tait CJ, Quantifying colour appearance, Part II. Testing colour models performance using LUTCHI Colour appearance data, *COLOR Res. & Appl*. **16** 181 - 197 1991.

116. Luo MR, Gao XW, Rhodes PA, Xin HJ, Clarke AA, Scrivener SAR, Quantifying colour appearance, Part III. Supplementary LUTCHI Colour appearance data, *COLOR Res. & Appl*. **18** 98 - 113 1993.

117. Luo MR, Gao XW, Rhodes PA, Xin HJ, Clarke AA, Scrivener SAR, Quantifying colour appearance, Part IV. Transmissive media, *COLOR Res. & Appl*. **18** 191 - 209 1993.

118. Hunt RWG, Luo MR, Evaluation of a model of colour vision by magnitude scalings: Discussion of collected results, *COLOR Res. & Appl*. **19** 27 - 33 1994.

119. Luo MR, Gao XW, Scrivener SAR, Quantifying colour appearance, Part V. Simultaneous contrast, *COLOR Res. & Appl*. **20** 18 - 28 1995.

120. Fairchild MD, Testing colour-appearance models: Guidelines for coordinated research, *COLOR Res. & Appl*. **20** 262 - 267 1995.

121 Technical leaflet: Colorimeter head, LMT Lichmesstechnik, Berlin, Germany

122. CIE Technical Report, Methods of characterizing illuminance meters and luminance meters, *CIE 69 - 1987*, CIE Central Bureau, Vienna.

123 Terstiege H, Gundlach D, Characterizing the quality of colorimeters, *SID 91 Digest* 641-644, 1991.

124. Technical leaflet: Colorimeter head, InPhoRa California, USA.

125. Technical leaflet: CCD-colorimeter, InPhoRa California, USA.

126. Schanda J, Lux G, On the electronic correction of errors in a tristimulus colorimeter, in Colour 73, Proc. AIC Congress, York, 1973, pp. 466 - 469, Adam Hilger, London, 1973.

127. Andor Gy, Temperature dependence of high accuracy photometer heads, *Appl. Opt*. **28** 4733 - 4734, 1989.

128. Raggi A, Barbiroli G, Colour-difference measurement: The sensitivity of various instruments compared, *COLOR Res. & Appl.* **18** 11 - 27 1993.

129. Rodgers J, Wolf K, Willis N, Hamilton D, Ledbetter R, Stewart C, A comparative study of color measurement instrumentation, *COLOR Res. & Appl*. **19** 322 - 327 1994.

130. Hirschler R, Colour standardisation — are we there yet? Colour Communication UMIST 1995 Conference.

131. CIE Technical Report, A review of publications on properties and reflection values of material reflection standards, *CIE 46 - 1979*, CIE Central Bureau, Vienna.

132. CIE Technical Report, The spectroradiometric measurement of light sources, *CIE 63 - 1984*, CIE Central Bureau, Vienna.

133. CIE Technical Report, Spectroradiometry of pulsed optical radiation sources, *CIE 105 - 1993*, CIE Central Bureau, Vienna.

134. Makai J, Czibula G, Vida D, Schanda J, Spatial distribution of colorimetric characteristics of metal halid lamps, Proc. CIE Symp. on Light and Colour Measurement '81, 51 - 56, 1981.

135. Martin G, Muray K, Réti I, Diós J, Schanda J, Miniature integrating sphere - silicon detector combination for LED total power measurement, *Measurement* **8** 84 - 89, 1990.

136. Engeldrum PG, Ingraham JL, Analysis of white point and phosphor set differences of CRT display, *COLOR Res. & Appl*. **15** 151 - 155 1990.

137. Brill MH, Derefeldt G, Comparison of reference-white standards for video display units, *COLOR Res. & Appl*. **16** 26 - 30 1991.

138. Cowan WB, Rowell N, On the gun independence and phosphor constancy of colour video monitors, *COLOR Res. & Appl*. **11** S34 - S38 1986.

139 *Brainard DH, Calibration of a computer controlled color monitor, COLOR Res. & Appl*. **14** 23 - 34 1989.

140. Berns RS, Motta RJ, Gorzynski ME, CRT colorimetry, Part I: Theory and Praxis, *COLOR Res. & Appl*. **18** 229 - 314 1993.

141. Berns RS, Gorzynski ME, Motta RJ, CRT colorimetry, Part I: Metrology, *COLOR Res. & Appl*. **18** 315 - 325 1993.

142. Bodrogi P, Schanda J, Testing the calibration model of colour CRT monitors, Displays (to be published).

143. Bodrogi P, Schanda J, Muray K, Kránicz B, Accurate colorimetric calibration of CRT monitors, *SID Conference*, Orlando, 1995.

144. Alessi PJ, CIE guidelines for coordinated research on evaluation of colour appearance models for reflection print and self-luminous display image comparisons, *COLOR Res. & Appl*. **19** 48 - 58 1994.

145. Schanda J, Colour and the Visual Display Unit, Proc. AIC '93 Congress, Budapest, I11-1 - 12 1993,

146. ISO Draft Standard, Visual display terminals (VDTs) used for office tasks — Ergonomic requirements Part 8: Requirements for displayed colours, IS/DIS 9241-8 1994.

147. CIE Research Note, Models of heterochromatic brightness matching, *CIE 118/2 - 1995*, CIE Central Bureau, Vienna.

148. Schanda J, Brightness description using different metrics, UMIST Internat. Conf. on Colour Communication, 1995.

149. CIE Technical Report, Brightness-luminance relations: Classified bibliography, *CIE 78 - 1988*, CIE Central Bureau, Vienna.

150. CIE Technical Report, Review of the official recommendations of the CIE for the colours of signal lights, *CIE 107 - 1994*, CIE Central Bureau, Vienna.

151. Collins dictionary of the English language, ed.: Patrick Hans, Thomas Hill Long and Laurence Urdang, Collins London & Glasgow 1983.

152. Billmeyer FW Jr, Metrology, documentary standards, and color specifications for fluorescent materials, COLOR Res. & Appl. 19 413 - 425 1994.

153. CIE Technical Report, Intercomparison on measurement of (total) spectral radiance factor of luminescent specimens, *CIE 77-1988*, CIE Central Bureau, Vienna.

154. Burns DM, Johnson NL, Pavelka LA, Colorimetry of durable fluorescent retroreflective materials, *COLOR Res. & Appl*. **20** 93 - 107 1995.

155. Donaldson R, Spectrophotometry of fluorescent pigments. *Brit. J. Appl. Phys*. **5** 210 - 224 1954.

156. Gundlach D, Terstiege H, Problems in measurement of fluorescent materials, *COLOR Res. & Appl*. **19** 427 - 436 1994.

157. ASTM standards on color and appearance measurement, sponsored by ASTM Committee E-12, ASTM, 1994.

Further Reading

ASTM standards on color and appearance measurement, sponsored by ASTM Committee E-12, ASTM, 1994.

Color in business, science and industry by D Judd and G Wyszecki, John Wiley & Sons, New York, 1975.

Color science; Concepts and methods, quantitative data and formulae, 2nd ed. by G Wyszecki and WS Stiles, John Wiley & Sons New York, 1982.

Computer generated color, A practical guide to presentation and display by R Jackson, L MacDonald and K Freeman, John Wiley & Sons Chichester New York, 1994.

Effective color display, Theory and practice by D Travis, Academic Pr., London 1991.

Einführung in die Farbmetrik, 2nd ed. by M Richter, Walter de Gruyter, Berlin - New York, 1981.

IESNA Lighting Handbook, Reference & Application, 8th edition, ed.: MS Rea, Chapters 3: Vision and Perception, 4 Color, Illuminating Engineering Society of North America, New York, 1993.

Measuring colour, 2nd ed. by RWG Hunt, Ellis Horwood, New York London, 1991.

OSA Handbook of Optics, ed.: M Bass, DR Williams, WL Wolfe, McGraw-Hill, Inc. New York 1995.

Praktische Farbmessung by Anni Berger-Schunn, Muster-Schmidt Verl., Göttingen, Zürich,1991.

The measurement of appearance by RS Hunter, John Wiley & Sons New York, 1975.

The reproduction of colour, 5th edition, Fountain Press, Kingston-upon-Thames, England, 1995.

Annex

Annex 1. CIE Standard Illuminant A and D65 relative spectral power distribution, 300 nm to 830 nm at 5 nm intervalls; Extract from Table 1.1, CIE 15.2-1986

λ	Ill.A	Ill.D65	500	59,861100	109,35400
300	0,930483	0,03410	505	62,932000	108,57800
305	1,128210	1,66430	510	66,063500	107,80200
310	1,357690	3,29450	515	69,252500	106,29600
315	1,622190	11,76520	520	72,495900	104,79000
320	1,925080	20,23600	525	75,790300	106,23900
325	2,269800	28,64470	530	79,132600	107,68900
330	2,659810	37,05350	535	82,519300	106,04700
335	3,098610	38,50110	540	85,947000	104,40500
340	3,589680	39,94880	545	89,412400	104,22500
345	4,136480	42,43020	550	92,912000	104,04600
350	4,742380	44,91170	555	96,442300	102,02300
355	5,410700	45,77500	560	100,000000	100,00000
360	6,144620	46,63830	565	103,582000	98,16710
365	6,947200	49,36370	570	107,184000	96,33420
370	7,821350	52,08910	575	110,803000	96,06110
375	8,769800	51,03230	580	114,436000	95,78800
380	9,795100	49,97550	585	118,080000	92,23680
385	10,899600	52,31180	590	121,731000	88,68560
390	12,085300	54,64820	595	125,386000	89,34590
395	13,354300	68,70150	600	129,043000	90,00620
400	14,708000	82,75490	605	132,697000	89,80260
405	16,148000	87,12040	610	136,346000	89,59910
410	17,675300	91,48600	615	139,988000	88,64890
415	19,290700	92,45890	620	143,618000	87,69870
420	20,995000	93,43180	625	147,235000	85,49360
425	22,788300	90,05700	630	150,836000	83,28860
430	24,670900	86,68230	635	154,418000	83,49390
435	26,642500	95,77360	640	157,979000	83,69920
440	28,702700	104,86500	645	161,516000	81,86300
445	30,850800	110,93600	650	165,028000	80,02680
450	33,085900	117,00800	655	168,510000	80,12070
455	35,406800	117,41000	660	171,963000	80,21460
460	37,812100	117,81200	665	175,383000	81,24620
465	40,300200	116,33600	670	178,769000	82,27780
470	42,869300	114,86100	675	182,118000	80,28100
475	45,517400	115,39200	680	185,429000	78,28420
480	48,242300	115,92300	685	188,701000	74,00270
485	51,041800	112,36700	690	191,931000	69,72130
490	53,913200	108,81100	695	195,118000	70,66520
495	56,853900	109,08200	700	198,261000	71,60910

705	201,359000	72,97900	775	239,370000	65,09410
710	204,409000	74,34900	780	241,675000	63,38280
715	207,411000	67,97650	785	243,924000	63,84340
720	210,365000	61,60400	790	246,116000	64,30400
725	213,268000	65,74480	795	248,251000	61,87790
730	216,120000	69,88560	800	250,329000	59,45190
735	218,920000	72,48630	805	252,350000	55,70540
740	221,667000	75,08700	810	254,314000	51,95900
745	224,361000	69,33980	815	256,221000	54,69980
750	227,000000	63,59270	820	258,071000	57,44060
755	229,585000	55,00540	825	259,865000	58,87650
760	232,115000	46,41820	830	261,602000	60,31250
765	234,589000	56,61180			
770	237,008000	66,80540			

Annex 2. CIE 1931 Standard Colorimetric Observer and CIE 1964 Supplementary Standard Colorimetric Observer colour matching functions, 360 nm to 830 nm at 5 nm intervalls; extract from Tables taken from CIE 15.2-1986

λ	$\bar{x}_2(\lambda)$	$\bar{y}_2(\lambda)$	$\bar{z}_2(\lambda)$	$\bar{x}_{10}(\lambda)$	$\bar{y}_{10}(\lambda)$	$\bar{z}_{10}(\lambda)$
360	0,0001	0,0000	0,0006	0,0000	0,0000	0,0000
365	0,0002	0,0000	0,0011	0,0000	0,0000	0,0000
370	0,0004	0,0000	0,0019	0,0000	0,0000	0,0000
375	0,0007	0,0000	0,0035	0,0000	0,0000	0,0001
380	0,0014	0,0000	0,0065	0,0002	0,0000	0,0007
385	0,0022	0,0001	0,0105	0,0007	0,0001	0,0029
390	0,0042	0,0001	0,0201	0,0024	0,0003	0,0105
395	0,0077	0,0002	0,0362	0,0072	0,0008	0,0323
400	0,0143	0,0004	0,0679	0,0191	0,0020	0,0860
405	0,0232	0,0006	0,1102	0,0434	0,0045	0,1971
410	0,0435	0,0012	0,2074	0,0847	0,0088	0,3894
415	0,0776	0,0022	0,3713	0,1406	0,0145	0,6568
420	0,1344	0,0040	0,6456	0,2045	0,0214	0,9725
425	0,2148	0,0073	1,0391	0,2647	0,0295	1,2825
430	0,2839	0,0116	1,3856	0,3147	0,0387	1,5535
435	0,3285	0,0168	1,6230	0,3577	0,0496	1,7985
440	0,3483	0,0230	1,7471	0,3837	0,0621	1,9673
445	0,3481	0,0298	1,7826	0,3867	0,0747	2,0273
450	0,3362	0,0380	1,7721	0,3707	0,0895	1,9948
455	0,3187	0,0480	1,7441	0,3430	0,1063	1,9007
460	0,2908	0,0600	1,6692	0,3023	0,1282	1,7454
465	0,2511	0,0739	1,5281	0,2541	0,1528	1,5549
470	0,1954	0,0910	1,2876	0,1956	0,1852	1,3176
475	0,1421	0,1126	1,0419	0,1323	0,2199	1,0302
480	0,0956	0,1390	0,8130	0,0805	0,2536	0,7721

485	0,0580	0,1693	0,6162	0,0411	0,2977	0,5701
490	0,0320	0,2080	0,4652	0,0162	0,3391	0,4153
495	0,0147	0,2586	0,3533	0,0051	0,3954	0,3024
500	0,0049	0,3230	0,2720	0,0038	0,4608	0,2185
505	0,0024	0,4073	0,2123	0,0154	0,5314	0,1592
510	0,0093	0,5030	0,1582	0,0375	0,6067	0,1120
515	0,0291	0,6082	0,1117	0,0714	0,6857	0,0822
520	0,0633	0,7100	0,0782	0,1177	0,7618	0,0607
525	0,1096	0,7932	0,0573	0,1730	0,8233	0,0431
530	0,1655	0,8620	0,0422	0,2365	0,8752	0,0305
535	0,2257	0,9149	0,0298	0,3042	0,9238	0,0206
540	0,2904	0,9540	0,0203	0,3768	0,9620	0,0137
545	0,3597	0,9803	0,0134	0,4516	0,9822	0,0079
550	0,4334	0,9950	0,0087	0,5298	0,9918	0,0040
555	0,5121	1,0000	0,0057	0,6161	0,9991	0,0011
560	0,5945	0,9950	0,0039	0,7052	0,9973	0,0000
565	0,6784	0,9786	0,0027	0,7938	0,9824	0,0000
570	0,7621	0,9520	0,0021	0,8787	0,9556	0,0000
575	0,8425	0,9154	0,0018	0,9512	0,9152	0,0000
580	0,9163	0,8700	0,0017	1,0142	0,8689	0,0000
585	0,9786	0,8163	0,0014	1,0743	0,8256	0,0000
590	1,0263	0,7570	0,0011	1,1185	0,7774	0,0000
595	1,0567	0,6949	0,0010	1,1343	0,7204	0,0000
600	1,0622	0,6310	0,0008	1,1240	0,6583	0,0000
605	1,0456	0,5668	0,0006	1,0891	0,5939	0,0000
610	1,0026	0,5030	0,0003	1,0305	0,5280	0,0000
615	0,9384	0,4412	0,0002	0,9507	0,4618	0,0000
620	0,8544	0,3810	0,0002	0,8563	0,3981	0,0000
625	0,7514	0,3210	0,0001	0,7549	0,3396	0,0000
630	0,6424	0,2650	0,0000	0,6475	0,2835	0,0000
635	0,5419	0,2170	0,0000	0,5351	0,2283	0,0000
640	0,4479	0,1750	0,0000	0,4316	0,1798	0,0000
645	0,3608	0,1382	0,0000	0,3437	0,1402	0,0000
650	0,2835	0,1070	0,0000	0,2683	0,1076	0,0000
655	0,2187	0,0816	0,0000	0,2043	0,0812	0,0000
660	0,1649	0,0610	0,0000	0,1526	0,0603	0,0000
665	0,1212	0,0446	0,0000	0,1122	0,0441	0,0000
670	0,0874	0,0320	0,0000	0,0813	0,0318	0,0000
675	0,0636	0,0232	0,0000	0,0579	0,0226	0,0000
680	0,0468	0,0170	0,0000	0,0409	0,0159	0,0000
685	0,0329	0,0119	0,0000	0,0286	0,0111	0,0000
690	0,0227	0,0082	0,0000	0,0199	0,0077	0,0000
695	0,0158	0,0057	0,0000	0,0138	0,0054	0,0000
700	0,0114	0,0041	0,0000	0,0096	0,0037	0,0000
705	0,0081	0,0029	0,0000	0,0066	0,0026	0,0000
710	0,0058	0,0021	0,0000	0,0046	0,0018	0,0000
715	0,0041	0,0015	0,0000	0,0031	0,0012	0,0000
720	0,0029	0,0010	0,0000	0,0022	0,0008	0,0000
725	0,0020	0,0007	0,0000	0,0015	0,0006	0,0000

730	0,0014	0,0005	0,0000	0,0010	0,0004	0,0000
735	0,0010	0,0004	0,0000	0,0007	0,0003	0,0000
740	0,0007	0,0002	0,0000	0,0005	0,0002	0,0000
745	0,0005	0,0002	0,0000	0,0004	0,0001	0,0000
750	0,0003	0,0001	0,0000	0,0003	0,0001	0,0000
755	0,0002	0,0001	0,0000	0,0002	0,0001	0,0000
760	0,0002	0,0001	0,0000	0,0001	0,0000	0,0000
765	0,0001	0,0000	0,0000	0,0001	0,0000	0,0000
770	0,0001	0,0000	0,0000	0,0001	0,0000	0,0000
775	0,0001	0,0000	0,0000	0,0000	0,0000	0,0000
780	0,0000	0,0000	0,0000	0,0000	0,0000	0,0000
785	0,0000	0,0000	0,0000	0,0000	0,0000	0,0000
790	0,0000	0,0000	0,0000	0,0000	0,0000	0,0000
795	0,0000	0,0000	0,0000	0,0000	0,0000	0,0000
800	0,0000	0,0000	0,0000	0,0000	0,0000	0,0000
805	0,0000	0,0000	0,0000	0,0000	0,0000	0,0000
810	0,0000	0,0000	0,0000	0,0000	0,0000	0,0000
815	0,0000	0,0000	0,0000	0,0000	0,0000	0,0000
820	0,0000	0,0000	0,0000	0,0000	0,0000	0,0000
825	0,0000	0,0000	0,0000	0,0000	0,0000	0,0000
830	0,0000	0,0000	0,0000	0,0000	0,0000	0,0000

Annex 3. Components $S_0(\lambda)$, $S_1(\lambda)$ and $S_2(\lambda)$ of daylight used in the calculation of relative spectral power distribution of daylight illuminants of different correlated colour temperatures, for wavelength 300 to 830 nm at 5 nm intervals (see Publ CIE. 15.2 Table 1.2 [19].

λ, nm	S_0	S_1	S_2
300	0,04	0,02	0,00
305	3,02	2,26	1,00
310	6,00	4,50	2,00
315	17,80	13,45	3,00
320	29,60	22,40	4,00
325	42,45	32,20	6,25
330	55,30	42,00	8,50
335	56,30	41,30	8,15
340	57,30	40,60	7,80
345	59,55	41,10	7,25
350	61,80	41,60	6,70
355	61,65	39,80	6,00
360	61,50	38,00	5,30
365	65,15	40,20	5,70
370	68,80	42,40	6,10
375	66,10	40,45	4,55
380	63,40	38,50	3,00
385	64,60	36,75	2,10
390	65,80	35,00	1,20
395	80,30	39,20	0,05
400	94,80	43,40	-1,10
405	99,80	44,85	-0,80
410	104,80	46,30	-0,50
415	105,35	45,10	-0,60
420	105,90	43,90	-0,70
425	101,35	40,50	-0,95
430	96,80	37,10	-1,20
435	105,35	36,90	-1,90
440	113,90	36,70	-2,60
445	119,75	36,30	-2,75
450	125,60	35,90	-2,90
455	125,55	34,25	-2,85
460	125,50	32,60	-2,80
465	123,40	30,25	-2,70
470	121,30	27,90	-2,60
475	121,30	26,10	-2,60
480	121,30	24,30	-2,60
485	117,40	22,20	-2,20
490	113,50	20,10	-1,80
495	113,30	18,15	-1,65
500	113,10	16,20	-1,50
505	111,95	14,70	-1,40
510	110,80	13,20	-1,30
515	108,65	10,90	-1,25
520	106,50	8,60	-1,20
525	107,65	7,35	-1,10
530	108,80	6,10	-1,00
535	107,05	5,15	-0,75
540	105,30	4,20	-0,50
545	104,85	3,05	-0,40
550	104,40	1,90	-0,30
555	102,20	0,95	-0,15
560	100,00	0,00	0,00
565	98,00	-0,80	0,10
570	96,00	-1,60	0,20
575	95,55	-2,55	0,35
580	95,10	-3,50	0,50
585	92,10	-3,50	1,30
590	89,10	-3,50	2,10
595	89,80	-4,65	2,65

600	90,50	-5,80	3,20
605	90,40	-6,50	3,65
610	90,30	-7,20	4,10
615	89,35	-7,90	4,40
620	88,40	-8,60	4,70
625	86,20	-9,05	4,90
630	84,00	-9,50	5,10
635	84,55	-10,20	5,90
640	85,10	-10,90	6,70
645	83,50	-10,80	7,00
650	81,90	-10,70	7,30
655	82,25	-11,35	7,95
660	82,60	-12,00	8,60
665	83,75	-13,00	9,20
670	84,90	-14,00	9,80
675	83,10	-13,80	10,00
680	81,30	-13,60	10,20
685	76,60	-12,80	9,25
690	71,90	-12,00	8,30
695	73,10	-12,65	8,95
700	74,30	-13,30	9,60
705	75,35	-13,10	9,05
710	76,40	-12,90	8,50
715	69,85	-11,75	7,75
720	63,30	-10,60	7,00
725	67,50	-11,10	7,30
730	71,70	-11,60	7,60
735	74,35	-11,90	7,80
740	77,00	-12,20	8,00
745	71,10	-11,20	7,35
750	65,20	-10,20	6,70
755	56,45	-9,00	5,95
760	47,70	-7,80	5,20
765	58,15	-9,50	6,30
770	68,60	-11,20	7,40
775	66,80	-10,80	7,10
780	65,00	-10,40	6,80
785	65,50	-10,50	6,90
790	66,00	-10,60	7,00
795	63,50	-10,15	6,70
800	61,00	-9,70	6,40
805	57,15	-9,00	5,95
810	53,30	-8,30	5,50
815	56,10	-8,80	5,80
820	58,90	-9,30	6,10
825	60,40	-9,55	6,30
830	61,90	-9,80	6,50